POLITECNICO
MILANO 1863

SCUOLA DI INGEGNERIA INDUSTRIALE
E DELL'INFORMAZIONE

A tool for the performance comparison between fixed block and moving block rail signalling systems

Tesi di Laurea Magistrale in
Automation and Control Engineering - Ingegneria dell'Automazione

Author: **Marco Barbaro**

Student ID: 10602783
Advisor: Prof. Andrea Collina
Co-advisors: Ing. Lorenzo Bernardini, Prof. Giuseppe Bucca, Ing. Ivano La Paglia
Academic Year: 2021-22

Abstract

The railway signalling system is one of the key players in controlling rail traffic, with the purpose of guaranteeing safety while respecting transport demand. Compared to road vehicles, trains are characterised by higher speeds and a lower wheel-to-rail adhesion coefficient than tyre-to-road, causing a considerable increase in braking distance. In addition, a railway convoy runs on lines with a predetermined route so the only option to avoid an obstacle in the path is to brake while having a sufficient length of line available. These factors make visual control performed by the driver unfeasible. Railway signalling systems are an answer to this issue, which arose historically with the first railways. Moreover, the increasing demand for rail traffic requires improved signalling system performance. Recent developments have led to the definition, within the framework of the European regulation (ERTMS), of the moving block (MVB) signalling system as an approach to overcome the limitations of current signalling systems, which are fundamentally based on the fixed block (FXB) approach. At present, there are no operational applications of the MVB system, except for some partial and limited experimentation. This work focuses on the development of a simulation tool to evaluate the performance of these two signalling systems, considering different operational scenarios. The evaluation is carried out using three performance indicators: line capacity, motion regularity and energy consumption. Among the factors considered, there is the response of signalling systems to degraded conditions or traffic disturbances due to various operational or infrastructural conditions. The results of this study show that the comparison between the two signalling systems is not unambiguous, since there is no railway signalling system that is convenient in each simulated scenario and according to each adopted indicator. With a view to developing a test laboratory able to combine simulated elements with physical components, the simulator was also implemented and tested on a real-time computing platform, thus enabling it to be connected with physical signalling elements.

Keywords: ERTMS/ETCS, signalling systems, fixed block, moving block, simulation environment, Hardware-in-the-Loop test bench

Sommario

Il sistema di segnalamento ferroviario è uno dei principali attori nel controllo del traffico ferroviario, con l'obiettivo di garantire la sicurezza nel rispetto della domanda di trasporto. Rispetto ai veicoli stradali, i treni sono caratterizzati da velocità più elevate e da un coefficiente di aderenza ruota-rotaia inferiore a quello pneumatico-strada, con conseguente notevole aumento dello spazio di frenata. Inoltre, un convoglio ferroviario viaggia su linee con un percorso predeterminato, per cui l'unica opzione per evitare un ostacolo sul percorso è frenare avendo a disposizione una lunghezza sufficiente di linea. Questi fattori rendono impraticabile il controllo visivo effettuato dal macchinista. I sistemi di segnalamento ferroviario sono una risposta a questo problema, sorto storicamente con le prime ferrovie. Inoltre, la crescente domanda di traffico ferroviario richiede un miglioramento delle prestazioni del sistema di segnalamento. I recenti sviluppi hanno portato alla definizione, nell'ambito della normativa europea (ERTMS), del sistema di segnalamento a blocchi mobili (MVB) come approccio per superare i limiti degli attuali sistemi di segnalamento, basati fondamentalmente sull'approccio a blocchi fissi (FXB). Al momento non esistono applicazioni operative del sistema MVB, ad eccezione di alcune sperimentazioni parziali e limitate. Questo lavoro si concentra sullo sviluppo di uno strumento di simulazione per valutare le prestazioni di questi due sistemi di segnalamento, considerando diversi scenari operativi. La valutazione viene effettuata utilizzando tre indicatori di prestazione: capacità della linea, regolarità del movimento e consumo energetico. Tra i fattori considerati, vi è la risposta dei sistemi di segnalamento a condizioni degradate o a perturbazioni del traffico dovute a varie condizioni operative o infrastrutturali. I risultati di questo studio mostrano che il confronto tra i due sistemi di segnalamento non è univoco, poiché non esiste un sistema di segnalamento ferroviario che sia conveniente in ogni scenario simulato e secondo ogni indicatore adottato. Al fine di sviluppare un laboratorio di prova in grado di combinare elementi simulati con componenti fisici, il simulatore è stato implementato e testato anche su una piattaforma di calcolo in tempo reale, consentendo così di collegarlo con elementi fisici di segnalamento.

Parole chiave: ERTMS/ETCS, sistemi di segnalamento, blocco fisso, blocco mobile, ambiente di simulazione, banco Hardware-in-the-Loop

Contents

1 | Introduction

Railway transport has a much larger capacity than road transport and operates at higher speed with better energy efficiency per passenger. Since its early development, it was clear that to achieve an acceptable level of safety in operation, the issue of the length of the breaking distance exceeding the visual capability of the train driver had to be managed. Two main reasons cause the braking distance of a train to be much longer than the one of a road vehicle, namely the speed, which can be higher by a factor of two, and the adhesion friction coefficient, which is about three-fold lower. As a consequence, the braking distance of a train is of the order of a kilometre, clearly exceeding the visual capability of the train driver.

The basic safety case is the avoidance of a collision between two trains on the same line. To achieve this goal, a sufficient distance must be kept between two consecutive trains during their operation: this is among the tasks performed by the signalling system. The first issue of a signalling system is to transfer the information on the status of the line ahead to the driver. In most railway systems, this role has been taken on by a device called radio block center (RBC). The RBC collects information on the state of the trains (like their position and velocities) and provides them with their movement authority (MA), which is the permission to move from one position of the line to another, in compliance with the specifications of the infrastructure and the presence of all the other trains.

A widely spread signalling system is the so-called fixed block (FXB) system, in which the line is divided into sections called blocks: each block can be occupied by one train only at a time. The line is sectioned in the line stage, so when the trains travel on it, the blocks are already set. If the blocks are dimensioned correctly, the trains will have enough space to stop within them travelling at the maximum allowed speed in that line section. Thus, the signalling system guarantees preventing any collision between trains by providing them with the state of the blocks ahead. To this end, a set of coloured signal lights are used, representing the train MA in terms of the number of free blocks ahead of it. The aspects of the signals are shown on trackside light poles at the beginning of each block. Moreover, in most modern applications the driver is provided directly with

the reference speed it must follow, which is evaluated by the on-board computing system on the basis of the coloured signalling and shown on the driver machine interface (DMI).

Another signalling system is the so-called moving block (MVB) system, in which the blocks are not set a priori, but rather, they follow the trains during their motion. This means that the movement authority cannot be provided in terms of a discrete set of coloured signal lights, but it needs to be provided by comparing the distance between two trains and the minimum safety distance that needs to be kept in order to avoid a collision in the event of a sudden stop of the leading train.

Figure 1.1 represents a diagram of the two signalling approaches. Figure 1.1(a) concerns the FXB system: the line is divided into blocks, marked by the coloured lines and circles that represent their state. A thorough description of the coloured signal lights meaning will be provided in Section 2, but to give a general idea, with a green signal the train can proceed without constraint, with a yellow signal it has to follow a prescribed deceleration curve to stop before the end of the block, and with a red signal it has to stop promptly. The end of the movement authority of the second train coincides with the beginning of an already occupied block, signalled by a red light. Considering this requirement, a braking curve has been drawn starting from the block before the end of MA, which is yellow signalled. Figure 1.1(b), on the other hand, concerns the MVB system: the line is not divided into blocks, but there is a zone around each train that cannot be occupied by other vehicles. The end of the movement authority of the second train coincides with the beginning of the occupation zone of the first train. Considering this requirement, a braking curve has been drawn by evaluating the safety distance that allows the second train to reliably stop without colliding with the first one.

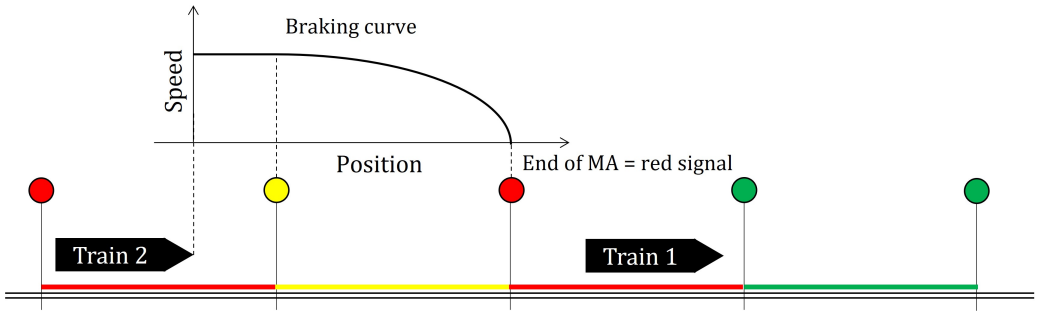

(a) FXB related diagram. The red dots and lines represent the states of the fixed blocks; if the second enters a yellow-signalled block, it has to follow a prescribed deceleration curve.

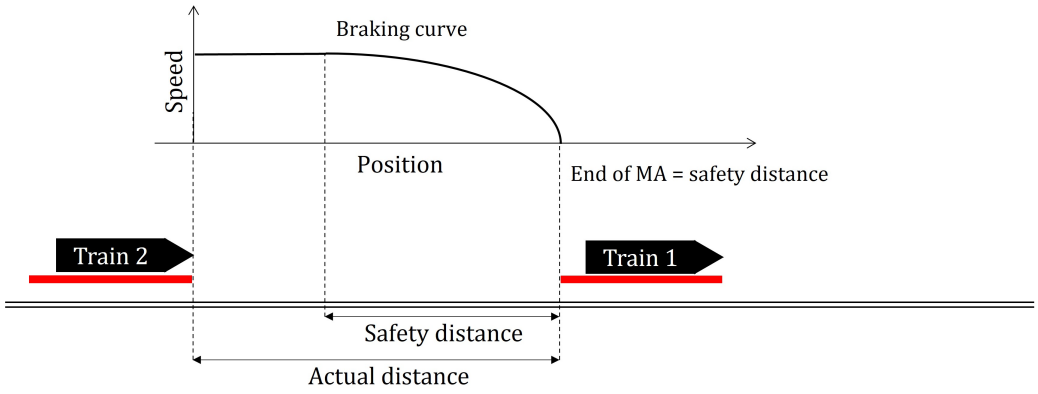

(b) MVB related diagram. The red lines represent the occupation zones of the trains; if the second train violates a safety distance with the occupation zone of the second one, it has to follow a prescribed braking curve.

Figure 1.1: Fixed block and moving block signalling systems diagrams.

This thesis aims to develop a simulation environment to compare the block-based signalling systems, i.e., fixed block (FXB) and moving block (MVB). The two will be compared in a diverse set of scenarios, so that a comparative evaluation can be carried out by means of a set of chosen KPIs, respectively Line Capacity (LC), Motion Regularity (MR) and Energy Consumption (EC). The developed simulator has to be structured in a modular way so that it will be possible to integrate it gradually in a physical laboratory.

The thesis will be organized according to the following structure. Chapter 2 will be devoted to the description of the state of the art, which includes a detailed presentation of the FXB and MVB signalling systems and the exposition of the scientific literature on the signalling systems simulation and comparison. In Chapters 3 and 4, attention will be paid to the virtual simulation tool built, respectively for the FXB and MVB environments. Chapter 5 will be dedicated to the description of the scenarios and KPIs considered for the comparison of the results obtained through the simulations according to

both signalling systems. In Chapter 6, attention will be paid to the possibility of applying the simulator in conjunction with real-time devices, which represents a first step in the direction of the broader aim of building a Hardware-in-the-Loop laboratory for signalling system comparison and certification. Finally, the conclusions and future development of this work will be presented.

In this respect, note that this thesis was developed within the framework of the Italian PNRR - Piano Nazionale di Ripresa e Resilienza, in particular with regard to Mission 4, Component 2, Investment 1.4. It is part of the research carried out by the National Centre for Sustainable Mobility (MOST), Spoke 4 - Rail Transportation.

2 | State of the Art

This Chapter will cover the state of the art related to the topic of simulating fixed block (FXB) and moving block (MVB) signalling systems. First, a thorough description of the signalling system will be provided, as well as their collocation inside a more general system of standards for railways management. Then, a literature review will be presented, with special attention to the comparison between these two signalling systems.

2.1. Presentation of ETCS levels and signalling systems

Given the relevance of railway signalling, multiple systems have been designed either at national or international level. Among these, the European Train Control System (ETCS) is the standard train protection system, which is the aim of signalling. This system has been designed to replace the many incompatible safety systems used by European railways, even though it has been applied also outside of Europe. As presented by Abed (2010) [1], it is a component of the European Rail Traffic Management System (ERTMS), which also include the Global System for Mobile Communication - Railways (GSM-R), regarding communication between the various players of the railway system, and the European Traffic Management Layer (ETML), regarding operation management and route planning.

Since its development, the ETCS system has evolved coherently to technological advancement, in order to provide an increment in the transport capacity and general performance of the railway system while still fulfilling the crucial safety requirements. Considering the different duties attributed to onboard (i.e., part of the train) and trackside (i.e., part of the infrastructure) equipment, as well as the degree of interaction prescribed between the two, the following levels can be defined as different signalling strategies adopted as the ETCS standard for different:

- level 0 (L0), which applies when an ETCS-fitted vehicle is used on a non-ETCS (legacy) route. It does not prescribe any interaction between on-board and trackside equipment, as the driver is appointed to observe and react to the trackside signalling;

- level NTC (National Train Control), in which the onboard equipment is standardised ETCS driver interfaces equipped with additional Specific Transmission Modules (STM, also the former name of the level) to interact with legacy systems;
- level 1 (L1), in which both the onboard and trackside equipment are ETCS standardised and the communication between those components is directed through trackside devices such as Eurobalises or Euroloops. Thus, the movement authority is transmitted to the train only when it interacts with one of those devices. At this level, fixed block signalling is adopted;
- level 2 (L2), which is designed according to a principle similar to that of L1, as fixed block signalling is still adopted, but the communication between on-board and trackside equipment is digital radio-based, through the use of GSM-R. Thus, the movement authority is continuously transmitted to the train, apart from the technical discretization of the information. This level is the first to introduce the radio block center (RBC) as an intermediary between trackside and onboard equipment. At this level, the train positioning is evaluated by trackside equipment such as track circuits or axle counters, which verify whether the section of the line that they are monitoring is occupied or not. Thus, even if the communication between the train and the RBC is continuous, it still concerns discrete movement authority, which is provided in terms of block state.
- level 3 (L3), which still makes use of the RBC as an intermediary on the communication of the trains, but the train positioning is evaluated on-board and their movement authority is provided in terms of absolute braking distance spacing. Thus, the signalling system applied at this level is the moving block one;
- hybrid level 3 (HL3), which develops on L2 by utilizing a further subdivision of the fixed blocks into virtual blocks to produce an approximation of L3.

After presenting the hierarchical organization of the ETCS/ERTMS signalling systems, a thorough description of FXB and MVB signalling will be provided. Note that for the rest of the dissertation, FXB systems will be associated with ETCS L2, while MVB systems will be associated with ETCS L3.

Regarding the FXB system, the MA is provided to the trains in terms of blocks state. Each block is assigned a colour depending on the rail traffic at that specific time instant. For a three-aspect signalling system, there are three colours that a block can assume according to the following criterion (however, there are also four:

- if a block is free, it is assigned the green signal light. If a train is approaching a

green-signalled block, it can proceed with its motion without applying any braking curve;

- if a block is occupied, it is assigned the red signal light. If a train is approaching a red-signalled block, it must brake as quickly as possible. The FXB signalling system is designed so that there will never be a compresence of two trains in a single red coloured block, as each train will stop before crossing a red signal light;
- if a block is free, but the one immediately after it is occupied, it is assigned the yellow signal light. If a train is approaching a yellow-signalled block, it has to follow a braking curve that leads it to stop before reaching the next block, which will be red-signalled.

With the correct dimensioning of the block system, the trains will never enter a red-signalled block, as they will have decreased their speed with a prescribed braking curve along a yellow-signalled block, and stopped before the red signal light. This is not a trivial task, as the length of the blocks depends on a set of parameters, the most relevant being the maximum speed allowed in that line segment. The procedure to evaluate the fixed block length will be presented in Section 3.2.2, but to give a preliminary overview, the block must be long enough that a train travelling at the maximum allowed speed can stop with a "comfortable" deceleration rate before reaching the end of the block, also considering a safety margin for robustness.

Regarding the MVB system, the MA is provided by comparing the actual distance of the trains and a safety distance evaluated at each time instant, as represented in Figure 1.1(b). The safety distance is evaluated in a similar manner to how the fixed block length is evaluated: it must be long enough that even in the unrealistic scenario of the first train stopping instantaneously, the second one is able to stop with a "comfortable" deceleration rate before colliding with it, also considering a safety margin behind the first train. The theoretical advantage of the moving block system is that while for FXB signalling the block length has to be evaluated considering the worst-case scenario, which is represented by the second train travelling at the maximum allowed speed, for MVB signalling the safety distance is evaluated considering the actual speed of the second train, which could be lower than the limit. Therefore, in general, the safety distance evaluated for MVB signalling, which represents the second train MA, is shorter than the block length evaluated for FXB signalling, on which the second train MA is based.

Once the signalling systems have been described, a review of the scientific literature of interest will be presented.

2.2. Review of signalling systems literature

Regardless of the signalling system considered, a high level of complexity and the need for strict test procedures before real-world implementation can be highlighted. In this sense, simulations of the signalling systems represent a fundamental tool. Specifically, the simulation of a railway line can be mainly performed by means of event-based or time-based approaches. The former relies on a discrete set of events that, when triggered, make the simulation proceed by performing the related computations; the latter divides the simulation time into evenly spaced intervals, and the computation of all variables of the system is performed for each time interval. A time-based simulation approach is more computationally demanding than an event-based one. However, it better resembles the trains movement along the railway line, making it simpler to design. Moreover, it is more suitable for applications related to signalling system analysis, as a higher level of detail can be obtained, as stated in [2]. Thus, the simulation environment has been developed using Matlab and Simulink, by considering a time-based approach.

That being said, there are researches that addressed the analysis of the signalling system impact on train performance also with event-based or hybrid approaches. An example is the study performed by Hill and Bond in [3], which pays particular attention to the relationship between minimum headway (the distance between the two trains front ends) with respect to the maximum speed permitted on the line, for bothFXB and MVB signalling. To this end, SIMSCRIPT [4] was adopted, which is a procedure-based language that programs the simulation model in terms of routines, processes and events. In [5], Chang et al. consider the conjunction of object-oriented programming techniques and discrete event-based simulation modelling to develop a simulator for fuzzy automatic train control under both nominal and disturbed conditions. The study by Basile et al. [6] represents a hybrid case between time-based and event-based simulation, in which attention is paid to the realization of a satellite-based ERTMS L3 moving block signalling system, through the use of event-based real-time UML [7], Simulink and UPPAAL [8] software. In their research, Ho et al. [9] report a model of train movement, and of the power supply and transmission, with a focus on the importance of adopting a modular approach in the development of a simulation tool for signalling systems. Lastly, Martin [10] pays attention to the simulation techniques and tools suitable to perform an assessment on train performances under different operating conditions, like different signalling systems.

One of the first steps in the procedure of designing the signalling system, which is a crucial aspect of this research, is the definition of the braking curves that the train has to follow in order to be in compliance with their movement authority. To this end, the

braking distance of the trains must be evaluated thoughtfully. In [11], Barney presents a tool for calculating train braking distances for various train classes with attention to the effect of the parameters in play, such as the physical properties and the state of the train and the line configuration. After evaluating the braking distance, a motion law over that space has to be imposed on the train so that the deceleration is performed in accordance with the particular requirements. In [12], Havryliuk provides a description of the braking curves prescribed in ERTMS/ETCS signalling systems. In [13], Friman reports a thorough review of the methods that can be applied for the calculation of those braking curves, considering three main factors: actual train speed, target speeds and line gradient.

The FXB signalling system design procedure goes on with the dimensioning of the blocks. These have to be long enough that a train travelling at the maximum allowed speed on the line segment of interest can decelerate completely within their margins. Simultaneously, the performance of the signalling system increase as the fixed blocks shorten, as with a denser discretization of the line railway traffic can be controlled more accurately. Thus, the dimensioning of the fixed blocks can be carried out as an optimization study, as reported by Vignali et al. [14]. On the same topic, Quaglietta [15] proposes another study on the design of the signalling system, considering a stochastic simulation-based optimization to design railway signalling systems, with the aim of optimizing the implementation and operational costs of the signalling system while respecting the robustness and capacity requirements.

For what concerns testing systems Mazini et al. in [16] provide an integrated test system that is backwards compatible, i.e., it applies to all levels of ETCS up to L3, based on the stakeholders' needs and requirements. Solas et al. in [17] and [18] designed a laboratory to advance towards the "Zero On-Site Testing" paradigm by realizing internal saboteurs and injecting external disturbances, so that evidence regarding the safety and reliability functions of the equipment under test can be gathered. Another broad topic regards the connection of lines controlled through different ERTMS levels. This includes automatic level crossing, which is the faculty of the train to adapt to changes in the ERTMS level under which it is being controlled (Ghazel, [19]) as well as the connection of new railway segments with the existing railway system (Wang et al., [20]).

To conclude, it is worth mentioning that the signalling problem concerns all kinds of railway transportation. This thesis focuses on the application of the signalling systems to a low-speed line, but it could be equivalently interesting to perform such research on high-speed lines, heavy hauls (Roscoe et al. [21]), rapid transit (Hamidi et al. [22]).

Once an overview of the state of the art regarding the simulation techniques and tools, some modelling aspects and the testing procedure for the comparison between fixed block and moving block has been provided, the next Chapter will describe the simulation environment designed to perform the preliminary comparison of the two technologies.

3 | Simulation environment for fixed block signalling systems

This chapter will present the virtual environment built to simulate train behaviour and its interaction with the railway and other trains, considering the fixed block (FXB) approach. It will be organized by first providing an overview of the model, listing the components on the highest level, and then explaining each component thoroughly.

This Section aims to provide a deep understanding of the simulation environment so that it will be possible to appreciate the modifications made to suit the moving block technology (Section 4), and most importantly the results of the simulations (Section 5).

3.1. Introduction and model overview

The simulation tool has been developed in Matlab and Simulink. More precisely, the former is used to initialize all the parameters and variables needed to perform the simulation, as will be thoroughly explained over the next chapters. The latter holds all the code to perform the simulation. On the highest level, the model consists of just a few blocks, as shown in Figure 3.1, which represent the main components of the real system.

The *Trackside* block contains all the parts external to the train, namely the limit speed profile generation and the radio block centre (RBC). It takes as input the state of the trains, containing their positions and bock occupancies and reports to them the coloured signal light they are to be shown when entering a new block, as well as limit speed profile they must follow. Note that in the FXB approach, the RBC does not receive the continuous position of the trains, but rather their (discrete) block occupancy. Still, that information is used in the limit speed curve generation blocks, which report the reference speed the trains must follow at each point on the line, thus, their position is needed as input for the trackside block even for the fixed block environment.

The *Train* block contains the train dynamics model and the driver's behavioural model. It takes as input the coloured signal light and the limit speed profile as well as the state

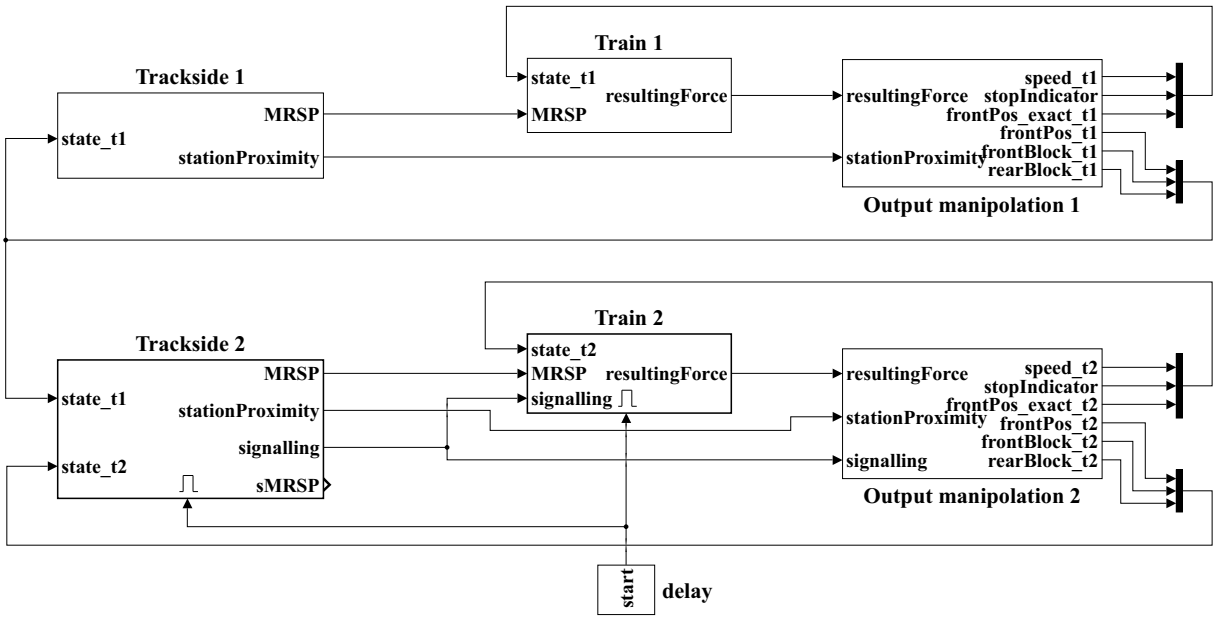

Figure 3.1: Overview of the Simulink block diagram.

of the train containing its exact position and speed, and returns as output the resulting force acting on the train at any given time instant.

The *Train output manipulation* block contains all the functions required to realize the communication between train and RBC, mainly the numerical integration to evaluate the position of the vehicle given the force acting on it and the evaluation of the block occupancy. The block takes as input the force acting on the train and returns as output all the train information, in the form of:

- speed;
- the stop indicator, which is a boolean variable that reports when the train is fully stopped (it will be thoroughly described in chapter 3.4.4);
- the position of its front end;
- the block occupancy of its front and rear ends.

Note that Figure 3.1 represents the simulation environment of two trains travelling on the line. This means that the first train is subject to no constraints (i.e., there are no other trains in front of it), while the second one has to consider the first into account during its motion. For this reason, the arrow related to the coloured signal lights (labelled *signalling*) is not present in the upper half of the diagram, concerning the first train. Likewise, the *Trackside 1* block only receives as input the block occupancy of the first train, while the *Trackside 2* block receives the block occupancy of both the first and second train.

3.2. Description of the trackside components

The main function of the *Trackside* block is to provide the train with the reference speed it has to follow to travel optimally along the line. This reference speed is named most restrictive speed profile (MRSP), and it is built taking into account the line specifics and configuration, the location of the stations and the coloured signal lights.

The trackside block can be subdivided into static MRSP generation, RBC model and dynamic MRSP generation. The difference between static and dynamic MRSP will be thoroughly explained in Sections 3.2.1 and 3.2.3, but as the name suggests, the static MRSP is generated at once before the simulation, while the dynamic MRSP is drawn during the simulation. This differentiation is useful to consider separately the factors of speed limit evaluation which are known before the simulation start (the overall speed limit profile on the line and the presence of stations), and the ones that manifest only during the simulation (the coloured signalling). The RBC model generates the coloured signalling to be shown to the train, based on the block occupancy of the two trains.

Figure 3.2 shows the Simulink block diagram for the Trackside block, highlighting the three sub-components and their interactions. In the next Sections, each of these modules will be explained thoroughly. Notice the RBC only receives as inputs the block occupancies of the trains and returns the coloured signalling. The other two blocks concern the generation of the MRSP: the static MRSP generator takes as input the continuous position of the train, while the other block aims to decrease the static MRSP when yellow or red signal lights are shown to the train, thus, it takes as inputs the position of the train, the static MRSP and the signalling provided by the RBC.

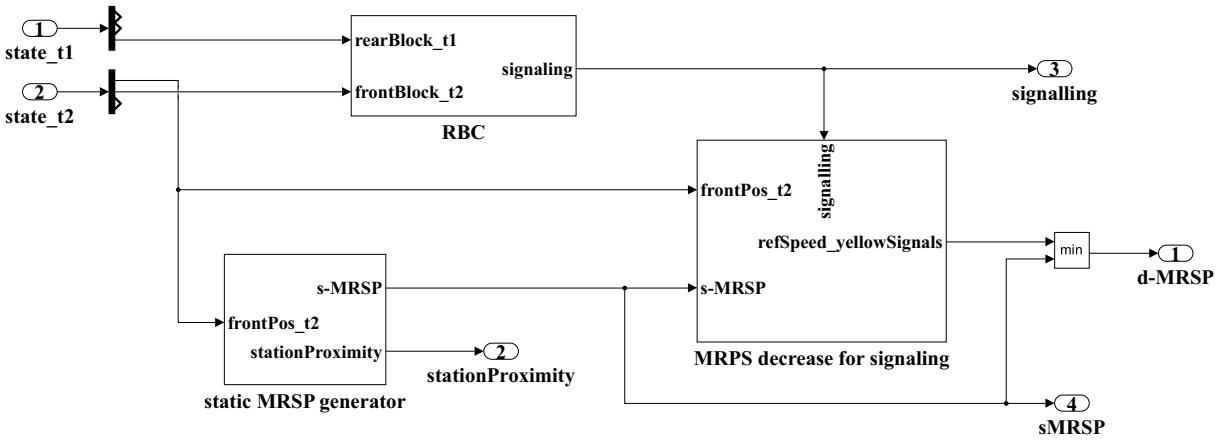

Figure 3.2: Trackside block diagram.

3.2.1. Static MRSP generation and line definition

The aim of the static MRSP (s-MRSP) generation block is to generate the static speed limit curve, that is the speed curve a train travelling on the reference line should follow in case no other trains were running on the considered line, i.e., if the signalling was not considered. Instead, at this stage, only the line-imposed speed limit and the presence of stations are considered. To do so, the railway line has to be properly defined, meaning that the following aspects have to be specified:

- the geometrical properties (length, gradient);
- the imposed speed and the VCP location;
- the information about the stations, such as location, approaching speed, and stop time;

These features allow the definition of the reference speed profile that a train travelling alone on the line must follow, i.e., the s-MRSP.

The speed limit curve generation procedure can be divided into two steps: first, the presence of stations is neglected to obtain the look-up table (LUT) shown in Figure 3.3, which shows the speed limit with respect to any position on the line.

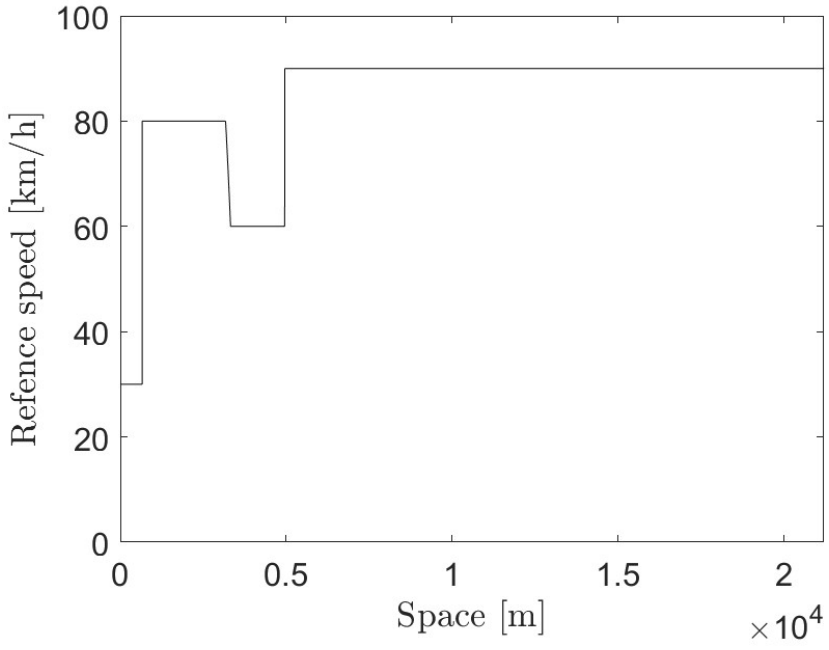

Figure 3.3: Speed look-up table without considering stations.

The LUT is obtained as follows:

- the speed changes at fixed locations, called velocity change points (VCP);
- when the speed increases, the change happens instantaneously exactly in correspondence with the VCP;
- when the speed decreases, it follows a curve defined to ensure that the train can reach the target speed in correspondence with the target VCP;
- the speed decrease is obtained by prescribing a uniformly decelerated motion (the choice of the uniform deceleration value will be discussed shortly). Of course, it is crucial to determine the braking distance needed to perform the deceleration. To this end, the following relationship is considered:

$$l_{dec} = \frac{1}{2}\frac{{v_0}^2 - {v_1}^2}{a_B} \tag{3.1}$$

  where:

  · l_{dec} represents the braking distance;

  · v_0 represents the approaching speed at the VCP;

  · v_1 represents the speed after the VCP;

  · a_B represents the prescribed deceleration;

- by prescribing a constant deceleration, the speed decreases linearly with respect to time, but parabolically with respect to space, as shown in Equation 3.2 and in Figure 3.4 (which is a zoom of Figure 3.3 around the speed decreasing VCP).

$$v_{lim}(s) = \sqrt{2a_B * (s_{VCP} - l_{dec} - s) + {v_0}^2}\text{ , with } s \in [s_{VCP} - l_{dec},\ s_{VCP}] \tag{3.2}$$

  where:

  · s_{VCP} represents the position of the VCP;

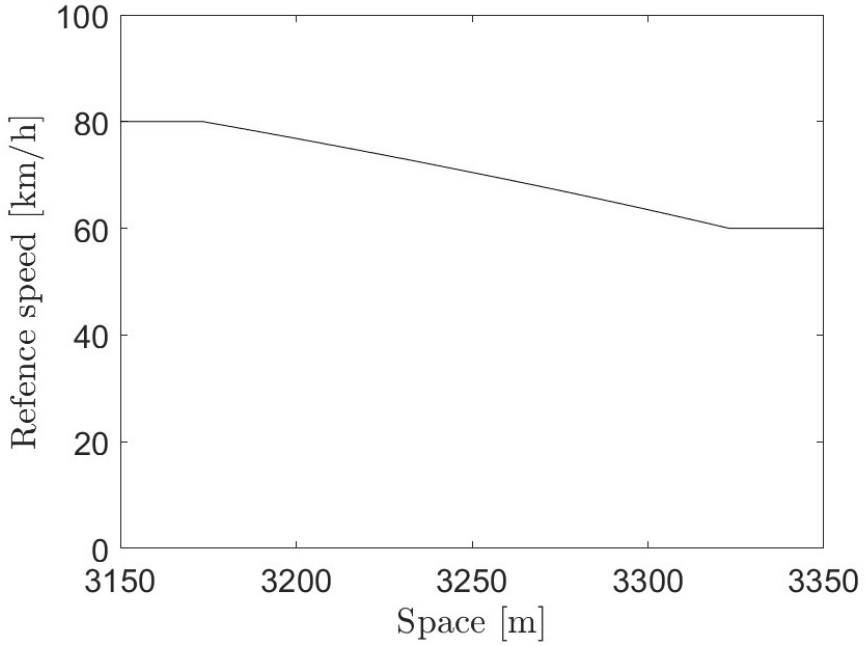

Figure 3.4: Look-up table zoom on braking curve.

Moving ahead with the second step of this procedure, it requires to consider the presence of the stations to obtain the look-up table in Figure 3.5.

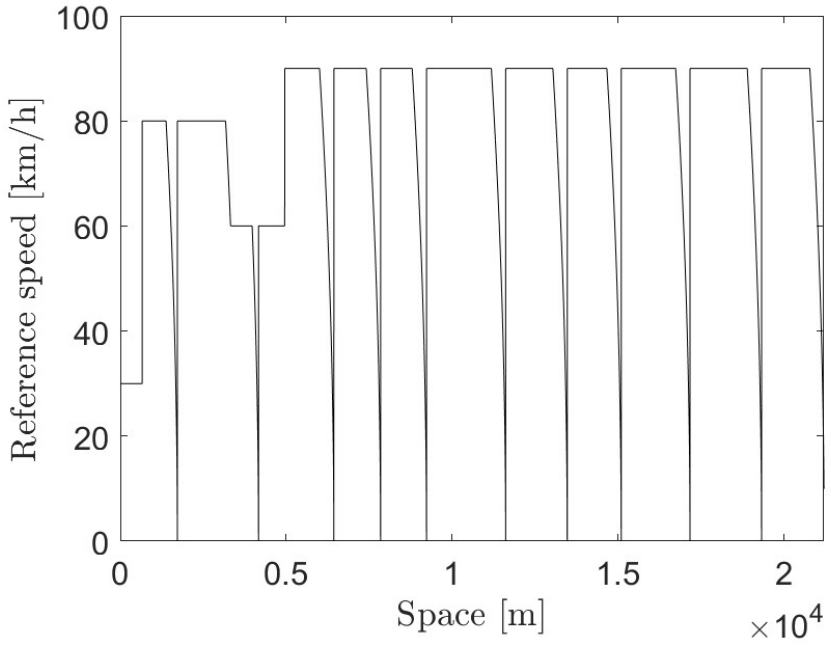

Figure 3.5: Speed look-up table considering stations.

Starting from the first LUT, this LUT is obtained as follows:

- For each station, the braking distance needed to stop the train considering the station approach speed is evaluated (the same uniform deceleration considered for the VCP is prescribed). To this end, the following relationship is considered:

$$l_{stop} = \frac{1}{2}\frac{v_0^2}{a_B} \tag{3.3}$$

  where:

  · l_{stop} represents the stopping distance;

  · v_0 represents the approaching speed at the station;

  · a_B represents the prescribed deceleration;

- Then, a uniformly decelerated motion is imposed so that the train stops exactly at the station with a curve of the same shape as described for speed-decreasing VCP's, as shown in Equation 3.4 and Figure 3.6 (which is a zoom of Figure 3.5 around a station).

$$v_{lim}(s) = \sqrt{2a_B * (s_{station} - l_{stop} - s) + {v_0}^2}, \text{ with } s \in [s_{station} - l_{stop},\ s_{station}] \tag{3.4}$$

where $s_{station}$ represents the position of the station.

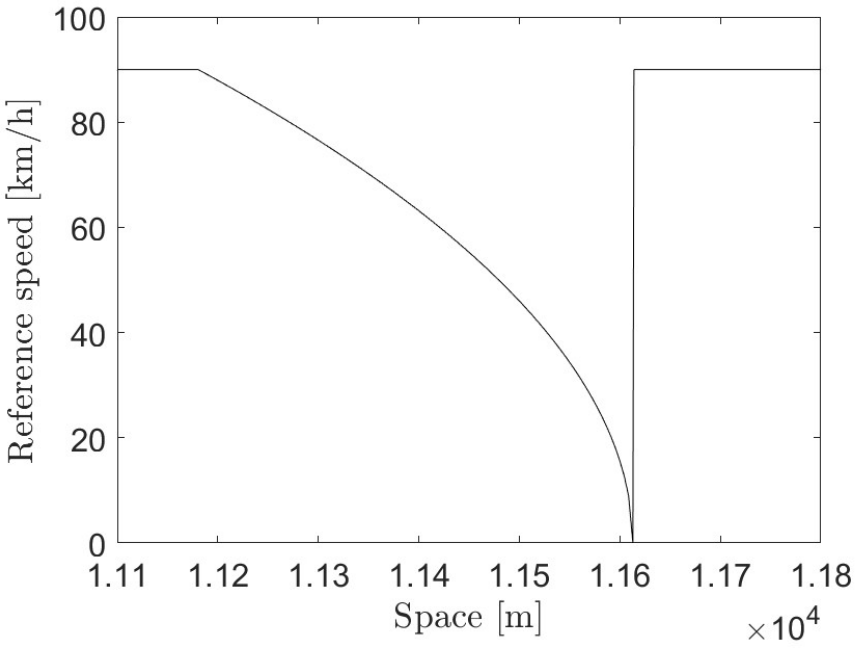

Figure 3.6: Look-up table zoom on stopping curve

Clearly, Equations 3.3 and 3.4 are analogous to Equations 3.1 and 3.2, i.e., the ones obtained for a decreasing VCP. The differences are that the target speed is null ($v_1 = 0$), the VCP is placed on the station ($s_{VCP} = s_{station}$) and the braking distance is actually a stopping distance ($l_{dec} = l_{stop}$).

As mentioned, these LUT's express the reference speed for each point of the line, while Simulink works with signals that vary through time. Thus, the reference speed can be seen also with respect to time, as shown in Figure 3.7. As expected, the portions of the curve that were parabolic with respect to space, are now linear with respect to time, as the train is prescribed to follow a uniformly decelerated motion law. The obtained signal is referred to as the static most restrictive speed profile or s-MRSP.

In practice, this signal is obtained by adopting a look-up-table block containing the LUT in Figure 3.5, controlled by the position of the train. As a result, a time signal containing the reference speed at the position that the train is occupying at any time instant is obtained.

To correctly simulate the train stop at any station, the s-MRSP around the stations is refined on top of the one generated through the look-up table. In particular:

- there is a small position range where the train can be considered at the station so that inside it, the s-MRSP is null;
- when the s-MRSP reaches 0, it remains null for the stop time prescribed in the Matlab script for the considered station;
- after that time has passed, the s-MRSP is fixed to a small positive value to let the train out of the station without allowing excessive speeds;
- this value is kept until the train has moved away enough from the station, and beyond that point, the s-MRSP resumes following the look-up table.

Figure 3.7 shows the s-MRSP for a train travelling on a line with 12 stations. Note that the first station is located at the start of the line, i.e., at position $s_0 = 0\ m$, thus, it is considered to be reached as soon as the simulation starts, i.e., at time $t_0 = 0\ s$. As desired, the speed decreases linearly as the train approaches the stations. Between the first and the fourth one, there are also 3 VCPs. Note that the intermediate steps that the s-MRSP reaches after each station are not VCPs, but rather the exit velocity prescribed so that the trains depart from the station after the stop time has elapsed without reaching excessive speeds. As desired, speed increases happen instantaneously at the VCP, while speed decreases follow a deceleration curve, which are be linear with respect to time.

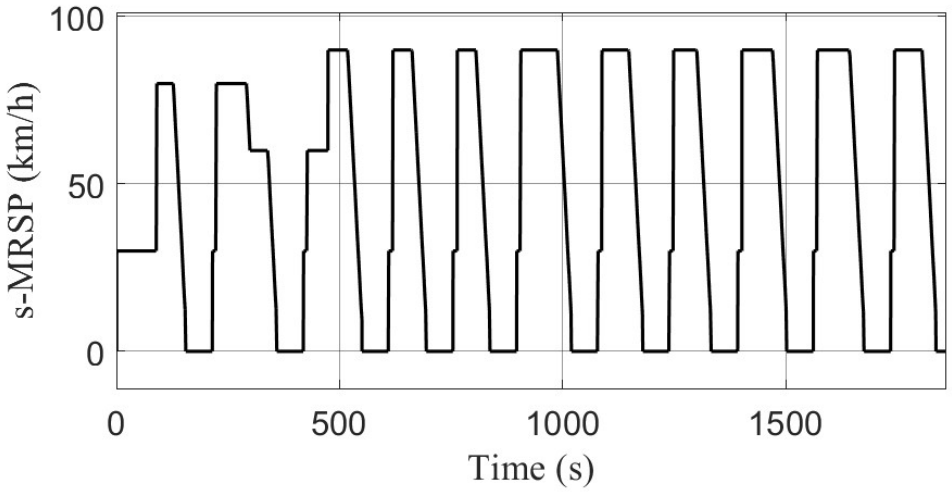

Figure 3.7: Static MRSP.

The next paragraphs will be devoted to the evaluation of the deceleration to prescribe in the braking phases (both for approaching a station or a speed-decreasing VCP), which is performed in the Matlab script. Considering a maximum deceleration for passenger safety and comfort, the reference deceleration is obtained by subtracting the contribution that external forces may generate on the most brake-inducing scenario, i.e. the case in which external forces generate the highest deceleration. As maximum deceleration theoretically achievable, the following value has been considered:

$$a_{max} = 1\ ms^{-2} \tag{3.5}$$

To take into account the aerodynamic drag and the wheel-track contact friction the following relationship has been considered:

$$a_{friction} = g * \left(\frac{{vlim_{max}}^2}{4500} + 1.5 \right) \tag{3.6}$$

Likewise, to take into account the motion resistance due to the effect of an uphill the following relationship has been considered:

$$a_{gradient} = g * sin(\alpha_{max}) \tag{3.7}$$

where α_{max} is the angle of the steepest uphill stretch present along the line.
Finally, to ensure some level of reliability, a safety margin of the following value has been considered:

$$a_0 = 0.05\ ms^{-2} \tag{3.8}$$

Thus, the prescribed deceleration for braking a_B can be evaluated as follows:

$$a_B = a_{max} - a_{friction} - a_{gradient} - a_0 \tag{3.9}$$

The regarded modelling approach can be considered conservative, as the two components of the maximum external deceleration evaluated in Equations 3.5 and 3.6 are evaluated in the worst case independently, meaning that they consider the critical scenario in which the point on the line with the maximum speed limit coincides with the point with the maximum uphill gradient. Moreover, if that scenario were to actually occur, the safety margin ensures that the actual braking deceleration will not increase past the 1 ms^{-2} limit.

Once the procedure to evaluate the braking deceleration has been described, in the next paragraphs attention is paid to another key piece of information for line definition, that is the balise model. Balises are track-side devices that contain information on their position so that they can transmit it to the train when it passes on them. This is particularly useful to make sure that the train position is regularly updated and corrected, especially in case it drifts because of integration errors.

Considering the balises installed on railway lines, they are typically arranged in groups called clusters to ensure that communication occurs even if a single balise is incapable to communicate with the train. Figure 3.8 provides a scheme of the balise disposition on a line:

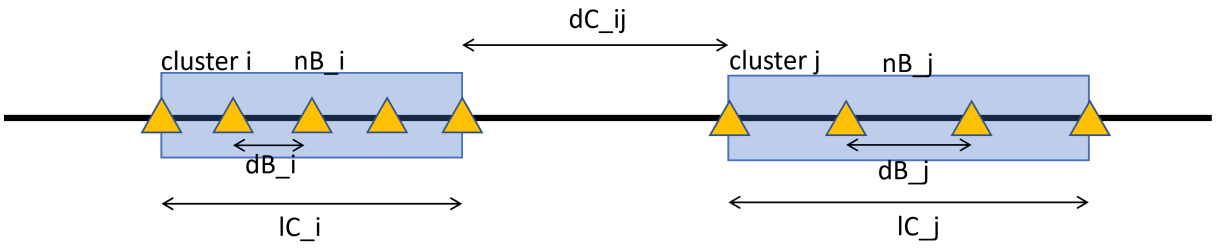

Figure 3.8: Balise cluster scheme

The specifics of the balise arrangement are the number of balises for each cluster n_B, the distance between each pair of balises in a cluster d_B and the distance between the clusters d_C. As shown in the figure, all of these quantities can vary from one balise cluster to the other, i.e., each cluster may consist of a different number of balises, and the distance one apart from the other may also change depending on the specific section of the line (for example, it may depend on the maximum speed allowed in the line segment). Thus, there

is no specific value for these quantities, rather than only some boundaries:

- the minimum number of balises in a cluster is $nB_{min} = 1$;
- the maximum number of balises in a cluster is $nB_{max} = 8$;
- the minimum distance between the balises within a cluster dB_{min} depends on the maximum reference speed as reported in Table 3.1;
- the maximum distance between the balises within a cluster is $dB_{max} = 12\ [m]$;
- the minimum distance between two clusters is $dC_{min} = vlim_{max} * 100\ [ms]$

$vlim_{max}\ [km/h]$	$dB_{min}\ [m]$
180	2.6
300	3
500	5

Table 3.1: Minimum balise distancing with respect to maximum line speed

This makes the definition of a realistic balise model overly complex, especially for the scope of this project. The modelling choice made is to consider clusters of single balises, evenly spaced across the line of a distance dB, as shown in Figure 3.9.

Figure 3.9: Balise simplified scheme.

Once the static MRSP generation process and the definition of the line have been extensively described, in Section 3.2.2 attention will be paid to the radio block center, which acts as the intermediary between the trains, making communication between them possible.

3.2.2. Radio block center (RBC)

The radio block centre (RBC) is a switchboard that communicates with the trains travelling in its area of influence, by collecting the relevant information from them and sending back the movement authority (MA). Movement authority represents the permission of a train to move from one point of the line to another with supervised speed and in accordance with the constraints of the infrastructure and the traffic state of the line segment.

In the case of a fixed block signalling system, the information that the trains send to the RBC is their block occupancy, represented by an integer stating in which section of the line the train is located, and the MA is sent back in the form of coloured signal lights, representing the state of the block the train is about to enter. As previously stated the following signalling colours are used:

- a green signal means that the block is free, so the train can proceed as specified by the s-MRSP;
- a yellow signal means that the block is free, but it's followed by an occupied block. In this case, the train must start decelerating so that if the following block does not clear, it can stop before trespassing on an occupied block.
- a red signal means that the block is occupied, so the train must stop as quickly as possible. In ideal conditions, the red signal is never encountered as it is always preceded by a yellow signal that slows the train down and eventually stops it before the following block.

Clearly, a crucial aspect of this procedure lies in the definition of the block length, which is performed prior to the simulation in the Matlab setup script. The fixed block length (FBL) must be sufficiently long that when a train is travelling at the maximum permitted speed and enters a yellow-signalled block, it can still slow down to a full stop with a comfortable braking curve before entering the following block.

Ideally, the FBL could be set to coincide with the stopping distance at the maximum reference speed. That can be evaluated in two ways:

- the Pedelucq formula, which takes into account the effective brake weight of the train Λ_C, a coefficient dependant on the maximum reference speed $\varphi(vlim_{max})$ and the maximum downhill gradient i_{max}, as shown in Equation 3.10:

$$Sa_{Pedelucq} = \frac{{vlim_{max}}^2}{(1.09375 \cdot \Lambda_C \ + \ 0.127)/\varphi(vlim_{max}) \ + \ 0.235 \cdot i_{max}} \tag{3.10}$$

- the application of a uniformly decelerated motion with the same prescribed deceleration evaluated in chapter 3.1.1, Equations 3.5 to 3.9, as shown in Equation 3.11:

$$Sa_{deceleration} = \frac{{vlim_{max}}^2}{2 \ a_B} \tag{3.11}$$

In order to adopt a conservative strategy, the modelling choice adopted is to consider the maximum between the two, meaning that when they are evaluated in the Matlab script,

the selection is made depending on which one provides the greater answer.

To simulate the behaviour of a human driver, the braking action does not start exactly as the yellow signalling is shown, but rather after a delay caused by the driver's reaction time. Thus, in addition to the stopping distance, the space travelled during that reaction time must be considered. Once more, the computation of this distance is performed prior to the simulation in the Matlab script, and it considers the worst-case scenario, i.e., the one in which the most space is travelled during the reaction time. Thus, for the whole duration of the reaction time the train moves at the maximum permitted speed over the whole line, as shown in Equation 3.12:

$$Sr = tr \cdot vlim_{max} \tag{3.12}$$

Finally, to add another level of reliability, a safety margin So is considered. Thus, the overall block length FBL will be the sum of the three components described, as shown in Equation 3.13:

$$FBL_{evaluated} = max\{Sa_{Pedelucq},\ Sa_{deceleration}\} + Sr + So \tag{3.13}$$

The previous reasoning and Equations provide some guidelines to evaluate the block length depending on the behaviour of the vehicle. Alternatively, there is a standardized method to define the FBL: if the line is a low-speed one, i.e., the maximum reference speed is lower than 160 km/h, the FBL is set to 1350 m; otherwise, the FBL is set to 1800 m. As all the simulations are performed on a low-speed line Equation 3.14 can be considered:

$$FBL_{standard} = 1350\ m \tag{3.14}$$

To choose between the evaluated and the standard FBL, presented in Equations 3.13 and 3.14, two possible strategies could be adopted: on the one hand, taking the maximum of the two leads to be more conservative, on the other hand, taking the minimum leads to be more efficient, so it's useful to understand what the benefits of selecting one over the other are.

- $FBL_{evaluated}$ is tuned to fit the specifications of the line, so it represents the optimal block length that ensures the safety constraints fulfilment (even by a margin) without over-dimensioning the block.
- $FBL_{standard}$ is a widely spread measure of the block length, so it is well suited for

applying the line in a pre-existing railway system.

Clearly, any FBL greater than the evaluated one could be chosen; the standard measure is just an example. The effect of the choice of the FBL will be thoroughly described in chapter 5.5. Up to that point, all the preliminary results reported have been obtained with the standard FBL, i.e., 1350 m.

As will be shown in chapter 3.3.3, the block occupancy is evaluated from the exact position of a train through a discretization and normalization of the space. Both trains then send their block occupancy to the RBC, which then compares them and sends the appropriate signal according to Algorithm 3.1.

Algorithm 3.1 Evaluation of the coloured signal light to show the second train depending on the block occupancy of the first and second train.

if $rearBlock_{T1} - frontBlockT2 == 0$ **then**
  $colouredSignalLight = RED$
else if $rearBlock_{T1} - frontBlockT2 == 1$ **then**
  $colouredSignalLight = YELLOW$
else if $rearBlock_{T1} - frontBlockT2 > 1$ **then**
  $colouredSignalLight = GREEN$
else
  $ERROR$
end if

The block diagram of the RBC block is represented in Figure 3.10, and it follows the aforementioned Algorithm:

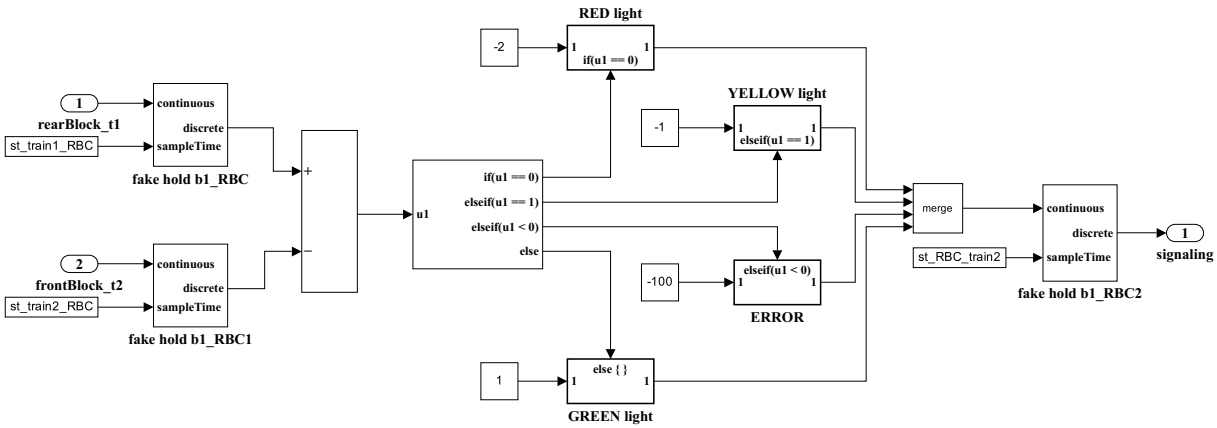

Figure 3.10: RBC block.

The last case (ERROR) occurs when the second train has overtaken the first one. This scenario is not considered in our simulation since the railway line is designed with a single

track for each travelling direction, therefore the "else" case is added just for the sake of code completeness.

The coloured signal light is shown to each train when it enters a new block, as well as regularly during the travel. This means that the RBC may send a yellow signal to the second train as it enters a new block, but then send a green signal after the first train has cleared the following block, while the second train is slowing down. In these cases, the second train is not required to come to a full stop. Instead, it should recognize that the way became free and go back to the nominal travelling conditions, i.e., following the s-MRSP.

Once the description of the RBC logic has been addressed, attention needs to be paid to the communication between the RBC and the train. In a real application, it is not possible to send and receive information continuously, so the simulator mimics this aspect by adding a discretization to the input/output ports of the RBC. It's possible to set the discretization time independently for each communication front between the RAB and the trains. In practice, this could be obtained through a zero-order hold block, which lets the input signal pass only at regular points in time, called sample times, while in the intervals between them, it holds the value of the signal at the last step, i.e., at the last sample time.

Aiming at the realization of a real-time testing environment, however, this kind of block appeared to be incompatible with the real-time application equipment (for a description of said equipment, please refer to chapter 6). Thus, the discretization is implemented through a "fake" hold. As shown in Figure 3.11, a fake hold block is composed of a switch that closes on the continuous signal at regular sample time intervals (a different sample time can be defined for each communication front), while outside of those time instants, it closes on the value it let through last. It's important to notice that each sample time must be a multiple of the overall integration step, to avoid any asynchrony between signals.

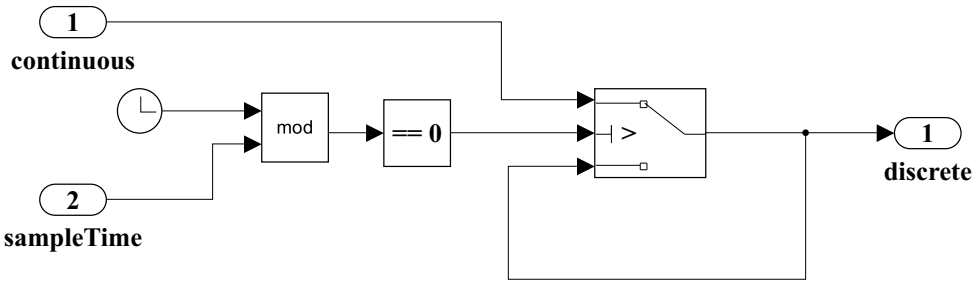

Figure 3.11: Fake hold block.

Once the RBC block and its operational rules have been described, in the following Section attention will be paid to the generation of the dynamic reference speed profile that the trains should follow, on account of both the railway line characteristics and the movement authority provided by the RBC, i.e., the d-MRSP.

3.2.3. Dynamic MRSP generation

When a train receives a green or yellow signal, the behaviour of the train doesn't change in terms of the forces applied to it or the logic that controls them. Instead, what changes is the reference speed curve. Indeed, in chapter 3.2.1 the static speed profile, or s-MRSP, was evaluated, on account of the line speed limits and the presence of stations along it, but disregarding the speed decreases induced by the signalling. To this end, a new signal should be generated, which consists in the dynamic most restrictive speed profile (d-MRSP). Note that in the block diagrams, a signal labelled simply MRSP will always refer to the d-MRSP. The dynamic MRSP generation block detects when a yellow signal is received, and it measures the speed and position of the train at that time instant. Then, it builds a curve starting from the current position at the actual speed and ending at the end of the block with null speed.

The curve describing the speed profile as a function of the position of the train s can be described according to a parabolic curve, as reported in Equation 3.15:

$$vlim_{brake} = \sqrt{2a_B \cdot (s_{block} - s) + v_0^2} \tag{3.15}$$

where s_{block} is the position of the start of the block the train is currently occupying, and v_0 is the speed measured at yellow signal detection.

The d-MRSP is then obtained according to the following procedure:

- if the train didn't receive a yellow signal, then the d-MRSP follows the s-MRSP;
- otherwise, the d-MRSP is evaluated step by step as the minimum between the s-MRSP and the $vlim_{brake}$ evaluated in Equation 3.15. Note that if the train received a yellow signal, but it is about a station, the d-MRSP still follows the s-MRSP, as it contains the speed curve to approach and stop at the station.

Figure 3.12 shows the graph of both the s-MRSP (solid black line) and the d-MRSP (dotted light blue line). The Figure represents a scenario which will be thoroughly described in Section 5.1.4, but to have a general understanding, it has been obtained by performing a FXB simulation in which the first train covers all stations on the line and the second

train covers only a subset of the stations on the line, namely the first four and the last one. Thus, the first train s-MRSP is the one represented in Figure 3.5, while the second train s-MRSP will prescribe stopping only at the aforementioned subset of stations (look at the s-MRSP between 400 s and 1000 s). However, the d-MRSP still prescribe additional stops and deceleration traits because of the impact of the signalling system (look at the d-MRSP after 1200 s). Each time the d-MRSP deviates from the s-MRSP, the second train has encountered a yellow signal light, making it slow down to prevent the violation of a red signal light.

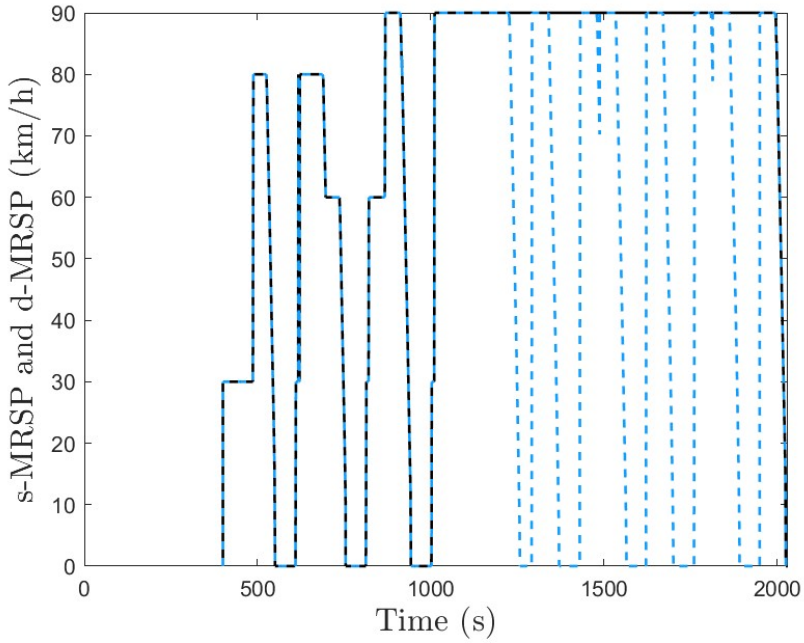

Figure 3.12: s-MRSP and d-MRSP.

3.3. Description of the vehicle and driver models

In the previous Section, the Trackside block has been explained thoroughly; now, attention will be paid to the *Train* block (recall Figure 3.1), which contains the model of the vehicle dynamics, the speed control algorithm and the driver's behavioural model.

The model of the vehicle dynamics considers the trains as a point mass to which all the relevant forces are applied. Three sources of force are considered: the motor, which can produce traction, braking or null force depending on the speed control system, the wheel-track contact and the aerodynamic drag, which generate a force component against the motion, and the gradient of the line, which generates a force component directed as or against the motion, depending on the slope of the line. As shown in Figure 3.13, these

components are summed algebraically to obtain the resultant force acting on the overall train, which will be later utilized to obtain its acceleration, and thus, speed and position.

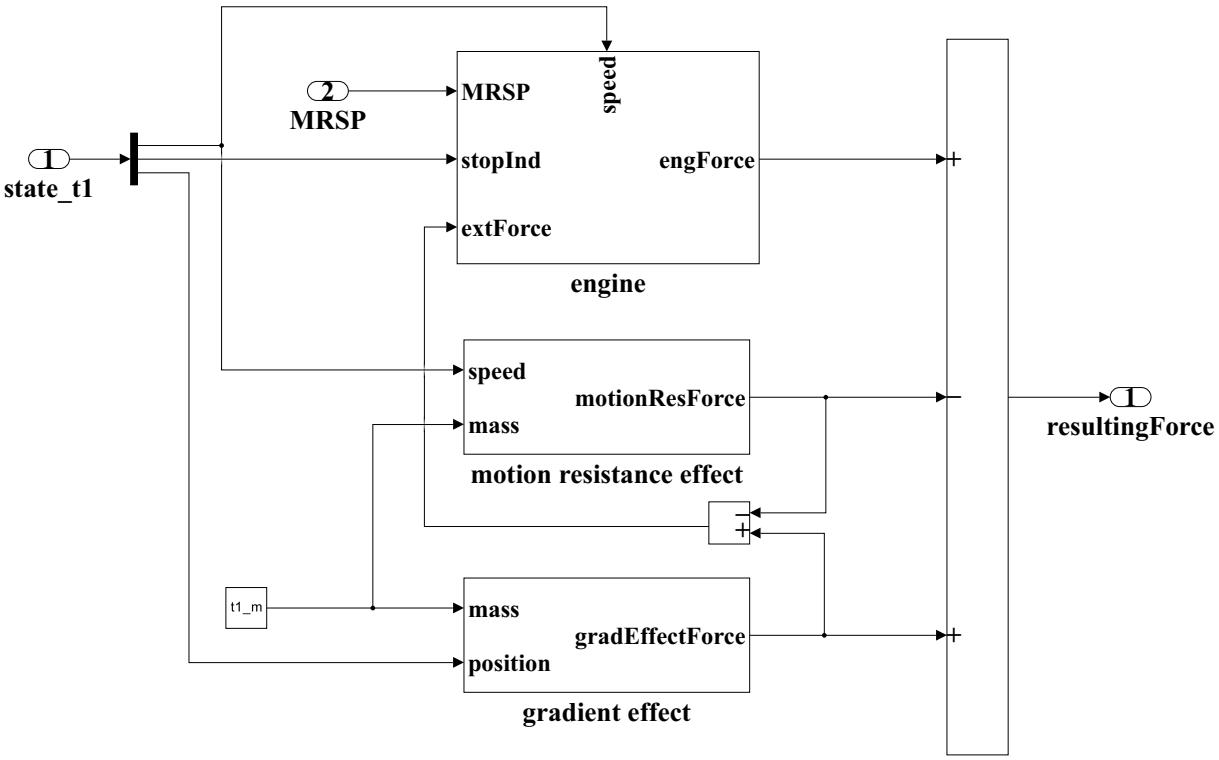

Figure 3.13: Vehicle model

Together with the mechanical parameters of the vehicle, also the driver's behaviour is introduced at this modelling stage. It is the main factor that determines the motor force component, both in its nature (traction, braking or coasting, meaning null) and magnitude. It is based upon the d-MRSP sent by the Trackside block, which acts as a reference for the driver.

3.3.1. Rail vehicle dynamics

This Section will expand on the force components listed in the previous paragraph, namely the motion resistance, the gradient effect and the motor-generated force.

The motion resistance includes both aerodynamical drag and wheel-track interaction. The former varies quadratically with the speed of the train, while the latter is modelled as friction with a constant coefficient, as shown in Equation 3.16.

$$F_{friction} = mg \ * \ \frac{{v_{kmh}}^2}{4500} \ + \ 1.5 \tag{3.16}$$

The gradient effect is modelled simply as the dynamics of an object on a tilted plane. The slope of the plane is obtained through a look-up table that associates an incline to each point on the line, given in per-thousands, and is controlled by the train position. The sign of the slope, as well as of the gradient effect force component, will be positive in downhill segments (in favour of the motion) and negative in uphill segments (in opposition to the motion).

$$F_{gradient} = mg * sin(\alpha) \tag{3.17}$$

Note that Equations 3.16 and 3.17 resemble Equations 3.6 and 3.7, which were presented in chapter 3.2.1 for the external deceleration components. The difference is the fact that in Equations 3.6 and 3.7 the speed used in the computation was the maximum one permitted on the whole line, while in Equations 3.16 and 3.17 the speed used is the current one. Also, as they evaluate forces rather than acceleration, Equations 3.16 and 3.17 include the mass of the train as well.

As for the motor force, it can be divided into traction and braking case. The force depends on the current speed of the train as shown in Equations 3.18 and 3.19:

$$F_{trc} = \begin{cases} \frac{325*40}{v_{ms}} * 10^3 & \text{if } v_{kmh} > 40 \\ (427 - \frac{427-325}{40} * v_{ms}) * 10^3 & \text{otherwise} \end{cases} \tag{3.18}$$

$$F_{brk} = \begin{cases} (419.5 - 187.5 + \frac{187.5*84}{v_{ms}} * 10^3 & \text{if } v_{kmh} > 84 \\ 419.5 * 10^3 & \text{if } 0 < v_{kmh} < 84 \\ 0 & otherwise \end{cases} \tag{3.19}$$

These formulas identify the maximum force that can be generated at a certain speed, i.e., the force characteristic curve depending on the speed: $F(v)$. However, the actual force could be anywhere below that limit. In practice, the motor force is multiplied by a coefficient of usage, meaning that the driver may push the train with only a fraction of the possibly achievable force. The evaluation of this coefficient will be covered in Section 3.3.2, devoted to the driver's behaviour.

To simulate the train behaviour more realistically the model of the train dynamics also include the possibility of actuating the emergency brake. In critical scenarios, the emergency brake overrides the motor force. Its value is constant and equal to the maximum

braking force deliverable, as shown in Equation 3.20:

$$F_{emergBrk} = 419.5 * 10^3 \ N \tag{3.20}$$

The overall resulting force on the train will be the algebraic sum of these three components. Thus, Equations 3.21 and 3.22 summarize the current modelling approach:

$$F_{mot} = \begin{cases} F_{trc} & \text{if command traction} \\ -F_{brk} & \text{if command braking} \\ 0 & \text{if command coasting} \\ -F_{emergBrk} & \text{if issued emergency brake} \end{cases} \tag{3.21}$$

$$F_{res} = F_{mot} - F_{friction} + F_{gradient} \tag{3.22}$$

Figure 3.14 shows the force characteristic with respect to train speed for traction and service brake. The vertical lines divide the various working regions of the characteristics.

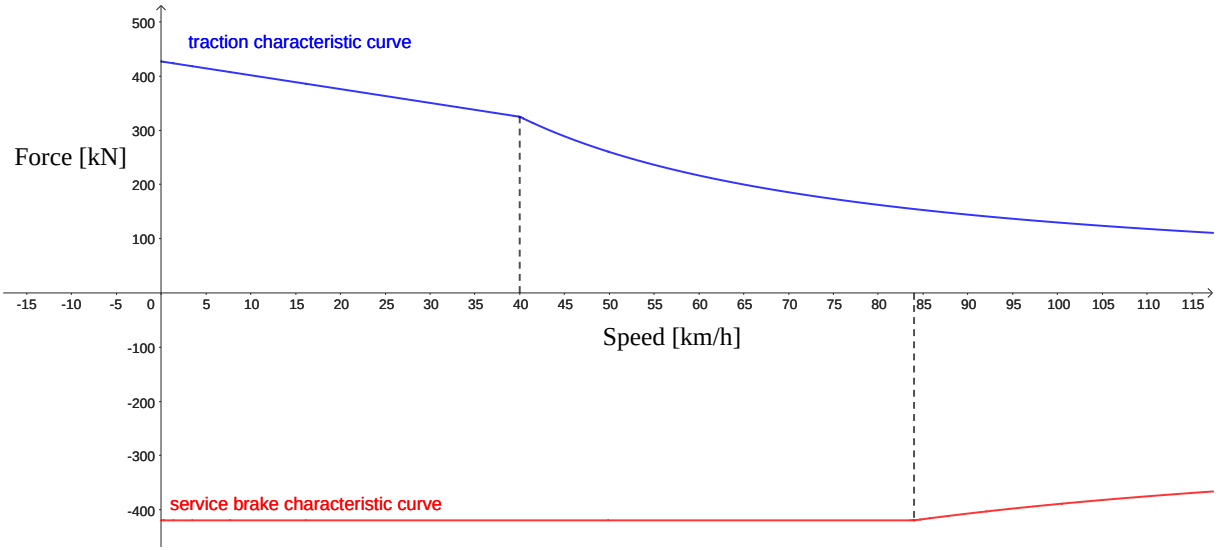

Figure 3.14: Force characteristic with respect to speed

Once the train dynamics model has been described, in the next Section attention will be paid to the driver's behavioural model.

3.3.2. Model of the driver's behaviour

This aim of this module is to mimic the main aspects of the driver's behaviour in specifying the commands that the train has to follow, namely traction, braking and coasting, based

on the speed reference profile provided by the RBC, i.e., the d-MRSP. Note that for brevity, it will be referred to as just MRSP.

To this end, it is useful to define the reference curves built upon the MRSP for speed control execution. The general idea is to provide an upper and lower limit around the MRSP so that an ideal driver will manually command braking and traction making the speed vary inside that range without needing any automatic response from the train. Thus, the Warning Curve (WC) and the Lower Curve (LC) are defined respectively above and below the MRSP through a constant asymmetrical offset (meaning that the difference between WC and MRSP could be different from the difference between MRSP and LC). When the speed reaches the WC, the driver will be alarmed with a warning signal (WS). An ideal driver is reactive enough to switch between traction and braking as soon as they hear the warning signal.

However, it may happen that a realistic driver will not react immediately to the exceedance of the WC, making the speed increase indefinitely. Thus, additional limits are needed to account for realistic driver behaviour. These limits will serve as thresholds for the automatic intervention of the brakes. Thus, the Service Brake Intervention (SBI) and the Emergency Brake Intervention (EBI) are defined, both obtained through other offsets above the MRSP (of course, at any time instant it will be $WC < SBI < EBI$). If the speed reaches these curves, the train automatically issues the relative braking force, overcoming the driver's directives.

The offset between MRSP and LC is defined arbitrarily by the driver, and it identifies their tendency to travel below the speed limit, i.e. it's a parameter of the driver's model. A conservative driver will consider a wide margin below the MRSP, and vice versa for an aggressive one. The other curves are defined at prescribed intervals from the MRSP, independently from the driver's behaviour, thus, they are not parameters of the driver's model. However, they still contribute to the speed control of the train and become relevant in critical scenarios. Figure 3.15 shows all the reference curves previously described for a motion over four stations.

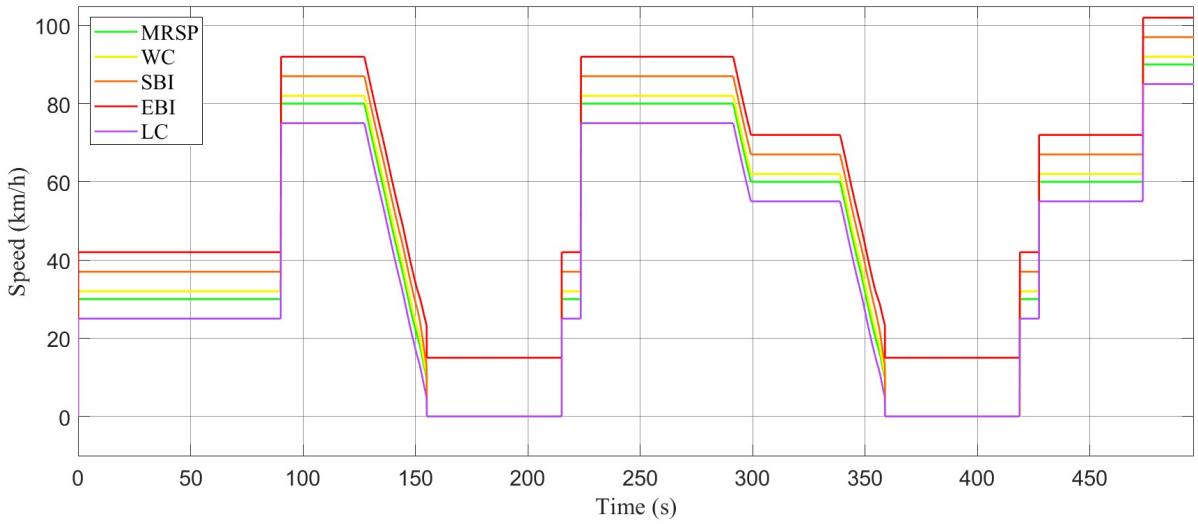

Figure 3.15: Reference speed curves.

Inside the nominal speed control range, i.e., LC-WC, the speed is controlled as follows:

- once reached the LC, the driver will command traction;
- the speed will increase, and upon reaching the MRSP, the driver will command coasting. The speed will vary depending only on the motion resistance (which will make it decrease) and the gradient of the line (which instead may make it increase or decrease at different points on the line).
- then, the train will move according to the external forces, namely the motion resistance component, which will always decelerate the train, and the gradient effect component, which will accelerate or decelerate the train depending on the slope of the line.
- if the external forces result in a negative component, the train will slow down back to the LC;
- otherwise, the train will accelerate to the WC, making the driver command braking all the way down to the LC.

This algorithm is shown in Figure 3.16, which represents the state chart of the driver's behaviour inside the nominal speed control range. Each rectangle, representing the state of the train in terms of speed range with respect to the reference curves, contains the action performed by the driver when that state is reached. The arrows connecting the rectangle represent the transitions between states, and they are labelled with the associated condition. Notice that when the speed reaches the MRSP-WC range, the driver does not command anything, meaning that the last command will remain active also in

this range. Finally, if the speed reaches the WC, the driver commands braking until the speed decreases below the MRSP (and not just the WC).

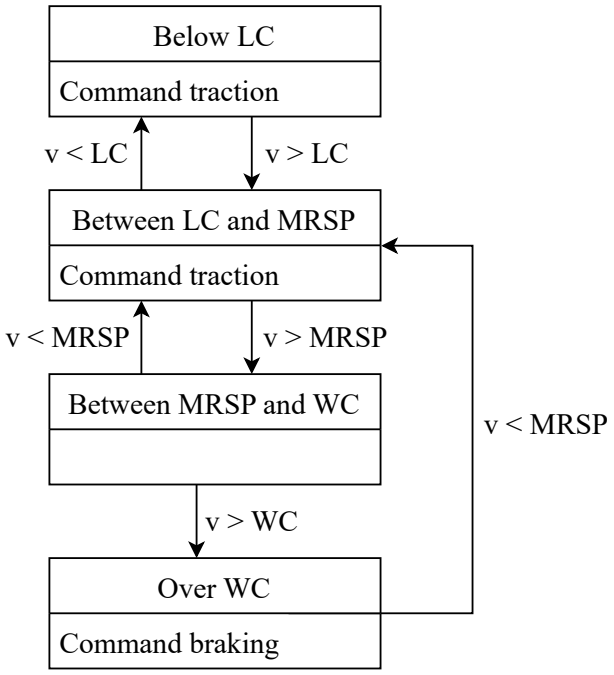

Figure 3.16: Driver's behaviour statechart

As previously stated, when the speed reaches the WC the braking force is not activated automatically, but rather a warning signal (WS) is sent to the driver. The behavioural model of the driver includes the possibility that they do not answer immediately to a WS, through the use of a probabilistic approach.

The driver is characterized by a base probability of reacting to the WS, which may be different between steady or decelerating motions, to simulate the fact that during a deceleration (decreasing MRSP), the driver will surely be at the board, so they will respond to a WS compared to cruise when they could be attending other tasks.

When the WS is issued, the driver's reaction probability starts to increase with a linear trend, up to 100% in a prescribed time. The model describes mimics the fact that the longer the duration of the WS, the more likely the driver will respond to it.

By tuning the base probability to be high enough, or the time needed for the probability to reach 100% to be short enough, it is possible to simulate the case in which the driver always commands service brake before the speed increases too much over the WC. On the other hand, by reducing the base probability or elongating the time of it reaching 100%, it is possible to include the cases of the speed increasing significantly over the WC. Therefore, other thresholds are needed to be reactive to such cases, namely the Service

and Emergency Brake Intervention (SBI and EBI) already introduced in the previous paragraphs.

A conservative driver will be highly reactive to any warning signal, meaning that their base probability both in cruise and deceleration will be high and the time for it to reach 100% will be short, to the point that it's impossible for the speed to reach the SBI. A case like this one is represented in Figure 3.17, where the actual speed varies inside the LC-WC range at all times. Vice versa, an aggressive driver will be characterised by a low base reaction probability and a high time for it to reach 100%. Note that it is possible to consider a relatively aggressive driver while still ensuring the non-exceedance of the SBI caused by their unreactivity towards warning signals.

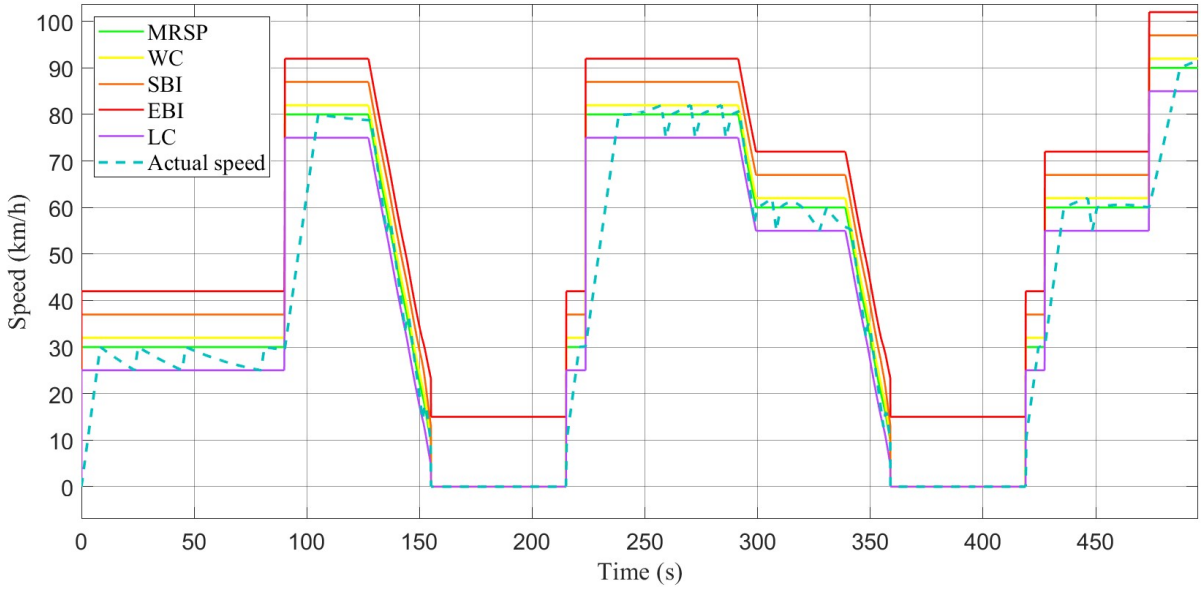

Figure 3.17: Reference speed curves and actual speed. Figure obtained from the same simulation as Figure 3.15.

Outside of the LC/WC range, the speed control is automatic. When the speed reaches the SBI the service brake is issued immediately, slowing the train down to the LC; then the driver regains control over the motor force.

If the SBI doesn't manage to slow the train down, its speed will reach the EBI. In this scenario, instead of immediately issuing the emergency brake, which should be used as the last resort, coasting is issued, and a timer starts. At the end of it, if the speed has not decreased below the EBI, the control system issues the emergency brake, which brings to a complete stop of the train. Clearly, this only happens in critical situations, as it requires the service brake to be broken, or the MRSP to decrease very steeply for unexpected reasons. Thus, during an emergency brake, the train decelerates with the

maximum force regardless of the actual speed, as shown in Section 3.3.1. Thus, also the deceleration during an emergency brake will be constant. Finally, the constraint on maximum deceleration equal to 1 ms^{-2} is removed during emergency brakes. When the train is stopped by an emergency brake, the model considers it unable to start the motion over, meaning that it will spend the remaining simulation time still in the spot where it stopped.

Another aspect of the driver's model is the usage of the force characteristic curve. As previously stated in Section 3.3.1 (recall Equations 3.18 and 3.19 and Figure 3.14), the equations that link velocity to force (both tractive and braking) draw a characteristic curve which is the upper limit of the functioning region, meaning that the actual force that can be imposed by the motor could be anywhere below that curve. This is modelled by multiplying the force by a coefficient, which can be modulated by the driver, depending on the situation and their own general attitude: a conservative driver will use a low coefficient for traction and a high one for braking, and vice versa for an aggressive one. Also, this coefficient varies depending on the gradient of the line at any point, meaning that the driver will be inclined to approach the limit traction force more closely during an uphill segment rather than a downhill one, and vice versa for the braking force.

In the last Section, the driver's behavioural model has been described, as well as the general speed control system. This concludes the description of the train motion model, which included the dynamics model and the driver's behavioural model. The output of the *Train* block is the resultant force acting on it, which will later be used to evaluate its acceleration and later, speed and position through integration. This is performed in the *Output manipulation* block, described in Section 3.4.

3.4. Evaluation of the train states

The *Output manipulation* block is the one that performs the manipulation of the force acting on the train to evaluate the states of the trains, i.e., the sets of information to convey to the RBC. This manipulation includes the following steps:

- evaluating the train acceleration given its mass and the resultant force acting on it;
- evaluating the train odometry of the train via numerical integration, i.e., the integration of the acceleration to obtain the speed and position of the train;
- applying a model of the position drift and its correction through the balise model;

- performing a discretization of the space in blocks and evaluating their occupancy;
- determining an indication of when the train stops completely so that the simulator can handle those scenarios correctly.

Before going on with the description of the single components mentioned in the previous list, it is useful to show a typical graph that represents the position of the train with respect to time, alongside a graph that represents the speed of the train in the same time interval, as shown in Figure 3.18.

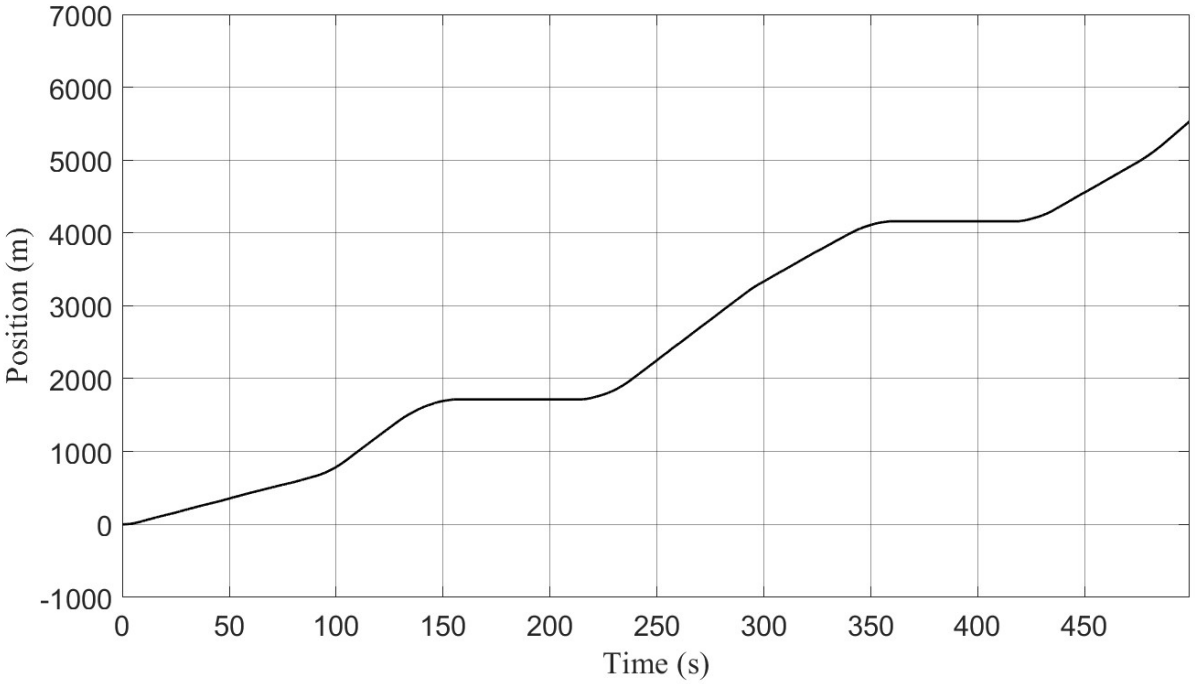

Figure 3.18: Position over time. Figure obtained from the same simulation as Figure 3.15 and 3.16.

As expected, in the segments where the speed is constant (or better, varying in a small interval around a constant MRSP), the position increases linearly, while in the segments where the speed is null (for instance, due to the stop at a station) the position is stationary. These two segments are connected smoothly as the speed doesn't change instantaneously but follows the train dynamics.

The next Sections will be devoted to expanding the components of the output manipulation block mentioned before. The evaluation of the acceleration, speed and position of the train, as well as the application of the drift model and subsequent correction will all be covered in Section 3.4.1, while the block occupancy evaluation and the determination of the stationarity periods of the train will be covered Sections 3.4.2 and 3.4.3 respectively.

3.4.1. Calculation of the train position

The evaluation of the train position is carried out in two phases: first, the computation of the exact position through double integrating the acceleration; then, the addition of the drift error and the subsequent correction to obtain the measured position. These two quantities are used for different scopes, as the exact position is useful to evaluate the external physical phenomena that act on the train, such as the force applied to it by the slope of the line, while the measured position is the one reported to the RBC, thus, it is the one considered in evaluating the block currently occupied by the train, as well as to control the reference speed look-up table (please recall Section 3.2.1, Figure 3.5) to generate the s-MRSP.

At first, attention is paid to the computation of the train exact position along the railway line. To this end, the force provided by the motor at any time instant is considered, to compute the corresponding acceleration (given the mass of the vehicle). Then, the position is computed by double integration of the acceleration signal. The procedure is iterated for the entire trip.

As previously mentioned, the upper limit of train acceleration is imposed by a constraint on passengers' safety and comport to 1 ms^{-2}, exception made in the case of emergency brake, when this constraint is disregarded and the maximum achievable acceleration is considered for safety reasons. The speed is saturated to a lower limit of 0 ms^{-1}, meaning that the case of the train going backwards is not considered. In addition, it is hard-constraint to 0 ms^{-1} when a full stop indication signal is received (please refer to Section 3.4.3 for a detailed explanation of this signal).

Secondly, attention is paid to the computation of the position that the train measures. To this end, a disturbance is added to the exact position, which will later be compensated through the use of the balises. Indeed, the integration inherently carries some error on the position, called drift. This could be simulated thoroughly by introducing a model of its causes, such as pseudo-slipping of the wheels. Given the simplified modelling choice, the drift error has actually been introduced as a black box disturbance that augments the position at every integration step. This starts at 0 at the beginning of the simulation and increases like a ramp with time.

To compensate for this error, the balises have been introduced, which were presented in Section 3.1.1. Each time the train passes on a balise and receives its information in terms of position along the line, the current train position is updated to match the one provided by the balise, which is assumed to be the exact one. Thus, the error added to obtain the drifted position is reset to 0, starting a new error ramp. In this way, the position detected

by the train is obtained, as shown in Figure 3.19.

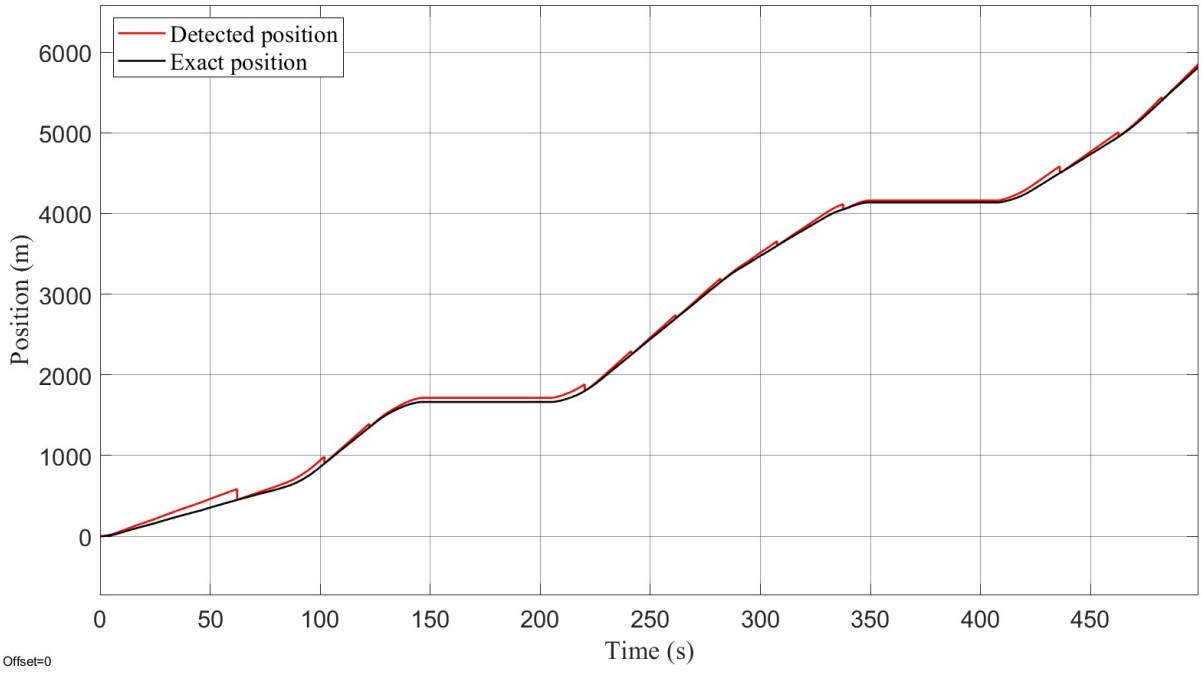

Figure 3.19: Exact and detected position, i.e., the one obtained after applying the drift error model and the balise correction model. Figure obtained from the same simulation as Figure 3.15, 3.16 and 3.17.

3.4.2. Block occupancy evaluation

Once the accurate positioning of the train along the railway line has been obtained, attention is paid to the working rules of the fixed block signalling system. Indeed, the input of the RBC is not the train position along the line, but only the information on which block it is occupying. To obtain the block occupancy, a discretization of the line is performed based on the length of the block, dividing the line into blocks with a set length equal to FBL (recall chapter 3.2.2 for its evaluation). By comparing the position of the train with the block ends, the block occupied by the train can be identified. Thus, the result of this computation is an integer specifying the bloc occupancy of the train.

It's important to remark that a block is occupied by a train even if just a portion of it is inside the section at issue. This means that as soon as the front end of a train enters a new block, or as long as its rear end doesn't leave it, that block is occupied. Thus, one train can occupy two subsequent blocks simultaneously. However, the information on the occupancy of the front and rear end of the train have different scopes:

- the front end of a train is used to evaluate the coloured signal light it receives from

the observation of the following blocks;

- the rear end of a train is used to let the RBC decide the coloured signal light to show the trains following it.

As a result, the RBC handles the communication between just two trains only based on the rear end of the first one and the front end of the second one.

In Figure 3.20, the block occupancy of the train is presented, as well as its continuous positioning inside the block, which is obtained by normalizing the position of the train with respect to the block length. (remark: the positioning is useful just for visualization purposes, as it is not sent to the RBC).

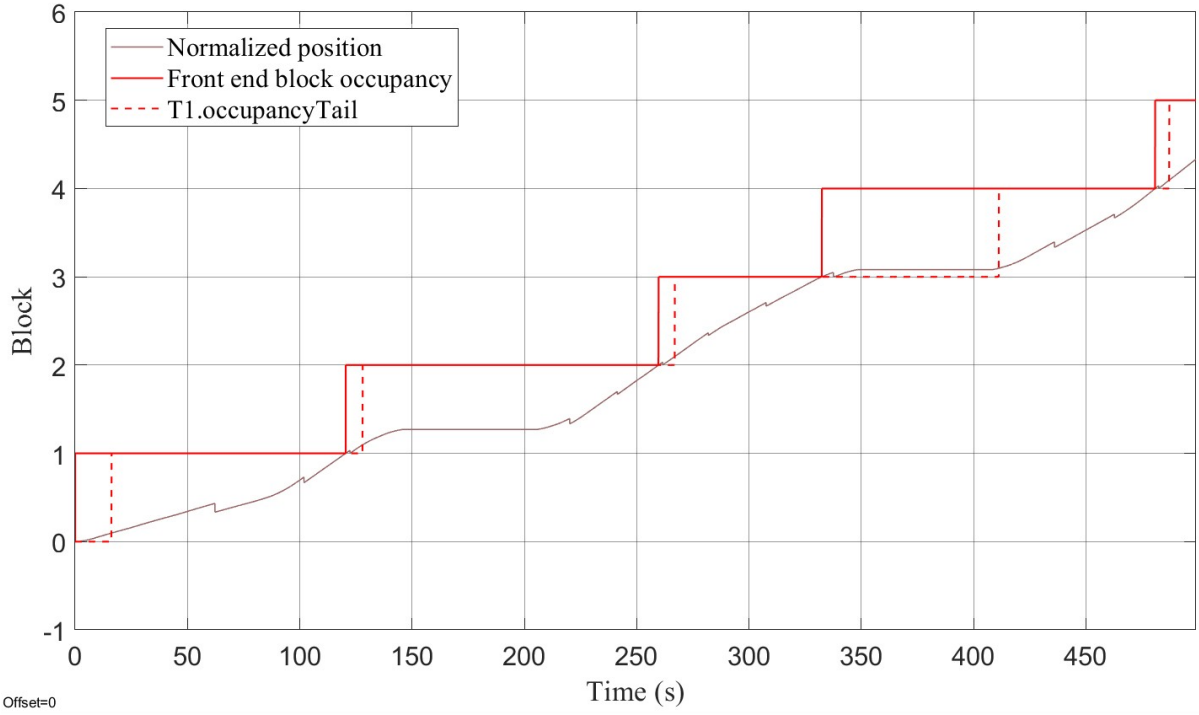

Figure 3.20: Front and rear end block occupancy and normalized position. Figure obtained from the same simulation as Figure 3.15, 3.16, 3.17 and 3.18.

3.4.3. Full stop indication

Once evaluated the block occupancy, the train and RBC can communicate correctly, and thus, the simulation can be run. In particular, the current modelling strategy allows to reproduce correctly the behaviour of two trains travelling in sequence on the line, interacting with each other through the RBC. However, at this stage the train stops cannot be modelled yet, either in correspondence of a station or after a deceleration curve

dictated by the coloured signalling, i.e., the trains are not able to fully stop and maintain null velocity for the required time, as what actually happens in these cases is that the speed oscillates around zero.

The reason behind this problem lies in the definition of the dynamics of the train: the braking action is a force oriented opposite to the motion, with a magnitude defined by its characteristic curve. At negative or null speeds, the braking force is identically zero, but at positive, however low, speeds it holds a constant value, as described in Equation 3.19 and shown in Figure 3.14. When the train is approaching a stop, the driver will command braking and the speed will decrease, potentially down to a negative value. As previously stated, the speed is saturated to be at least 0 ms^{-1}, but that saturation happens after the integration of the acceleration, so if the speed holds a negative value, that is visible to the driver. Then, as the speed has decreased below the Lower Curve (which in case of a full stop is identically 0), commands traction. Thus the speed reaches positive values again, the driver commands braking and the cycle starts again.

The adopted solution is to consider a Boolean signal that indicates when the train must stay still, called *stopIndicator* in the current model. This signal works on both the force and speed control sides. When the indicator is true:

- on the motor side, it sets the motor force to be opposite to the algebraic sum of the external forces (gradient effect and motion resistance). In this way, the resultant force is 0, as well as the acceleration, and the speed remains constant until the stop indicator keeps the true value;
- on the speed control side, it sets the speed to 0 ms^{-1}. Otherwise, if at the reception of a true stop indicator the speed was not 0 ms^{-1} because of the fluctuations around 0 ms^{-1} described earlier, it would remain constant at the last value it held, and not at 0 ms^{-1}.

.

To obtain this signal, we look at the possible causes of stops of the train, namely being at a station or having received a yellow or red signal for long enough. If either one of these causes is true, and the MRSP is low enough, the stop indicator becomes true. As soon as the cause of the stop ceases to be valid, or the MRSP increases over a threshold, the stop indicator turns back to false. Figure 3.21 shows how the block related to the generation of the stop indicator works. In particular, notice the input signal called *stationProximity*, which is another boolean variable that becomes true when the train is about a station. This signal is provided by the *Trackside* block, as shown in Figure 3.1, and in particular,

it is evaluated at the static MRSP generation stage.

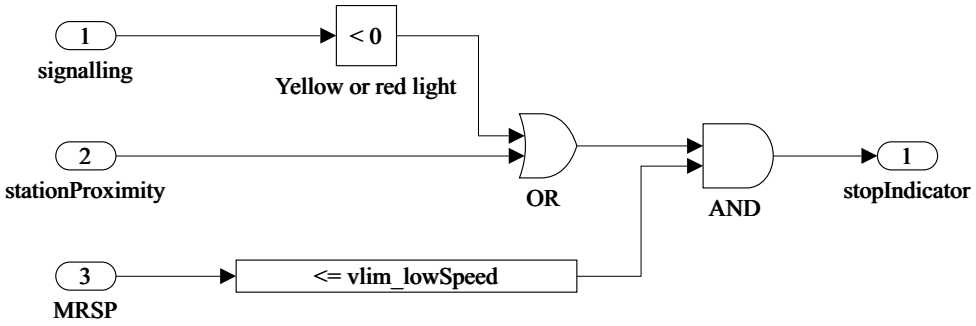

Figure 3.21: Stop indicator block diagram.

3.5. Final remarks

In conclusion, this Chapter has been devoted to describing the components of the simulation environment built to simulate the behaviour of two trains travelling on a line. To summarize, its main features are the generation of the reference speed curves, the definition of the RBC as an intermediary in the communication between the trains, the handling of the interaction of the vehicles travelling on the line through the coloured signal lights system and the model of the trains in terms of their dynamics, their automatic speed control system and their driver's behaviour. In the following Chapter, the modification to the simulation environment necessary to reproduce a moving block signalling system will be presented.

4 | Simulation environment for moving block signalling systems

This chapter presents the changes made to the simulation environment to suit the adoption of the moving block (MVB) signalling approach.

4.1. Introduction

The model works similarly to the one presented in Chapter 3 in most of its parts, especially for what concerns all the components that strictly relate to the train (its dynamics, the driver's behaviour and the odometry). The major differences appear in the radio block center (RBC) model, as:

- it must be able to handle continuous valued signals indicating the positions of the trains, instead of discrete block occupancies (note that time discretization still occurs to represent the communication discontinuity between train and RBC);
- it must evaluate and continuously update a safety distance to be maintained between the trains, based on their current speed and position;
- it must evaluate the movement authority not in terms of a set of coloured signals to be shown to the following train, but rather an indication of its distancing from the leading train, compared to the safety distance previously evaluated.

It is worth mentioning that the safety distance is not to be intended as uninfrangible, meaning that it is allowed for the second train to violate it. In fact, the safety distance is evaluated so that when a violation happens, a deceleration curve is imposed on the following train so that the collision would be prevented even in the (unrealistic) case where the leading train stops in the very same place of the last recorded position. In this sense, the possibility to violate the safety distance can be regarded as dual to the reception of the yellow signal light in the fixed block signalling system.

Another notable difference is that verification about the train integrity is performed on the train itself. It is here reminded that train integrity is verified when no wagon has detached from the main body of the train. Thus, integrity can and must be handled by the simulator, meaning that if the first train reports a loss of integrity, the second one must be able not to collide with the detached wagon.

The following differences complete the description of the MVB approach simulation environment:

- even though the balises are still considered in the model, their role is significantly reduced as they are considered just to verify the train position. In fact, in MVB systems, the position evaluated on board vehicle must comply with stricter accuracy requirements than in FXB ones.
- the block occupancy must not be evaluated anymore, as the state of the train is reported to the RBC directly in terms of its position;
- all conditions previously based on the signalling are now based on the safety distance observation. For example, recalling Section 3.4.4, one of the stop indication causes was having received a yellow signal for long enough; now it will be having violated the safety distance for long enough.
- while in FXB systems entering a red-signalled block would automatically issue the emergency brake, there is no equivalent way to do so by confronting the actual and safety distances of the trains; the emergency brake is still triggered if the speed exceeds the Emergency Brake Intervention for more than a prescribed timer.

Figure 4.1 contains the simulation environment developed for the MVB approach model. As expected, it is similar to Figure 3.1, but some high-level differences can be already noted, such as the $d/dmin$ signal being sent from the Trackside 2 block instead of the *signalling* one, and the state of the two trains containing their positions instead of their block occupancies. The signal $d/dmin$ contains both the actual distance and the safety distance as sub-signals.

Once the main differences between FXB and MVB simulation environments have been brefly presented, they will be extensively described in the following Sections. Specifically, Section 4.2 will be devoted to the handling of the train integrity, a feature that was not present altogether in the FXB environment, as it was not required.

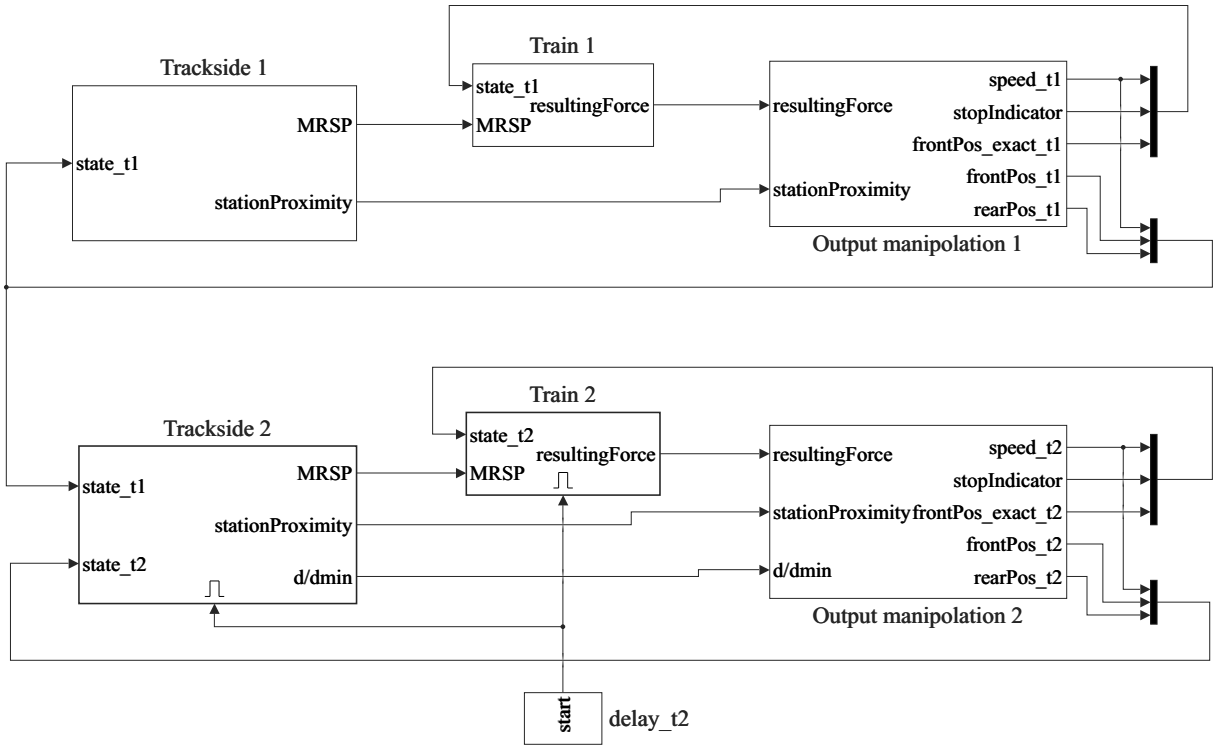

Figure 4.1: MVB approach simulation environment overview. Notice that the *Trackside 2* block reports the signal *d/dmin* instead of *signalling* to the *Output manipulation 2* block .

4.2. Handling of train integrity

The first component to describe is the one related to train integrity. The procedure can be split into two parts:

- first, the generation of an indicator stating whether integrity is confirmed, i.e. whether the train realizes a unique piece;
- then, the communication of this indicator to the RBC so that it generates the movement authority for the following train considering this critical occurrence.

Note that only the integrity of the first train is considered in the model, as compromising the integrity of the second train would not affect the simulation results, as there are no vehicles following it.

The integrity signal comes from the circuitry on the whole train: if integrity is lost, the circuitry gets broken and the error can be identified. In the model, the signal is a boolean variable generated virtually in the *Train* block with the meaning expressed in Equation

4.1:

$$\text{integritySignal} = \begin{cases} 1 & \text{if train 1 integrity is confirmed} \\ 0 & \text{otherwise} \end{cases} \tag{4.1}$$

Confirmed integrity means that the rear end of the train follows the front end, shifted back of the train length. Not confirmed integrity means that a wagon may have detached from the main body of the train. When a wagon detaches from the train, its residual movement is not considered, and it is modelled to stay still in the place in which it detached. In reality, inertia may cause the wagon to move in the direction of motion for some distance, and the track gradient may then cause some acceleration (in either direction) even without the connection to the motor. These phenomena are not considered for modelling simplicity, but also because this approach is the most conservative, as we consider the wagon to stop immediately in place, leaving the least space for the second train to decelerate and stop in time.

The integrity signal is always initialized at 1. As mentioned before, and reported in Equation 4.1, a step to 0 of this boolean variable means a loss in the integrity of the convoy. Most commonly, however, it is due to a communication error, meaning that the wagon has not actually detached, but the control system did not receive confirmation of its presence. Thus, it is possible that the integrity signal steps back to 1, meaning that integrity is restored: the previous communication error has been resolved. The case with integrity loss and further restoration is the most interesting one from the signalling point of view: without integrity restoration, the second train sees the first train rear end stuck in place for the rest of the simulation. On the other hand, with integrity restoration, the second train can resume motion when the way becomes free. When integrity is restored, the rear end of the train reverts to its nominal position instantaneously, i.e., behind the front end, distanced as the train length.

In practice, the effect of an integrity loss is that the rear end of the train stops moving until integrity is restored, as shown in Figure 4.2: when integrity loss is detected, the current rear end position of the first train is detected and conveyed as the actual rear end position until the integrity is not restored; when integrity is restored, the actual rear end position returns to its nominal condition.

In Figure 4.3 the integrity signal for the first train and the position of both trains (regarding rear and front end) are shown. The simulated scenario considers two trains travelling on a line with no stops or velocity change points, thus maintaining a constant reference speed for the whole travel. At time $t_0 = 300s$ the integrity is lost (integrity signal steps to 0 from its initial value of 1), so the rear end of the first train stays still at its last

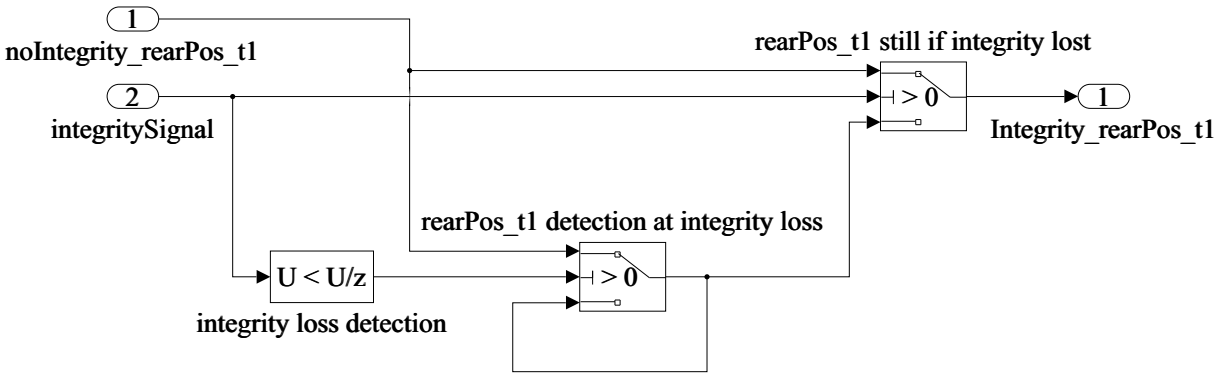

Figure 4.2: Integrity signal handling block

recorded position until integrity is recovered. Therefore, in accordance to the safety distance observation, the second train slows down and eventually stops not to collide with the detached wagon. At time $t_1 = 400s$ the integrity is restored (integrity signal steps back to 1), so the rear end of the first train recovers the space lost and positions itself at its nominal position (behind the front end according to the train length). Then, the second train can start accelerating, reaching again the reference constant speed.

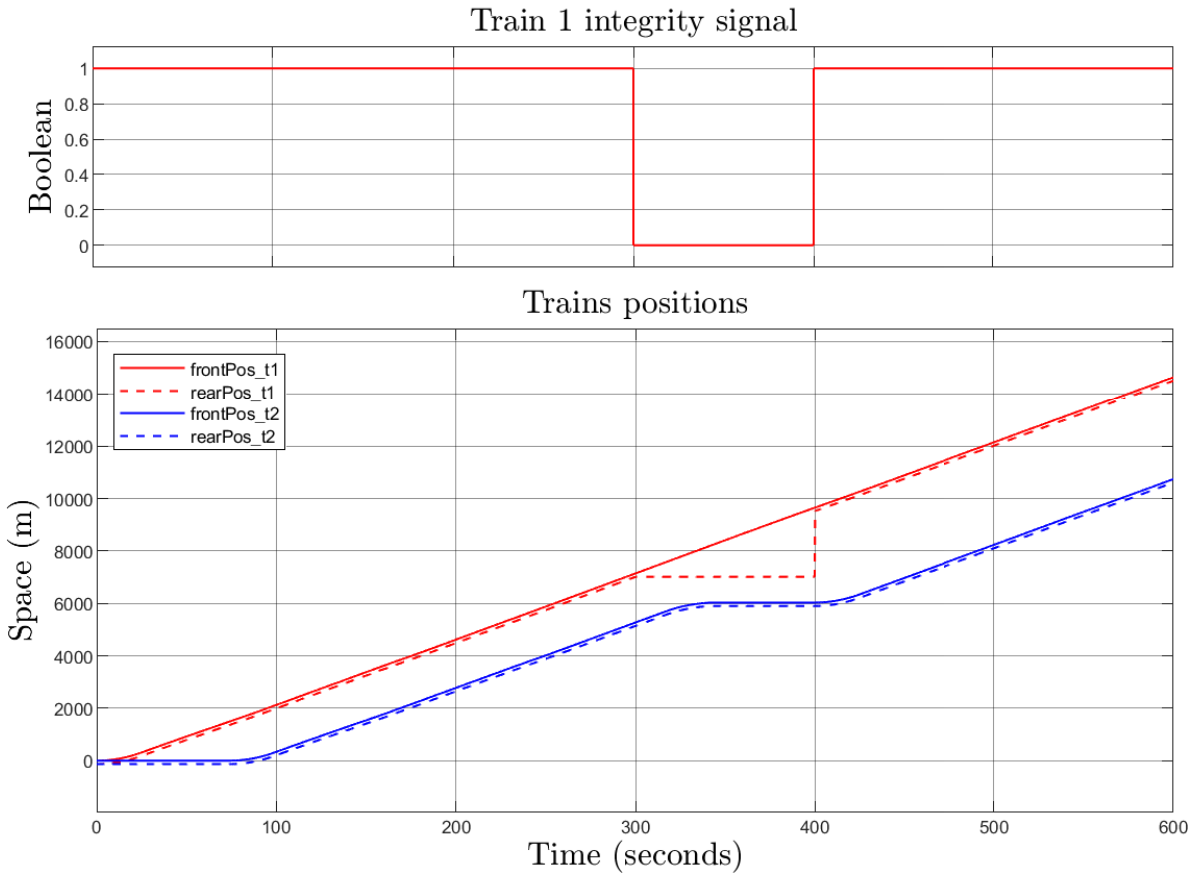

Figure 4.3: Integrity loss and restoration

In this Section, the modelling strategy adopted to allow the simulation of the loss of integrity has been presented together with the strategy to handle the cases of compromised integrity. Thus, the position of the rear end of the first train conveyed to the RBC is the one computed after the integrity verification and handling, so that the second train movement authority can be evaluated correctly.

4.3. RBC

This Section is devoted to describing the modifications made to the RBC to suit a MVB environment. The RBC component is the one that underwent the most changes, as it contains the main features of the signalling system, being the coloured signal lights for the FXB system and the actual and safety distances evaluation and comparison for the MVB one.

As shown in Figure 4.4, the RBC now takes as inputs the states of the trains, containing their positions (regarding both front and rear ends) and speeds, and returns the actual and safety distance of the trains, as well as the position and speed of the second train at the instant when the safety distance is violated. The rear end of the first train is the one obtained considering the train integrity in accordance to the strategy presented in Section 4.2. Each input and output signal is discretized through the use of hold blocks as described in Section 3.2.2. The RBC performs three main operations: distance evaluation, safety distance evaluation and state detection in case of safety distance violation.

The first operation performed by the RBC is to evaluate the actual distance between the trains. This is performed in the yellow-shaded area of the diagram by subtracting the position of the second train front end from the position of the first train rear end.

The second operation performed by the RBC is to evaluate the safety distance between the trains. This is performed in the green-shaded area of the diagram. This yealds to:

$$d_{safe} = S_a + S_r + S_o \tag{4.2}$$

where S_a, S_r and S_o hold the same meaning as the symbols presented in Section 3.2.2 on fixed block length evaluation, i.e., stopping distance, space travelled during the driver reaction time and safety margin. The difference is that in the fixed block case the evaluation was performed once for the whole simulation, considering the most critical scenario that could occur during the motion (for example, the stopping distance was evaluated using the highest permitted speed $vlim_{max}$). In the case of MVB system, on the other hand, the evaluation is performed with the actual quantities (following the same example,

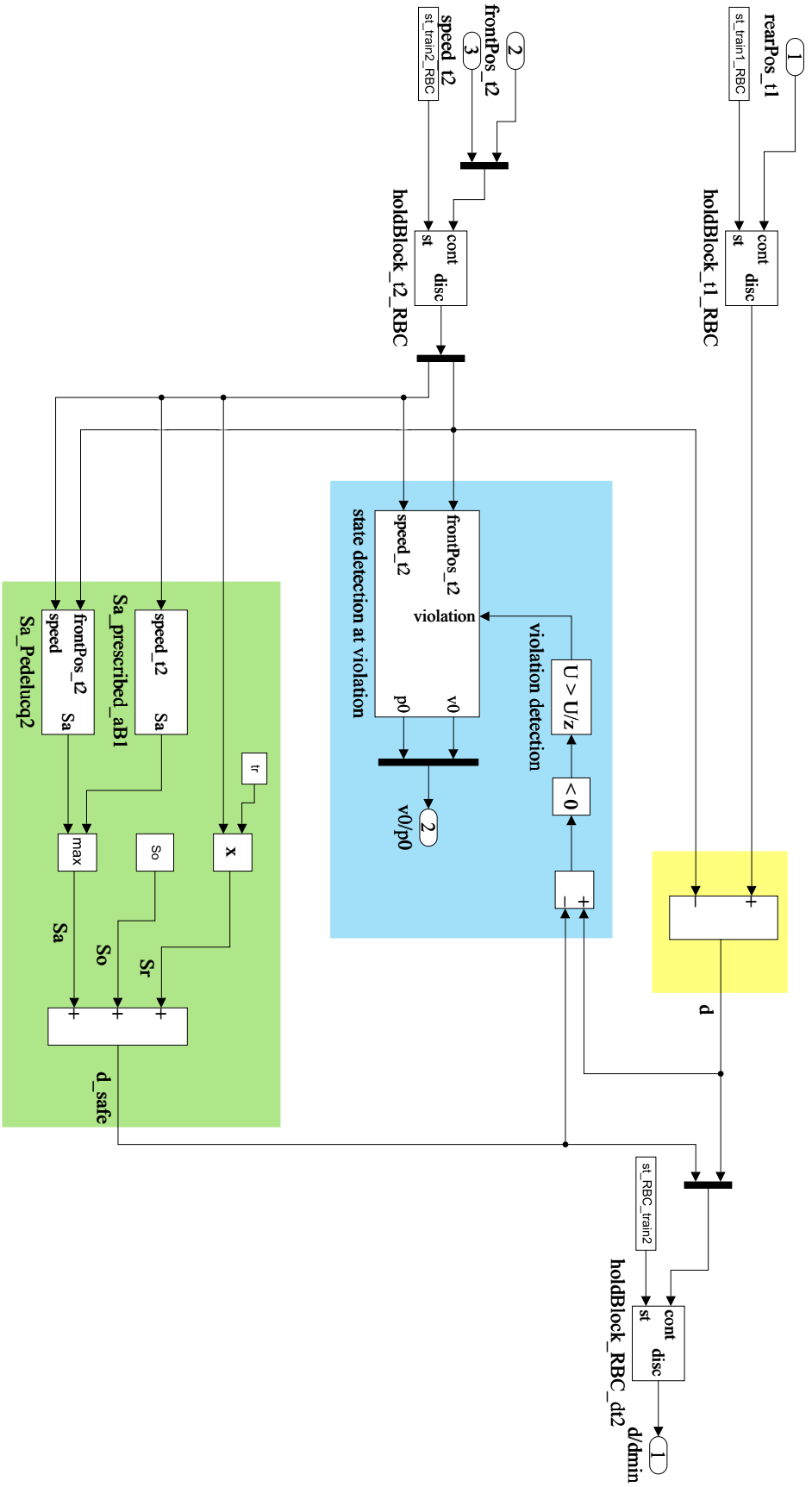

Figure 4.4: RBC block. In yellow: actual distance evaluation; in green: safety distance evaluation; in light blue: state detection at violation

the current speed of the second train v is now used for the stopping distance evaluation).

Thus, these quantities will have the following expressions:

$$Sa_{uniformDeceleration} = \frac{v^2}{2\ a_B} \tag{4.3}$$

$$Sa_{Pedelucq} = \frac{v^2}{(1.09375\ *\ \Lambda_C\ +\ 0.127)\ /\ \varphi(v)\ +\ 0.235\ *\ i(s)} \tag{4.4}$$

$$S_a = \max(Sa_{uniformDeceleration}, Sa_{Pedelucq}) \tag{4.5}$$

$$S_r = v_{ms} * t_r \tag{4.6}$$

$$S_o = 100m \tag{4.7}$$

where:

- a_B is the prescribed deceleration evaluated in Equations 3.5 to 3.9;
- Λ_C is the brake weight;
- $\varphi(v)$ is a coefficient dependent on the current speed of the second train;
- $i(s)$ is the gradient of the line expressed in per-thousands dependent on the current position s of the second train along the line;
- t_r is the reaction time of the driver;

Thus, the signal containing both the actual distance d and the safety distance d_{safe} can be returned as an output, after being discretized.

The last operation performed by the RBC is the detection of the position and speed of the second train when the safety distance is violated ($p_0,\ v_0$). This is performed in the light blue-shaded area of the diagram. This will be crucial to draw the deceleration curve, as that curve needs to start at a position p_0, with the corresponding speed v_0. This detection is performed as follows: when a violation is detected (d becomes lower than d_{safe}), the current position and speed are saved into the variables p_0 and v_0. If no violation occurred($d > d_{safe}$) or it had already been detected (it was already $d < d_{safe}$), the quantities inside p_0 and v_0 do not get updated.

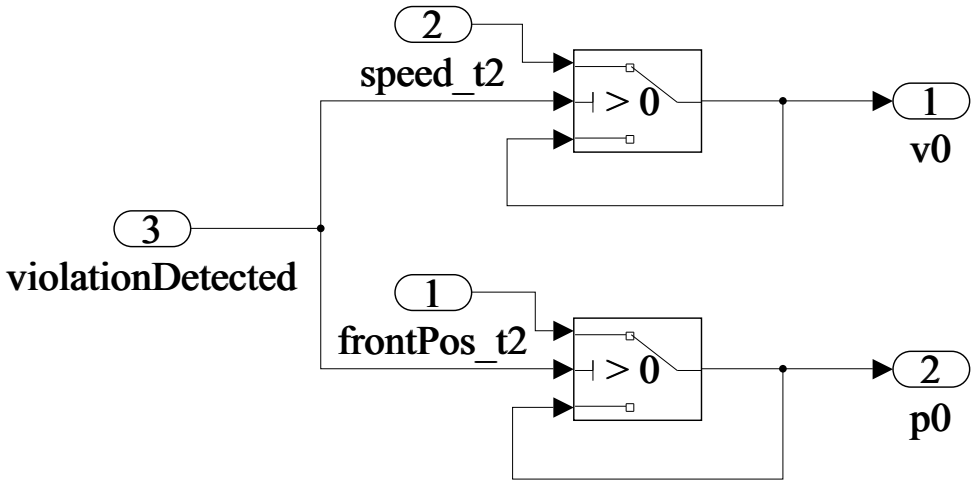

Figure 4.5: State detection at safety distance violation

In this Section, attention has been paid to the modifications applied to the RBC for it to be suitable for MVB applications. In particular, the output signals of the RBC, being the actual and safety distance of the trains and the second train position and speed in case of safety distance violation, are then used to generate the dynamic reference speed curve, similarly to how the coloured signal lights were used in the FXB environment. This topic will be covered in the next Section.

4.4. Dynamic MRSP generation

In the fixed block model, there were a static MRSP (s-MRSP) generator block, which considered only the stations and velocity change points, and a dynamic MRSP (d-MRSP) generator, which reduced the reference speed when a train entered a yellow-signalled block prescribing its stop before the following block (which would be red-signalled, until the train occupying it did not move past its limit). A similar distinction can be made in the moving block model as well. The s-MRSP generator block works in the same way as presented in chapter 3.2.1, while for what concerns the d-MRSP generation, it cannot rely on coloured signalling and blocks of fixed length in the moving block approach. Instead, it considers the safe distance evaluated in the RBC.

The d-MRSP generator block designed for the framework of MVB signalling receives as inputs the current and safety distance of the trains (d and d_{safe}), the current position of the second train (p_2) and the position and speed of the second train detected when the safety distance is violated (p_0 and v_0).

When a violation of the safety distance is not detected, the dynamic MRSP follows the

static one, while when a violation is detected, a deceleration curve is drawn so that starting from the state $(p_0,\ v_0)$, the train can decelerate with a prescribed deceleration a_B (evaluated in Equations 3.5 to 3.9) to a full stop before colliding with the leading train, considering the unrealistic worst case scenario of it stopping in place instantaneously. To generate this deceleration curve, the space needed for reaching a full stop l_{stop} has to be evaluated first, as shown in Equation 4.8:

$$l_{stop} = \frac{v_0^2}{2\ a_B} \tag{4.8}$$

Where l_{stop} depends on the approach speed of the second train at the violation point v_0. Because of how it has been defined, the safety distance d_{safe} will definitely be higher than this value. Then, the deceleration curve can be defined as shown in Equation 4.9:

$$v_{lim}(p_2) = \begin{cases} \sqrt{-2\ a_B\ (p_2 - p_0) + v_0^2} & \text{if } p_2 - p_0 < l_{stop} \\ 0 & \text{otherwise} \end{cases} \tag{4.9}$$

where p_2 is the position of the second train. This curve depends on both the approach speed and the position of the second train at the violation point v_0 and p_0.

4.5. Final remarks

In Chapters 3 and 4, the models specifically designed to simulate fixed and moving block signalling systems have been presented. The main features of the MVB environment are the same as the one described for the FXB one in Section 3.5, most notably, the definition of an RBC as an intermediary in the communication between the trains and the handling of the interaction of the vehicles travelling on the line through the safety distance observation. In the following Chapter, the results of the simulations carried out according to both signalling logics will be presented and compared, focussing the attention on possible advantages and drawbacks rising from the adoption of a MVB signalling system.

5 | Simulation results and signalling systems comparison

This Chapter contains the most significant results obtained by simulating different scenarios using the simulation environment described in Chapters 3 and 4. In particular, the focus will be on comparing the performances of the fixed block (FXB) and moving block (MVB) signalling systems.

First, a description of the services will be provided, which represent the specific scenarios, in terms of line conformation and station specifications, on which the simulations have been run. Then, a description of the key performance indicators (KPIs) considered to evaluate the simulations and compare the FXB and MVB signalling systems will be introduced. Lastly, the results of the services will be presented and discussed in terms of the KPIs.

5.1. Services

The comparison between the FXB and MVB signalling systems must be performed on appropriate services (SRV) that are able to point out their relevant features.

The following features characterize a service:

- the stations and the velocity change points (VCP) present on the line;
- the subset of stations where each train is required to stop to allow passenger service.

The number of trains travelling on the line in a simulation is not a feature of a service because, as already mentioned in Section 3, they all involve only two trains, called first (or leading) train and second (or following) train. The second train cannot ever overtake the first one. The two trains are the same, in terms of the model of their dynamics as well as the behavioural model of their driver (these models have been described in Sections 3.3.1 and 3.3.2).

Four services have been considered at the simulation stage, ordered according to their

complexity. The first two services are referred to as SRV0-A and SRV0-B, and are built on a fictional line containing respectively 0 and 1 stations and no VCPs in both cases. In the case of SRV0-B, both trains stop at the station. For the sake of simplicity, these services are characterized by no longitudinal gradient of the railway line, meaning that the force component modelling the gradient effect is null. This choice has been made to filter out the effect of the geometry of the line on these services results. The last two services are referred to as SRV1 and SRV2. These are built on a realistic line representing the Milano-Seveso route, which is the section of the longer Milano-Asso railway line containing one set of tracks for each direction (while in the Seveso-Asso section, there is only one for both directions). In all of these services, there are 12 stations on the line, but in SRV1 both trains cover all stations, while in SRV2 it skips 7 intermediate stations (while the first one still stops at all of them). The following Sections will present these service in detail.

5.1.1. SRV0-A

SRV0-A is the simplest service considered. In this case, the line does not contain any station or VCP, so the static MRSP that the trains have to follow is a constant one, as shown in Figure 5.1, where a MVB signalling system is considered as a preliminary example. The second train s-MRSP starts at 0 and steps up to the constant reference value when the initial delay of the second train (i.e., 240 s) has elapsed.

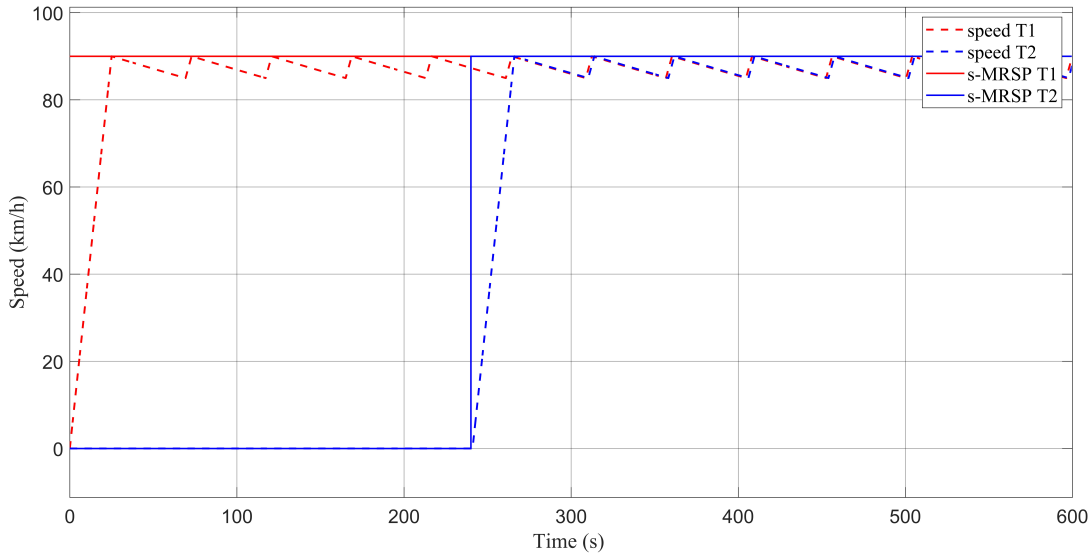

Figure 5.1: SRV0-A: s-MRSP and actual speed of both trains. The dotted lines model the dynamics of the trains when they are controlled to follow a constant reference speed. Figure obtained by performing a MVB simulation on the service.

Thus, the trains, if the presence of other trains does not hinder their motion, will accelerate to the reference speed, and then keep that for the rest of the simulation, as shown in Figure 5.2, where the red lines refer to the first train, solid for its front end and dashed for its rear end, and the blue lines refer to the second train, with the same line-style code as the first one.

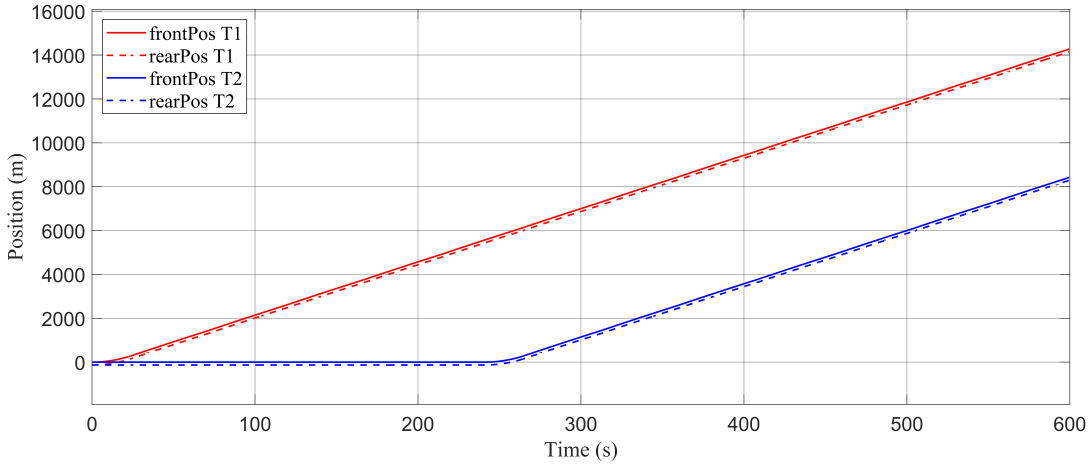

Figure 5.2: SRV0-A: position of both trains in time. Figure obtained by performing a MVB simulation on the service.

As the two trains and their drivers are characterized by the same model, they respond to MRSP changes in the same way. In particular, the time spent in the initial acceleration is the same, as well as the space travelled in that time. This means that from the moment the second train starts moving, the two trains always maintain the same distance between them.

5.1.2. SRV0-B

SRV0-B is a complication of SRV0-A, as it adds a station to the line. It will be shown that this modification alone leads to substantial differences from SRV0-A. The s-MRSP of both trains will not be constant, but it will instead be composed of deceleration, stop and acceleration stretches so that the train can correctly approach and stop at the station, as described in Section 3.2.1, Equations 3.3 and 3.4, and as shown in Figure 5.3, where the colour and line style code is the same adopted in Figure 5.1.

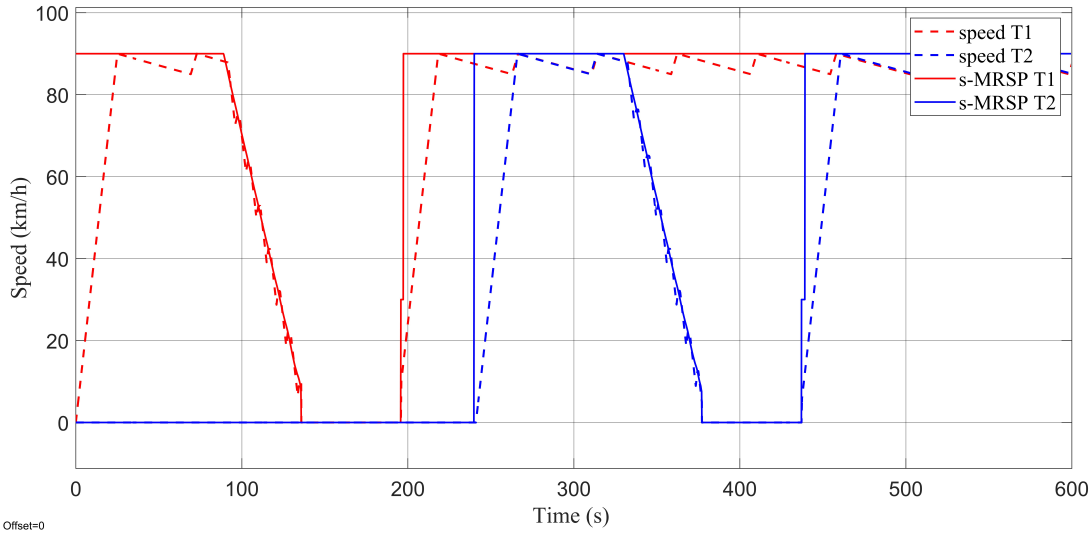

Figure 5.3: SRV0-B: s-MRSP and actual speed of both trains. The dotted lines model the dynamics of the train when it is controlled to follow a varying reference speed. Figure obtained by performing a MVB simulation on the service.

If the presence of other trains does not hinder their motion, the trains will move as shown in Figure 5.4 (a), where the colour and line style code is the same adopted in Figure 5.2. Figure 5.4 (b) represents the distance the trains keep between them. Clearly, it is not constant, meaning that the presence of even one station makes the trains not move in parallel anymore.

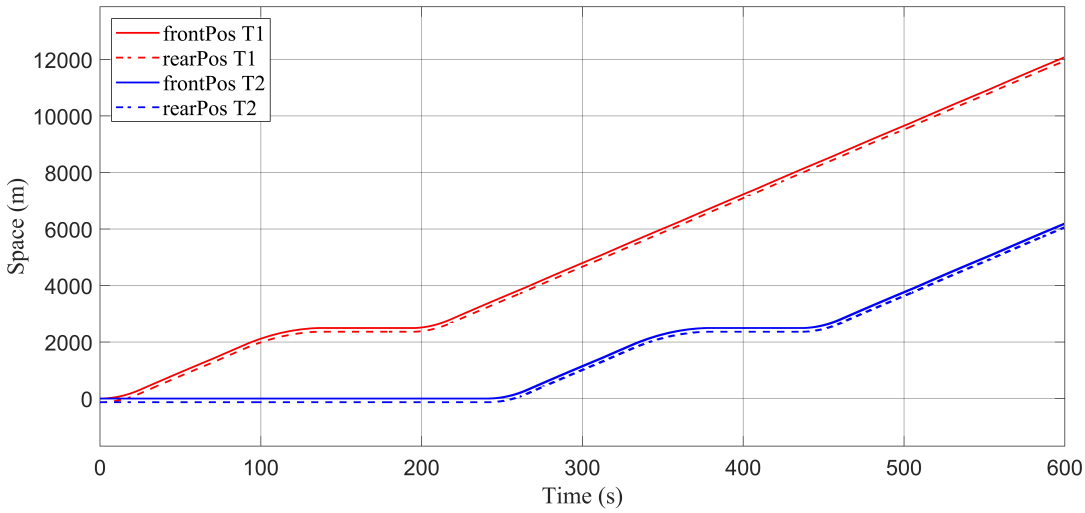

(a) Position of both trains.

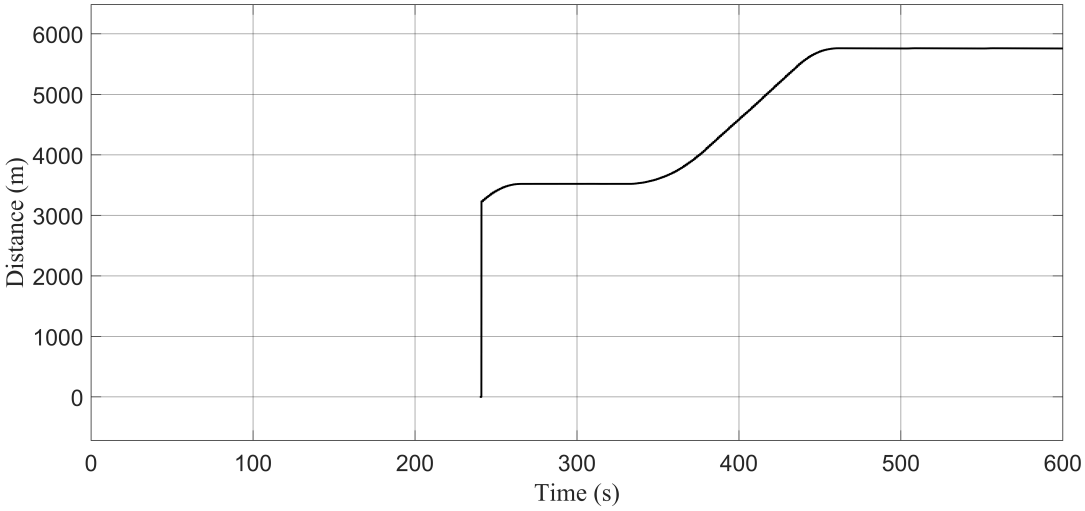

(b) Distance between trains. The graph starts when the second train departs from the initial station, i.e., 240 s in the presented example.

Figure 5.4: SRV0-B: position and distancing of the trains. Figures obtained by performing a MVB simulation on the service.

Given that an ideal line is considered, the position of the station is not imposed, thus it can be considered a parameter of the service, and the performance of the FXB and MVB signalling systems can be studied as a function of it.

5.1.3. SRV1

SRV1 is the first service built on a real-case scenario, the Milano-Seveso route. Table 5.1 collects information on the stations and VCPs. Each row represents one station or VCP,

depending on the element of the first column. The last column contains the speed allowed right after the station or VCP.

	Stop name or VCP	Position [m]	Reference speed [km/h]
1	Cadorna	0	30
	VCP	662	80
2	Domodossola	1 720	80
	VCP	3 323	60
3	Bovisa	4 165	60
	VCP	4 955	90
4	Affori	6 435	90
5	Bruzzano	7 843	90
6	Cormano	9 227	90
7	Paderno	11 613	90
8	Palazzolo	13 467	90
9	Varedo	15 094	90
10	Bovisio	17 167	90
11	Cesano	19 323	90
12	Seveso	21 208	90

Table 5.1: Stations and VCPs information for the Milano-Seveso line.

Each station prescribes the same stop time of 60 s. The only exception is represented by the first station, which prescribes a null stop time, as shown in Equation 5.1. This specification has been considered to simulate the train to immediately depart as soon as the simulation starts.

$$stopTime(s) = \begin{cases} 0\ s & \text{if } s = 1 \\ 60\ s & \text{if } s \in (2, 12) \end{cases} \tag{5.1}$$

Considering the method described in Section 3.2.1, this line definition results in the look-up table that links a velocity value to each position on the line, shown in Figures 3.3 (only considering the VCPs and neglecting the stations) and 3.5 (considering both the VCPs and the stations). The graph of the s-MRSP, which links velocity and time, is the one represented in Figure 5.5 with a black line, alongside the actual speed of the train with a light blue line. In particular, the graph depicts the motion of the second train, as can be seen from the presence of the initial delay of 240 s. The s-MRSP and actual velocity graph related to the first train would be identical but shifted leftward, so as to start its motion at time t = 0 s, i.e., with no initial delay. Notice that the actual speed follows closely the s-MRSP (considering the fluctuations derived from the train dynamics and speed control system). This is a result of the signalling being always green for the second train in the considered scenario. Thus, the second train is not affected by the presence of

the first one in its motion, and its s-MRSP and d-MRSP are identical.

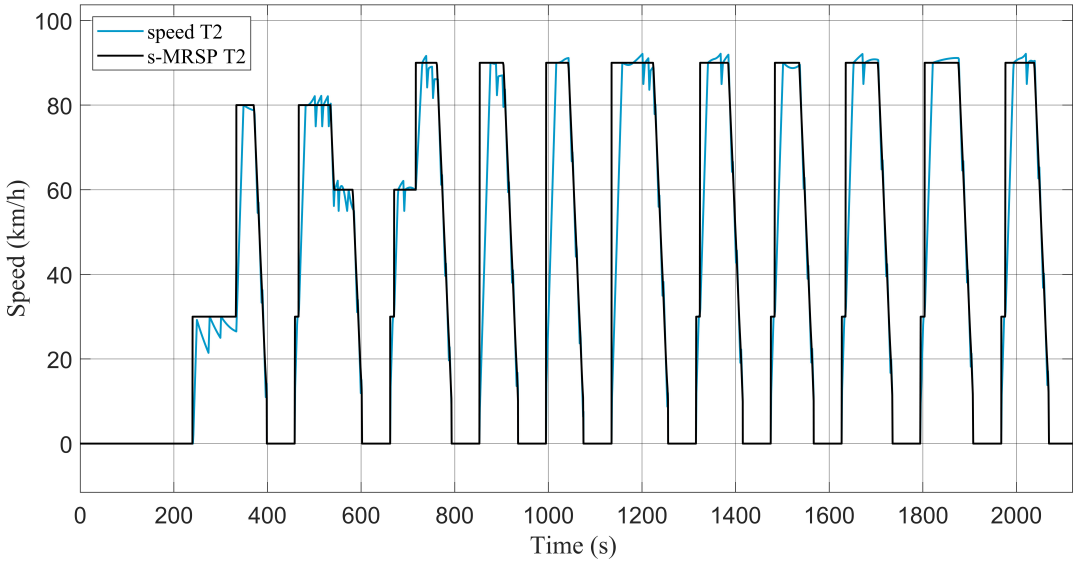

Figure 5.5: SRV1: s-MRSP and actual speed of the second train, which departs with an initial delay of 240 s from the first one. Figure obtained by performing a MVB simulation on the service.

In scenarios like this one, i.e., with no hindrance of the motion of the trains because of the presence of other vehicles, the trains will move as shown in Figure 5.6. Figure 5.6 (a) represents the trains positions, while 5.6 (b) shows their distance. The segments in which their distance increases correspond to the ones in which the first train is moving while the second one is still at a station, and vice versa for decreasing segments; the constant segments correspond to the ones in which the trains are either both moving or both still.

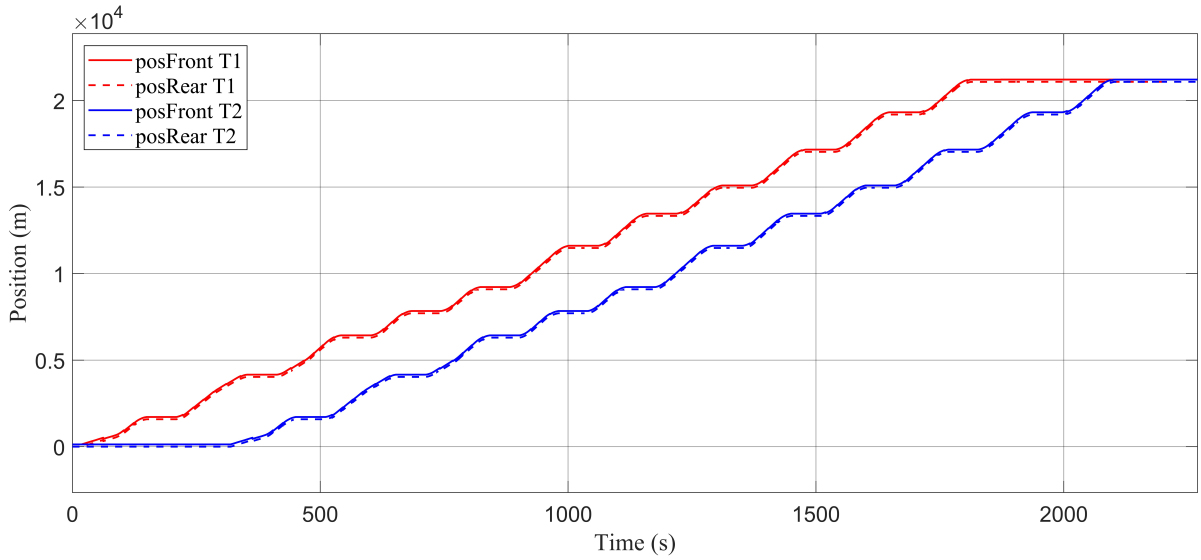

(a) Position of both trains

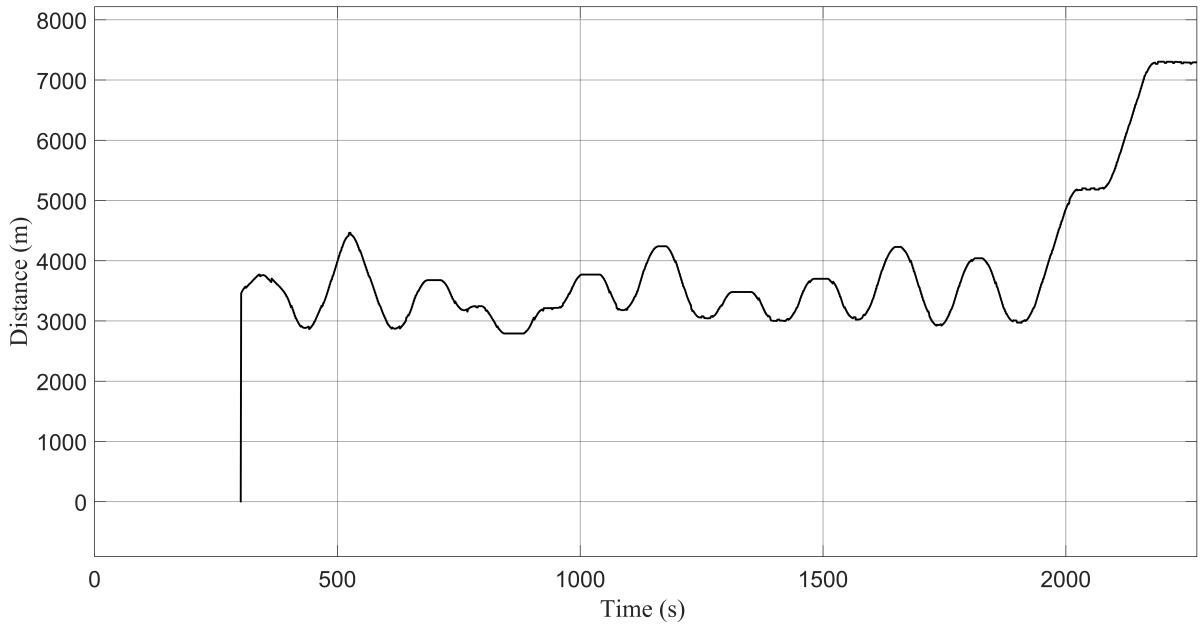

(b) Distance between trains. The graph starts when the second train departs from the initial station, i.e., 240 s in the presented example.

Figure 5.6: SRV1: position and distancing of the trains. Figures obtained by performing a MVB simulation on the service.

5.1.4. SRV2

The last service considered in this work, referred to as SRV2, is similar to SRV1 in terms of line configuration and railway stations. However, the second train skips all stations between number 5 (Bruzzano) and 11 (Cesano), while the first one is still stopping at all

stations.

Figure 5.7 shows the look-up table that links reference speed and position on the line and Figure 5.8 shows the s-MRSP and actual speed of the second train (note that the ones associated with the first train are the same as SRV0, shown in Figures 3.5 and 5.5 respectively). It can be observed that the actual speed deviates from the s-MRSP in the last portion of the graph in Figure 5.8: this happens because the second train encounters yellow signals along the line, thus making the d-MRSP differ from the s-MRSP. As the d-MRSP is used as the reference for speed control, a deviation between s-MRSP and d-MRSP results in a deviation between s-MRSP and actual speed.

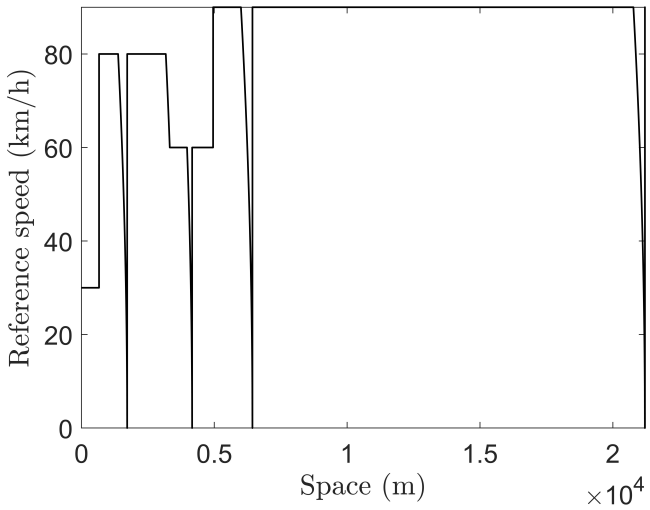

Figure 5.7: SRV2: Speed/position lookup Table of the second train considering stations.

Figure 5.9 shows that the second train may get too close to the first one because of the station it does not have to stop at. SRV2 is built specifically to simulate scenarios in which the second train catches up to the first one, thus receiving a yellow signalling in case of FXB signalling system, or violating the safety distance in case of MVB signalling system, making its d-MRSP deviate from the s-MRSP. Note that when the second train gets too close to the first one, it decelerates even though the s-MRSP would not prescribe so, as illustrated in Figure 5.8.

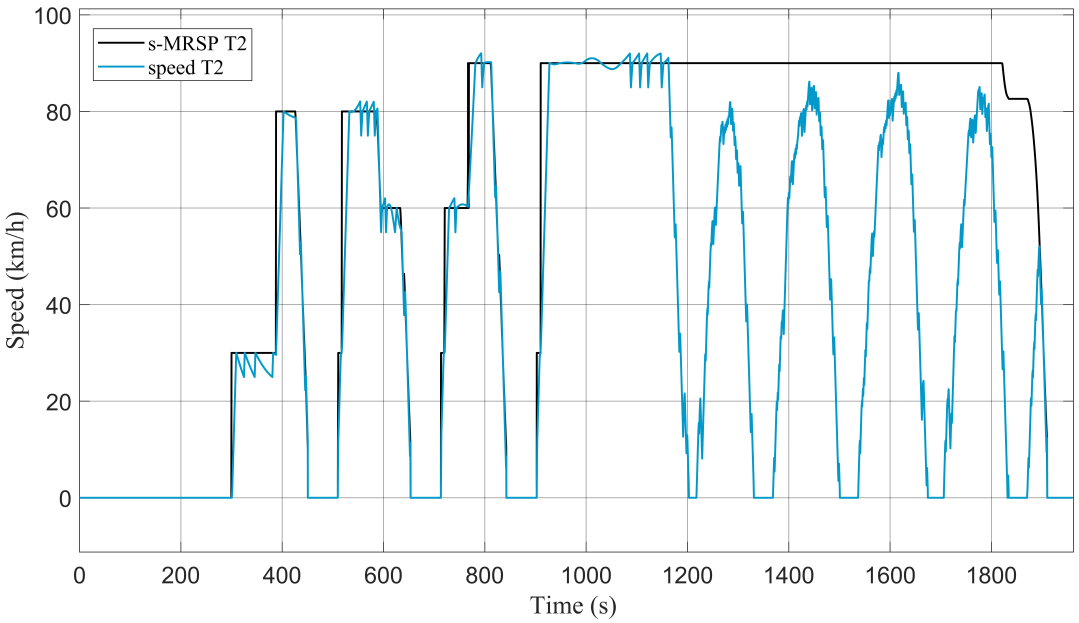

Figure 5.8: SRV2: s-MRSP and actual speed of the second train, which departs with an initial delay of 360 s. Figure obtained by performing a MVB simulation on the service.

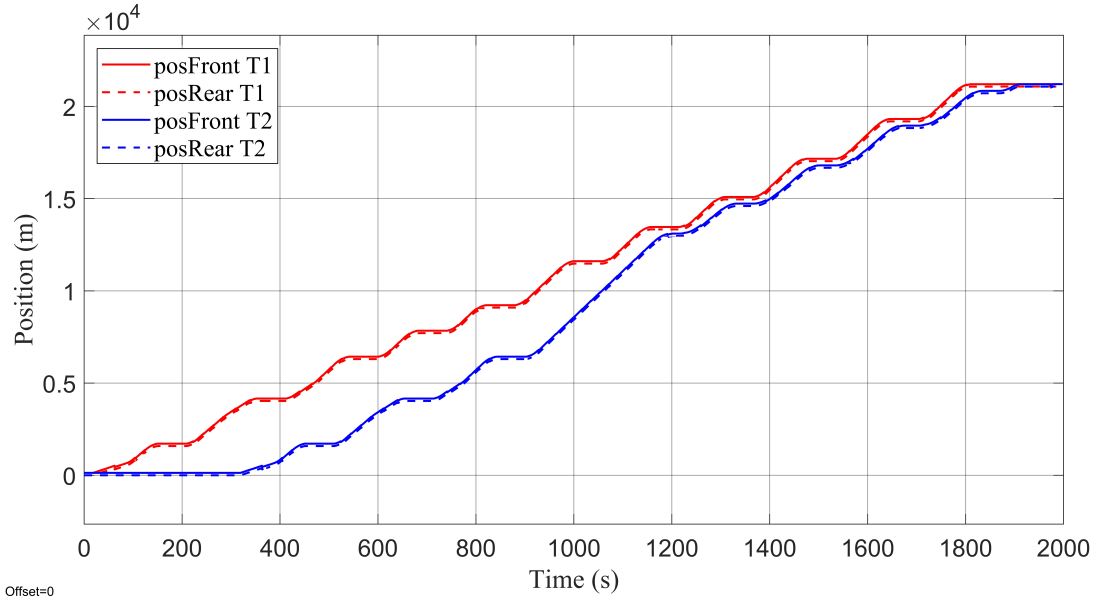

Figure 5.9: SRV2: Position of both trains. Figure obtained by performing a MVB simulation on the service.

5.2. Key performance indicators (KPIs)

The previous Section was devoted to the description of the services considered for the simulations. In this Section, attention will be paid to the key performance indicators

(KPIs) considered to compare the performances of the FXB and MVB signalling systems when applied to the services previously described. They will be thoroughly explained in the next Sections, but to give a general overview:

- safety is the most important indicator since signalling major priority is to ensure the safe operation of all vehicles. A positive safety indicator means that the trains did not collide during the execution of a service. It will be shown that safety is inherently respected in all the simulations performed, being an intrinsic principle from which the entire environment was built;
- line capacity (LC) measures the frequency of the service execution. It is usually expressed in terms of trains per hour, or, by multiplying by the average number of passengers per train, in terms of passengers per hour;
- motion regularity (MR) measures how much the d-MRSP follows the s-MRSP. It will be expressed as a percentage, reaching 100% only in the case of no hindrance of the second train motion;
- energy consumption (EC) measures the energetic efficiency of the trains.

In the following, each of these KPIs will be described as well as the method considered to obtain them from the simulations.

5.2.1. Safety

The first KPI is safety, which can be regarded as the most important aspect of the simulations since the trains must never collide. Providing a quantitative measure of safety is not trivial, as many methods could be designed. The simplest one is considering a boolean value set to 1 if safety is ensured and to 0 otherwise (Isobe et al. [23]). Whilst being simple, this method is suitable to show the most crucial aspect. Indeed, other methods could be designed by considering a continuous-valued variable that increases with the minimum distance the trains keep along the whole simulation. However, such methods overcomplicate the evaluation of the safety KPI, so that a boolean-valued safety variable is preferred to distinguish safe and not safe simulations and use other indicators to evaluate them more thoroughly in terms of their performances.

With specific reference to the simulation environment presented in this thesis, the safety KPI is always equal to 1, it was purposely realized to prevent any collision.

5.2.2. Line capacity

Line capacity (LC) is an indicator of how much traffic can be held by the line. Out of all the presented KPIs, it is the one with the most scientific literature coverage, at least in relation to the signalling systems. The effectiveness of the fixed block signalling system, i.e., ERTMS level 2 signalling system, compared to a non-ERTMS is discussed by Goverde et al. [24], putting emphasis on both nominal and disturbed scenarios and reporting a superiority of the ERTMS system. For a comparative analysis within the ERTMS environment, Ranjbar et al. [25] have carried out a comparison between the capacity performances of fixed block and hybrid moving block, i.e., ERTMS levels 2 and H3 signalling systems. The study reports that the hybrid MVB signalling system performs poorly with respect to the FXB one.

Before a detailed explanation of the KPI, one last element must be introduced, which is time distancing. Indeed, in all previous dissertations, the distance between the trains was always intended as space distancing d_s, obtained as the difference between the positions of the trains at a specific time instant. However, another notion of distance could be the one of time distancing d_t, obtained by evaluating the time that the first train needed to reach its current position from the second train current position. In Figure 5.10 both notions of distance have been highlighted.

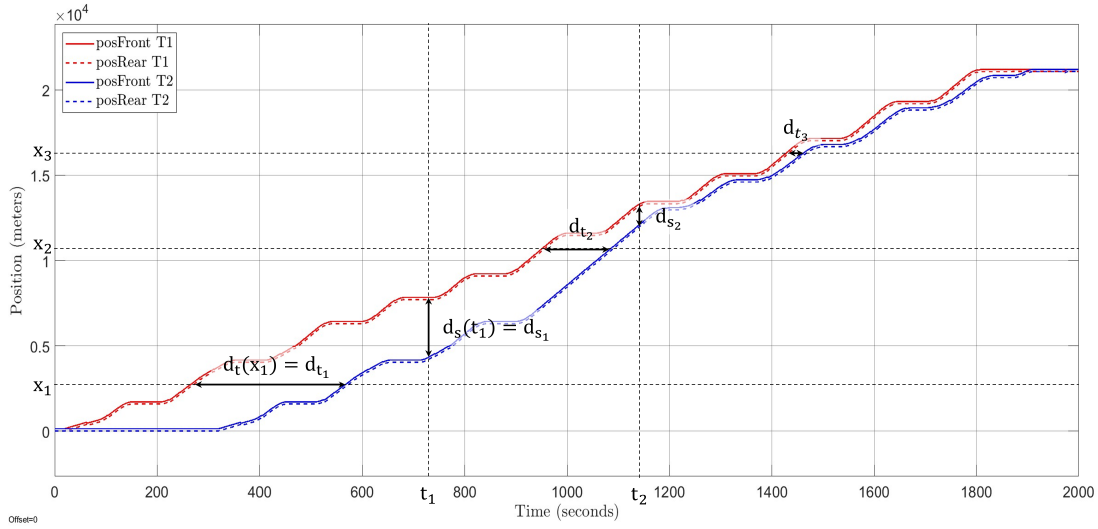

Figure 5.10: Space and time distance of the trains. For each value on the vertical axis (space) time distance between the trains can be evaluated as $d_t(x)$; likewise for the horizontal axis (time) and space distance as $d_s(t)$. Figure obtained by performing a MVB simulation on SRV2.

Line capacity LC is expressed as a frequency, obtained as the reciprocal of the time

distancing. Clearly, as shown in Figure 5.10, $d_s = d_s(t)$ can differ for any time instant t and $d_t = d_t(x)$ can differ for any point on the line x. Thus, LC is a local indicator. To obtain a global measure of the capacity over the whole line, the minimum over the local values must be considered: the bottleneck of the line is the section in which the least amount of vehicles can travel per unit of time.

Since the time distancing is expressed in seconds, to obtain the capacity in trains per hour it has to be multiplied by 3600. The capacity evaluation could be further refined by expressing it in terms of passengers per hour by multiplying the LC by an estimate of the number of passengers per train. However, this factor introduces a grade of complexity which is not required at this stage, especially since the number of passenger in a train strongly depends on the specific route considered and on the time of the day considered for the evaluation. Thus, the LC is expressed in trains per hour, as shown in Equations 5.2, for the local LC at a position s, and 5.3, for the global LC over the whole line.

$$LC(s) = \frac{3600}{d_T(s)} \tag{5.2}$$

$$LC = \min LC(s) = \frac{3600}{\max d_T(s)} \tag{5.3}$$

More in detail, different notions of line capacity can be defined as hereafter reported (Abril et al. [26]):

- The theoretical line capacity LC_T evaluated through Equations 5.2 and 5.3, which is the maximum number of trains that could be run by a railway line in ideal conditions during a given time period.
- The practical line capacity LC_P obtained as a fraction of the theoretical one (generally 60% to 75%), which is the traffic flow that can be offered under normal operating conditions, driving on the railway line with an accepTable level of reliability;
- The commercial line capacity LC_C evaluated on the actual timeTable of the service, which is the effective traffic flow that is canalized through the line.

Note that if not furtherly specified, the theoretical line capacity will be considered in all future Sections, thus $LC = LC_T$.

5.2.3. Motion regularity

Motion regularity (MC) is an indicator of how much the d-MRSP of a train deviates from the s-MRSP, i.e., how much the signalling system affects the motion of a train. The least

a train is affected by the signalling, the highest its MR will be. Figure 5.11 and Equation 5.4 provide an explanation of how the MR is defined.

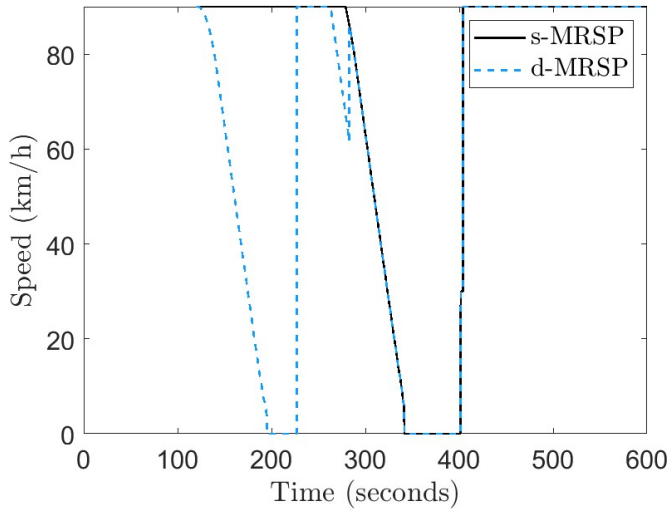

(a) d-MRSP (dotted blue) and s-MRSP(solid black) of the second train.

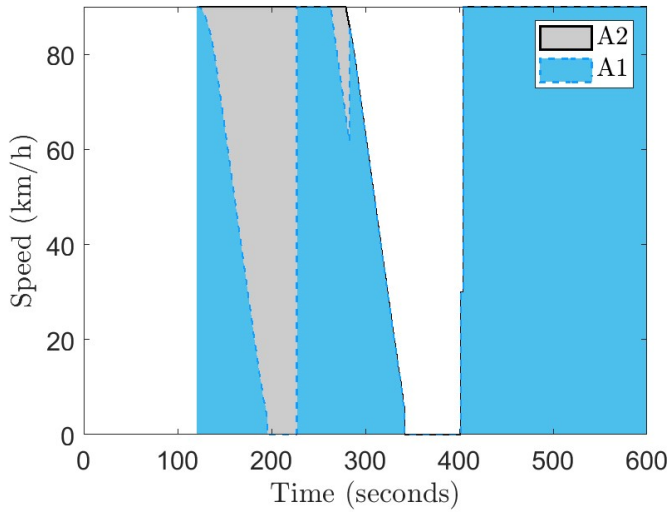

(b) Areas underneath the d-MRSP (A1, light blue) and s-MRSP (A2, grey) of the second train.

Figure 5.11: MR: s-MRSP and d-MRSP of the second train and area under those curves. Figure obtained by performing a FXB simulation on SRV0-B.

$$MR = \frac{A_1}{A_2} \tag{5.4}$$

Referring to Equation 5.4 and Figure 5.11 (b), A_1 is the area under the d-MRSP, light blue-shaded in the graph, while A_2 is the area under the s-MRSP, grey-shaded in the graph (clearly, the grey area extends below the whole light blue area).

MR could be evaluated with different signalling systems, such as counting the deviations of the d-MRSP from the s-MRSP, i.e., the number of unexpected decelerations, or counting the total time the train had to impose a null reference speed without it being required by the s-MRSP, i.e., the total unexpected stop time, or even more complex ones. The ratio of the areas under the curves is a synthetic parameter that takes into account both the amount of time in which d-MRSP deviates from the s-MRSP and the depth of those deviations, including also the case of full stops.

While line capacity was a property of each section of the line, motion regularity is a global property of the single train, meaning that one indicator for each train could be defined, but that indicator is global to the whole service and not local to a specific point on the line. Clearly, the MR of the first train will always be 100%, as its motion is not affected by the signalling, being that there are no trains running ahead of it. Thus, only the MR of the second train will be considered.

5.2.4. Energy consumption

Energy consumption (EC) is the final KPI considered in the comparison between FXB and MVB signalling systems. It measures the efficiency of the trains in terms of power consumption. Many studies have been conducted on the optimization of energy consumption for train motion, both analytic-based (Jong [27]) and simulation-based (Dullinger et al. [28]).

To evaluate the power usage, it is sufficient to multiply the force output of the motor F_{mot} (Equations 3.18 to 3.21) and the speed of the train v. Indeed, given the proposed modelling choices, F_{mot} is not evaluated on the motor itself, but rather on the train, considered as a point-mass. This means that the transmission ratio for the force is already included in the computation. Also, there is no need to consider the radius of the motor rotating part or of the wheels, as the power can be evaluated directly from the linear force and speed multiplication.

According to the nature of the motor force, its sign will be different (positive for traction and negative for braking forces). Thus, also the power will have positive and negative segments (recall that the train speed is always non-negative). When the power is positive, the train is absorbing power to perform its motion, while when it is negative, it is reconverting some of the previously spent power through the use of regenerative braking.

In practice, the amount of power that can be restored is limited by some efficiency factor η, the value of which will be discussed in chapter 5.7.

To express the power P in Watts, consider Equation 5.5.

$$P = F_{mot} \cdot v = \begin{cases} F_{trc} \cdot v & \text{if command traction} \\ -\eta \cdot F_{brk} \cdot v & \text{if command braking} \\ 0 & \text{if command coasting} \\ -\eta \cdot F_{emergBrk} \cdot v & \text{if issued emergency brake} \end{cases} \tag{5.5}$$

To obtain the energy consumption, the power has to be integrated over the whole simulation, as shown in the block diagram in Figure 5.12. This method would provide the energy consumption in $[W \cdot s = J]$, while the most suitable unit of measure to express this quantity is [kWh]. Thus, the result is scaled by $\frac{1}{3600 \cdot 10^{-3}}$, as shown in Figure 5.12, which is the Simulink block diagram that performs the evaluation of the energy consumption. Note that in the Figure, the unit conversion factor is divided into two gain blocks, placed upstream and downstream with respect to the integration. Of course, this does not change the EC results.

As previously mentioned, the energy consumption evaluation can be performed with or without regenerative braking (Wang and Rakha [29]), meaning that a portion of the energy consumed during traction segments can be recovered during braking segments. If the parameter *regenerativeBrake* is set to 1, a portion of the braking force is considered in the evaluation of the power, according to the value of the parameter η. Of course, as shown in Equation 5.5, the power consumed during braking traits is negative, meaning that it is actually power recovered. If the parameter *regenerativeBrake* is set to 0, during braking traits the force considered is multiplied by 0, as shown in the regenerative brake switch in Figure 5.12, meaning that no power recovery is considered.

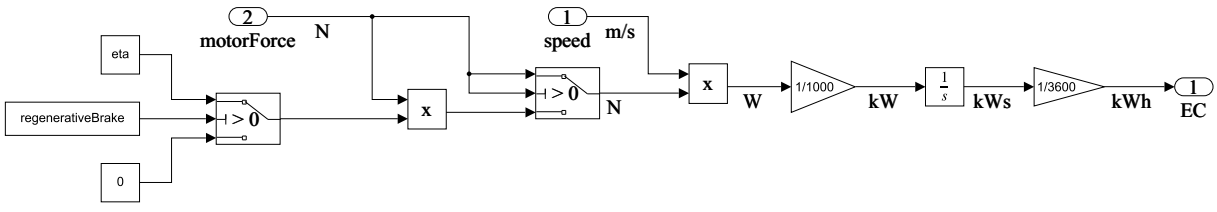

Figure 5.12: Energy consumption block diagram.

5.3. Introduction to results presentation

Sections 5.1 and 5.2 have been devoted to the presentation of the services and the KPIs considered to evaluate the performances of the two signalling systems, i.e., FXB and MVB.

In the following Sections, attention will be paid to the results obtained from the various simulation performed on a service, and considering the KPIs as comparison indicators for the two systems. For each KPI, only the most meaningful services that allow evidencing significant differences between FXB and MVB will be considered. A summary of the associations between KPIs and services can be found in Table 5.2. Note that to better emphasize the difference between the signalling systems, the services may undergo small changes from the nominal cases described in Section 5.2.

KPI	SRV0-A	SRV0-B	SRV1	SRV2
Safety	X			
Line capacity	X	X	X	
Motion regularity	X	X	X	X
Energy consumption		X	X	X

Table 5.2: SRV-KPI couplings.

5.4. Safety evaluation

In the following Sections, it will be shown that the model guarantees safety by simulating two critical scenarios:

- in Section 5.4.1, the driver does not react to a warning signal, making the speed increase past the service brake intervention curve (SBI) and automatically activating the service brake;
- in Section 5.4.2, in addition to the inactivity of the driver, the service brake is broken, making the speed increase not only past the SBI, but also past the emergency brake intervention curve (EBI) and automatically starting the emergency brake procedure.

It is here recalled that while an exceedance of the SBI immediately issues the service brake, an exceedance of the EBI activates a timer, at the end of which the emergency brake is issued. This is useful to allow the driver intervention before resorting to the emergency brake, that in the presented simulation environment stops the train for the whole remaining time of the simulation.

5.4.1. Safety in case of SBI exceedance

The first safety-compromising scenario is the one in which the speed reaches the service brake intervention (SBI). It can be simulated by simply reducing up to a null value the probability of the driver's reaction to 0 (for the definition of the probabilistic model of the driver's reaction to a warning signal, refer to Section 3.3.2). As a result, even when the speed crosses the warning curve (WC), the driver will not command the motor to generate the braking force. Instead, the motor will maintain the coasting state, meaning that the force generated by it will be null, and the train will move only according to the motion resistance and the gradient effect force components. Thus, if the line is inclined downhill enough, the train will keep on accelerating, eventually reaching the SBI.

This scenario is performed on SRV0-A, which includes the least amount of external factors that should not be considered when evaluating the safety of a service. For example, it is irrelevant to check if the train manages to stop at a station, as that takes a back seat with respect to safety when it could be compromised. Thus, the most appropriate scenario to test safety is the one without any station, and for the same reason, without any further complication. The only difference with the description of SRV0-A presented in Section 5.1.1 is that in this simulation the line presents a positive uniform gradient, meaning that it is a downhill segment and the train accelerates even if the coasting actuation is active, i.e., the motor generates null force.

The results show that even without the contribution of the driver, the train manages to slow down when the SBI is reached, bringing the speed back down to the lower curve (LC), below the MRSP. As this is still not an emergency case, the train does not have to be stopped, but rather, it can carry on with its normal behaviour after the automatic service brake. Thus, traction is commanded until the speed reaches the MRSP when coasting is issued again, and the cycle starts over (for a description of the nominal speed control algorithm, refer to Section 3.2.2, Figure 3.16). In this case, there are no differences in the behaviour of the train in FXB or MVB signalling system, as the criticality of the scenario only concerns a single train, in its dynamics and speed control, and these components are unchanged in the two signalling systems.

5.4.2. Safety in case of EBI exceedance

The second safety-compromising scenario is the one in which the speed reaches the emergency brake intervention (EBI). To simulate this scenario, the service brake module has to be disconnected from the rest of the simulation environment. In this way whatever curve the speed exceeds, the service brake is not actuated, nor manually by the driver at

the warning curve (WC), nor automatically at the SBI. Thus, the motor will stay in the coasting state, and if the line is inclined enough, the speed will eventually reach the EBI, starting a timer and automatically issuing the emergency brake at the end of it.

As explained in Section 3.2.1, Equations 3.20, the emergency brake holds a fixed value for any speed condition, which is the maximum braking force generable by the motor. Also, as mentioned in Section 3.4.1, the saturation on the acceleration is bypassed in case of emergency brake activation, meaning that the deceleration will have a constant value of:

$$a_{emergBrk} = \frac{-F_{emergBrk}}{m} = \frac{-419.5 \text{ kN}}{369 \text{ ton}} = -1.1369 \ \frac{\text{m}}{\text{s}^2} \tag{5.6}$$

Thus, the space needed to perform the whole deceleration, down to stopping the train is:

$$l_{emergBrk} = \frac{1}{2} \frac{v_0^2}{a_{emergBrk}} \tag{5.7}$$

where v_0 is the speed of the train at emergency brake activation.

The reasoning behind the service choice and specification stated for the previous scenario still stands for this one. Thus, the simulation is performed on SRV0-A with a positive uniform gradient (meaning downhill slope) over the whole line.

The results show that when the emergency brake activates, the train manages to stop in a relatively short time. Again, there are no differences in the behaviour of the train in the FXB or MVB signalling system, but it is worth noting that for the FXB signalling system if the emergency brake activation happens at a distance greater or equal to $l_{emergBrk}$ from the end of the block currently occupied by the train, it will stop before entering in the following block. If this was not the case, the following block would definitely not be red-signalled, as if it were, the train would have encountered a yellow signal at the start of its current block. Thus, even if the service brake were not active, the emergency brake would have taken control before getting closer than $l_{emergBrk}$ to the block boundary. Instead, the case of an emergency brake that spans over two blocks only happens when the service brake breaks in a green signalled block, meaning that there is no harm in crossing the block boundary.

Figure 5.13 shows the behaviour of the train in terms of its speed when both of these emergency situations happen in succession. Recall the meaning of the coloured lines, each representing a reference speed curve:

- the green line is the most restrictive speed profile (MRSP);
- the purple line is the lower curve (LC), used as a lower bound for the speed control;

- the yellow line is the warning curve (WC), used to send a warning signal to the driver, who will autonomously command braking and slow down the train;
- the orange line is the service brake intervention (SBI), used to automatically issue braking and slow down the train in case of unreactivity of the driver;
- the red line is the emergency brake intervention (EBI), used to start the emergency brake procedure and stop the train in case of malfunctioning of the service brake.

The light blue line is the actual speed of the train. In the nominal scenario, it fluctuates around the MRSP inside the LC-WC range, but looking at the simulation results of Figure 5.13, different events can be recognised. At first, focus the attention on time $t_0 = 150\ s$, when the driver becomes unreactive, so the first time that the speed reaches the WC, they do not command braking. Thus, the speed keeps on growing because of the slope of the line (recall that for these simulations, the line gradient is constant and positive, meaning that the train travels on a uniform downhill route). At time $t_1 \tilde{=} 170\ s$, when the speed reaches the SBI, the service brake is automatically issued, slowing down the train to the LC. Then, at time $t_2 = 300\ s$ the driver becomes reactive again, so the speed resumes fluctuating in the LC-WC range. This concludes the first safety-risking scenario. Now focus the attention on the second half of the diagram, starting from time $t_2 = 400\ s$, when the service brake stops working, so the first time that the speed reaches the SBI, it does not automatically issue braking. Thus, the speed keeps on growing and eventually reaches the EBI. When that happens, at time $t_3 \tilde{=} 450\ s$, 10 seconds of waiting time is left for the driver to restore its action and slow down the vehicle. If this is not the case (whether because of the inaction of the driver or because of the malfunctioning of the service brake), at the end of the 10 seconds, the emergency brake is automatically issued, stopping the train with the maximum available braking force. Finally, at time $t_4 \tilde{=} 490\ s$, the train reaches null speeds and it does not resume the motion at any time in the simulation, concluding also the second safety-risking scenario.

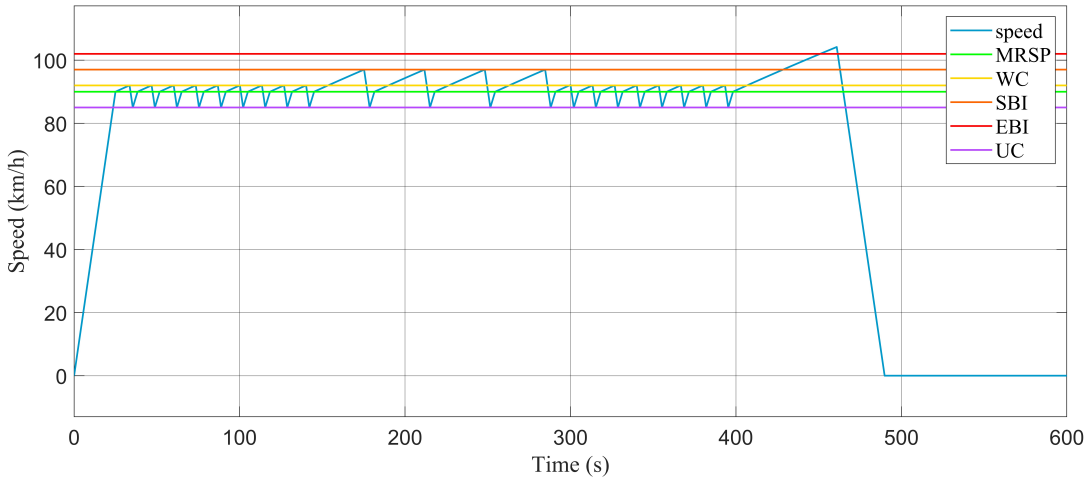

Figure 5.13: Automatic service and emergency brake activation with the exceedance of the SBI and EBI respectively. Figure obtained by performing a FXB simulation on SRV0-A with positive uniform gradient and prescribing a disconnection of the driver's reactivity module in the interval $(t_0, t_2) = (150, 300)\ s$ and of the service brake module at time $t_3 = 450\ s$.

These scenarios may become relevant in a number of critical situations, as any unexpected phenomenon has an impact on the limit speed, meaning that it can be answered through automatic service brake or emergency brake activation. Thus, safety is always guaranteed, and in all further dissertations, this KPI will be taken for granted for both FXB and MVB signalling systems, while the comparison will be made on the other performance indicators.

The next Section will be devoted to the evaluation of the theoretical line capacity over multiple services.

5.5. Line capacity evaluation

Theoretical line capacity (LC_T or just LC) is the first KPI used to compare the FXB and MVB signalling systems. It is here recalled that LC is defined as the reciprocal of the maximum time distancing the trains keep between themselves over the whole simulation, multiplied by 3600 to obtain the LC in terms of trains per hour. LC has been evaluated in various services. Specifically, SRV0-A and SRV0-B will be used to introduce the adopted method for the evaluation of the LC, while SRV1 will be used to present the results obtained with one or the other signalling system in a realistic scenario.

5.5.1. Line capacity for SRV0-A

Consider SRV0-A first. Since there are no stations on the line, the trains maintain always the same distance between them, both in terms of space and time. Thus, the line capacity will be uniform over the whole line. This statement stands under a fundamental hypothesis: the second train must never deviate from the s-MRSP during the whole motion. If this assumption is not confirmed, the second train will move differently from the first one (which is never affected by the signalling) and the time distance between the trains will vary during the motion. On the other hand, if it is confirmed, the time distance between the train will be constant and equal to the initial one, i.e., the delay of the second train $d_t(x) = d_{T2}$ $\forall$ position x.

The reason behind this analysis is the need to find a set of conditions and requirements to make the simulation conducted with the FXB and MVB signalling systems comparable. As explained in Section 4.1, the safety distance defined for MVB environments plays a similar role to the yellow signalling for FXB environments, while in case of MVB there is no signalling equivalent to the red signal light. Thus, a comparable situation is one in which the second train only encounters green signalling for what concerns the FXB signalling system, and never violates the safety distance for what concerns the MVB one.

For the FXB signalling system, to confirm this hypothesis the second train must be delayed at least as the time needed for the first one to reach the third block. Indeed:

- the second train is not allowed to move while the first block is occupied by the first vehicle (due to red signalling);
- if the second train starts moving when the second block is still occupied, it will immediately receive a yellow signal. Therefore, it will be able to start moving but its d-MRSP will decrease as it moves, thus violating the assumption for the evaluation of line capacity;
- if the second train starts moving only when the first two blocks have been freed, it will encounter a green signal at the first block, and because it moves exactly as the first train, also at any other block, confirming our hypothesis.

The times needed for the first train to reach respectively the second and third block are referred to as t_{B2} and t_{B3} To avoid encountering any yellow signalling, the second train must be delayed at least as t_{B3}, which takes the role of the optimal initial delay of the second train ${d_{T2}}^*$:

$$d_{T2} \geq t_{B3} = {d_{T2}}^* \tag{5.8}$$

Given that the LC is the reciprocal of time distancing, its minimum value is also the optimal one. Clearly, t_{B2} and t_{B3} depend on the length of the fixed block (FBL). If the blocks are short, the first train will quickly reach the third one, and vice versa in case of longer blocks. Thus, to obtain the optimal time distancing for any block length, the relationship between FBL and t_{B3} must be derived, as shown in Equation 5.9:

$$t_{B3}(FBL) = {d_{T2}}^*(FBL) = \begin{cases} \sqrt{\frac{4FBL}{a}} + \frac{l_T}{v} & \text{if } 0 \leq 2FBL < l_0 \\ t_0 + \frac{2FBL - l_0}{v} + \frac{l_T}{v} & \text{if } l_0 \leq 2FBL \end{cases} \tag{5.9}$$

where:

- a is the prescribed acceleration, set to 1 m/s^2;
- v is the reference speed, set to 90 $km/h = 25$ m/s;
- $t_0 = v/a$ is the time needed to perform the initial acceleration, which turns out to be 25 s;
- $l_0 = v^2/2a = v \cdot t_0/2$ is the space travelled during the initial acceleration, which turns out to be 312.5 m;
- l_T is the length of the train, set to 131 m

To have a general understanding of Equation 5.9, each of its cases is composed of the time needed for the front end of the train to reach the third block and the time needed for the rear end to catch up. It is recalled that a train reaches a block if it is completely contained in it, thus, if its rear end reaches it. The first case of Equation 5.9 refers to the case in which the train front end reaches the third block while it is still accelerating, so the time needed will be proportional to the square root of the block length; on the other hand, in the second case of Equation 5.9, the acceleration has concluded in a time t_0 making the train front end reach a position l_0, while the rest of the space to reach the third block is travelled at a constant speed.

Figure 5.14 represents the theoretical position of the first train in SRV0. As expected, it accelerates for a time t_0, covering a distance l_0, and then it reaches the constant reference speed. The time t_{B3} is the first coordinate of the point obtained by intersecting the curve representing the train position and a horizontal line crossing the vertical axis at twice the block length. In the Figure, the red curve stands for the acceleration, while the blue one represents the uniform motion, and point A is the delimiter between the two; thus its coordinates will be $(t_0,\ l_0)$. Points B and C are obtained as the intersection of the curve with horizontal lines representing the start of the second and third blocks; thus,

their time coordinates will be $(t_{B2},\ FBL)$ and $(t_{B3},\ 2FBL)$.

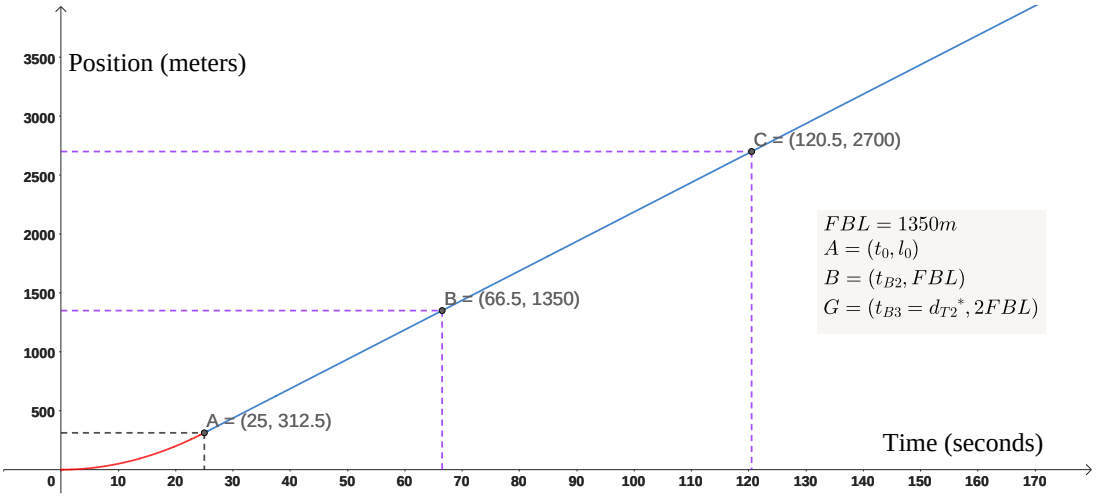

Figure 5.14: SRV0-A, FXB with FBL = 1350 m: position of the first train with respect to time, points of shape change of the curve and time needed to reach the second and third block for a specific value of the block length.

Table 5.3 shows the results obtained with Equation 5.9 compared to those achived by simulating the proposed service making use of the developed model. Note that different block lengths are considered, all belonging to the second case of Equation 5.9, meaning that the simulations regard only the scenario of the blocks being large enough that the first train reaches the third one only after having finished the initial acceleration.

FBL [m]	$d_{T2}{}^*$ [s]	t_{B3} from Simulink [s]
800	81.74	84.06
1150	109.74	112.22
1350	125.74	128.20
1800	161.74	164.39

Table 5.3: SRV0-A: Optimal second train delay (evaluated from Equations 5.9) and time for the first train to reach the third block (obtained empirically) with respect to different fixed block lengths

The difference between the analytical results and the simulation outputs reported in Table 5.3 is negligible, and most importantly, it is constant with the FBL. Indeed, by rewriting Equation 5.9, replacing the symbols with their numeric counterparts and considering only the second case, Equation 5.10 is obtained:

$$t_{B3}(FBL) = d_{T2}{}^*(FBL) = 17.74 + 0.08\ FBL \tag{5.10}$$

While making a linear regression on the last column of Table 5.3, Equation 5.11 is obtained:

$$t_{B3\ sim}(FBL) = 17.38 + 0.08\ FBL \tag{5.11}$$

The cause of the difference between the second and third columns in Table 5.3, as well as between Equations 5.10 and 5.11, lies in the fact that the analytical solution prescribes a constant speed after acceleration. On the other hand, during the simulation, the speed is never actually constant, but rather it oscillates around a constant reference speed (the MRSP), as explained in Section 3.3.2.

Expressing the line capacity in terms of the block length can be achieved by simply considering the reciprocal of the time distancing. For the considered case, i.e., the second case of Equation 5.9, Equation 5.12 can be derived with few algebraic steps:

$$LC(FBL) = \frac{v}{l_0 + l_T + FBL} \tag{5.12}$$

Once the description of the FXB signalling system has been completed, attention is paid to the MVB one. In this case, there are no equivalent time-based thresholds to t_{B2} and t_{B3}, making it harder to derive an analytic expression of the time distance and subsequently of the line capacity. However, given that no blocks are defined, no dependency over the block length has to be considered. Therefore, the minimum delay to guarantee the non-violation of the safety distance can be evaluated empirically, by performing simulations with decreasing values of d_{T2}, until the safety distance observation is not perfect anymore. Keeping all the specifications equal to the ones adopted for the FXB evaluation, it results in the following optimal time delay for the first train for MVB:

$$d_{T2\ MVB}{}^{*} <= 28\ s \implies LC_{MVB} = 128.57\ \text{trains/h} \tag{5.13}$$

To compare the results obtained considering the two signalling systems, consider Equation 5.9, specifically its first case: it can be reverted to obtain the value of the block length needed to guarantee a certain optimal delay of the second train, i.e., a certain minimum time distancing between the trains. By inserting the value $d_{T2\ MVB}$ obtained in the last paragraph, the FBL reported is the one needed to guarantee the same line capacity performances for the FXB and MVB signalling systems:

$$FBL(d_{T2\ MVB}{}^{*}) = 129.50\ m \tag{5.14}$$

The fixed block length obtained with this procedure is significantly lower than those

typically adopted (it is here recalled that the standard value is set to 1350 m). Recalling Section 3.2.2, Equations 3.10 to 3.14 evaluate the minimum FBL that could be chosen to still maintain a reasonable safety margin, and whatever the specifications of the model, the value obtained in Equation 5.14 will be lower than that minimum value. Thus, considering line capacity, it is practically impossible to build a line on SRV0 with a fixed block signalling system making it more convenient than a line with a moving block one.

5.5.2. Line capacity on SRV0-B

In this Section, attention is paid to SRV0-B, which resembles SRV0-A, but with the presence of a single station, at which both trains have to stop. The analysis will be conducted in a similar way as for SRV0-A, as described in the following:

- the fundamental requirement is that the time distancing must always be sufficiently long to prevent the reception of yellow signalling for the FXB signalling system, and the violation of the safety distance for the MVB one. Notice that if and only if this requirement is fulfilled, the time distancing between the trains is constant and equal to the initial delay of the second train (while the presence of a station makes the space distancing not constant under any condition).
- considering a FXB signalling system, the delay d_{T2} must be at least the time needed for the first train to reach the third block t_{B3}. Thus, an analytical expression for the optimal delay of the second train can be obtained as ${d_{T2}}_{FXB}{}^{*}(FBL) = t_{B3}(FBL)$, and its results confronted with the empirical ones;
- considering a MVB signalling system, that optimal initial delay ${d_{T2}}_{MVB}{}^{*}$ will be empirically obtained.
- finally, the FXB and MVB results can be compared, and if possible it will be stated if one is better than the other and in which cases.

Focus now the attention to the motion of the leading train along the line, considering Figure 5.15.

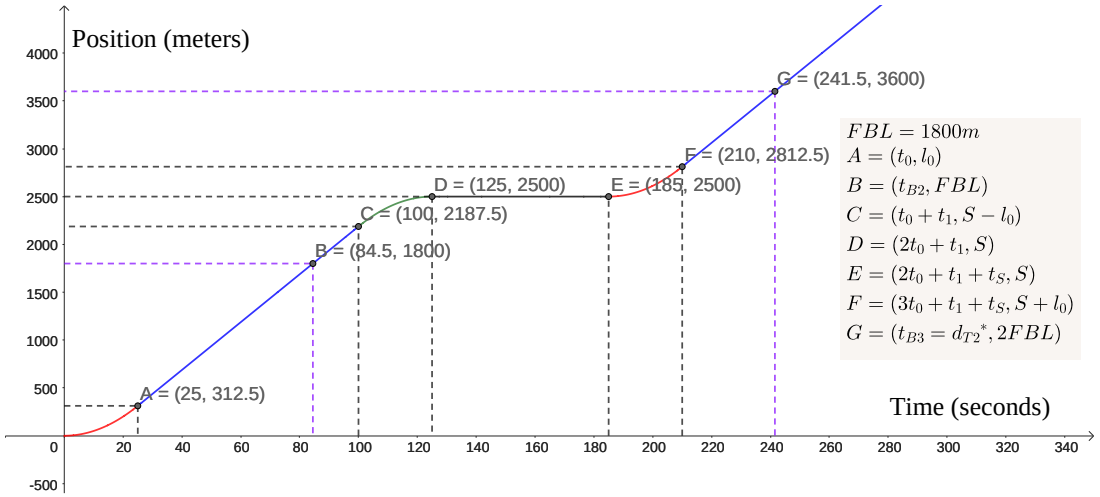

Figure 5.15: SRV0-B, FXB with FBL = 1350 m: position of the first train with respect to time and time needed to reach the second and third block for a specific value of the block length.

Following the Figure, the train will perform various kind of motion in sequence. First, it accelerates to the reference speed (reaching point A in the Figure). That speed is maintained until the train is close enough to the station that it has to start the deceleration (point C). Then, the train decelerates to stop at the station position (point D) and stays still for a prescribed stop time (point E). Finally, it accelerates again up to the reference speed (point F), furtherly maintaining it for the rest of the simulation. Thus, the relationship between block length and initial delay of the second train is composed of five cases (first acceleration, first uniform motion, deceleration, second acceleration and second uniform motion).

$$d_{T2}{}^*(FBL) = t_{B3}(FBL) = \begin{cases} \sqrt{\frac{4FBL}{a}} + \frac{l_T}{v} & \text{if } \ 0 \leq 2FBL < l_0 \\ t_0 + \frac{2\ FBL - l_0}{v} + \frac{l_T}{v} & \text{if } \ l_0 \leq 2FBL < S - l_0 \\ t_0 + t_1 + \frac{\sqrt{v^2 - 2a\ (2FBL - (S - l_0))}}{a} + \frac{l_T}{v} & \text{if } \ S - l_0 \leq 2FBL < S \\ 2t_0 + t_1 + t_S + \sqrt{2\ \frac{2FBL - S}{a}} + \frac{l_T}{v} & \text{if } \ S \leq 2FBL < S + l_0 \\ 3\ t_0 + t_1 + t_S + \frac{2FBL - (S + l_0)}{v} + \frac{l_T}{v} & \text{if } \ S + l_0 \leq 2FBL \end{cases} \tag{5.15}$$

where:

- S is the position of the station, which is equal to 2500 m;
- $t_1 = \frac{S-2l_0}{v}$ is the time spent during the first uniform motion, which is equal to 75 s;
- t_S is the time spent still at the station, which is equal to 60 s;

To have a general understanding of Equation 5.15, a few remarks need to be considered. The procedure to obtain each expression in Equation 5.15 is similar to the one described to obtain Equation 5.9. Apart from the time related to the train length, which is there to account for the delay of the rear end with respect to the front end, each Equation contains a constant term, which represents the time needed to reach the lower bound of the related condition interval, plus a term varying on the FBL: it will be linear for the cases of uniform motion and parabolic for the other cases, in particular, for the deceleration trait, ${d_{T2}}^*(FBL)$ will contain the term $-\sqrt{2FBL}$, while for the acceleration traits, it will contain the term $+\sqrt{2FBL}$. Moreover, the first two Equations are identical to the one presented for SRV0-A (Equation 5.10), as they represent the cases in which the third block is reached before the train has to start decelerating for the station, i.e., when the presence of the station has no influence in the evaluation of the optimal initial delay of the second train. Furthermore, the acceleration and deceleration rates are assumed to be equal ($+a$ for acceleration and $-a$ for deceleration), thus the t_0 is the time needed for reaching the reference speed from being still as well as for stopping completely from the reference velocity. Finally, The stop time t_S is added only for the last two cases, in which the third block is reached after stopping at the station.

By performing various simulations with different fixed block lengths (FBL), it is possible to empirically obtain the values of t_{B2} and t_{B3}, as reported in Table 5.4. The second

FBL [m]	${d_{T2}}^*$ [s]	t_{B3} from Simulink [s]
800	81.74	83.94
1150	110.24	127.43
1350	210.24	226.95
1800	246.74	263.86

Table 5.4: SRV0-B: Optimal initial delay for the second train (evaluated from Equation 5.15) and time for the first train to reach the third block (obtained empirically) with respect to different block lengths.

column contains the optimal second train delay ${d_{T2}}^*$, i.e., the minimum delay of the second train that prevents the reception of yellow signal by the second train. That is evaluated analytically through the use of Equation 5.15. The third column, which reports

empirical data, is obtained from simulating SRV0-B.

As for Table 5.3, the last two columns differ slightly. However, the difference between analytical and empirical data is now more significant and not constant with the block length. This happens because in addition to the difference in terms of speed control algorithm (already discussed commenting Table 5.3), also the effect of the acceleration and deceleration plays a significant role. In fact, as previously mentioned, Equation 5.15 is written assuming specularity between acceleration and deceleration, in particular regarding t_0 and l_0. However, while the acceleration is always limited at 1 $m \cdot s^{-2}$, the deceleration prescribed for lowering the speed is less than that value, as explained in Section 3.2.1, Equations 3.5 to 5.9. For example, if the prescribed deceleration had a modulus 50% lower than the acceleration, the deceleration time and space would be double the ones for the acceleration. For this reason, the second and third columns of Table 5.4 will differ especially in the last three elements, which are obtained by simulating cases of the third block being reached during or after the deceleration for stopping at the station.

An explicit expression for LC could be obtained by simply considering the reciprocal of Equation 5.15, which is not reported for the sake of simplicity. The analysis of the line capacity can be done equivalently on the optimal delay of the second train like it has been done for SRV0-A.

Once the description of the FXB signalling system has been completed, attention is paid to the MVB one. In this case there is no analytical expression of the optimal delay of the second train, that is the minimum delay that allows the train to perform the route without ever violating the safety distance from the first train. However, it is possible to empirically find a value for it, by performing simulations with various values of d_{T2} and looking for the minimum one that ensures the non-violation of the safety distance. Keeping all the specifications equal to the ones adopted for the FXB evaluation, it results:

$$d_{T2\ MVB} = 128\ s \implies LC_{MVB} = 28.125 \text{ trains/h} \tag{5.16}$$

By inverting Equation 5.15 and evaluating it for $d_{T2\ MVB}$, the FBL needed to guarantee the same line capacity performances for the FXB and MVB signalling systems is obtained:

$$FBL(d_{T2\ MVB}) = 1120\ m \tag{5.17}$$

This result is significant, as a FBL value of 1120 m is not so smaller than the standard

one (1350 m). Thus, a line with blocks of length equal or smaller to $FBL(d_{T2\ MVB})$ could be designed. In that case, the FXB signalling system would outperform the MVB one in terms of line capacity.

However, an interesting discussion can be made referring to the effect the station position can introduce over the time distancing ${d_{T2}}^*$ To this end, Equation 5.16 is evaluated at the boundaries of its cases:

- considering the third case at its condition upper bound, if $2FBL = S$ then ${d_{T2}}^* = 2t_0 + t_1 + \frac{l_T}{v} = 130.24\ s$;
- considering the fourth case at its condition lower bound condition, if $2FBL = S$ then ${d_{T2}}^* = 2t_0 + t_1 + t_S + \frac{l_T}{v} = 190.24\ s$;

Clearly, there is a difference coming from the time that the train has to spend still at the station, i.e., $t_S = 60\ s$. If $d_{T2\ MVB}$ were to fall in the interval (130.24, 190.24), there would be no fixed block length that made the two signalling systems equivalent in terms of line capacity.

In any case, the presence of even just one station makes the comparison not straightforward. Indeed, for SRV0-A the MVB signalling system was outperforming the FXB one for any reasonable choice of the block length. On the other hand, for SRV0-B there is a threshold value for FBL that allows making the two signalling systems perform in a similar way in terms of line capacity. Even though the identification of such threshold is not straightforward for the considered case, SRV0-B allows recognising that the benefits of MVB signalling is strongly dependent on the presence and location of the railway stations, together with the actual size of the blocks adopted in the framework of FXB signalling.

Table 5.5 reports the value for those thresholds with respect to the position of the station (recall that SRV0-B is built on a fictional line, so the station can be seen as a parameter of the simulation).

Station position [m]	FBL threshold [m]
900	470
1800	910
2500	1120
3200	1444

Table 5.5: FBL value that makes the FXB and MVB signalling systems equivalent in terms of line capacity with respect to the position of the station.

5.5.3. Line capacity on SRV1

After analyzing and comparing the signalling systems on the simplest services, the simulations have to be performed on a realistic and more complex line. The requirement of not encountering yellow signals or not violating the safety distance (depending on the signalling system adopted) is maintained to evaluate the line capacity.

In this case, it will be significantly difficult to give an analytical expression of the optimal delay of the second train, since it would require many cases depending on the fixed block length. Thus, the comparison procedure will only be based on the results of the simulations.

Table 5.6 reports the results obtained in the FXB environment, both in terms of minimum delay of the second train so that it never encounters a yellow signal $d_{T2}{}^*$ and of line capacity LC (the meaning of the last column will be explained shortly). Also in this case, if the "no yellow signal" requirement is fulfilled, the time distancing between the trains will be constant and equal to the initial delay of the second train. Thus, the LC can be obtained by considering the reciprocal of $d_{T2}{}^*$ and multiplying by 3600.

FBL [m]	$d_{T2}{}^*$ [s]	LC [trains/h]	Use of data point
800	230	15.65	T
900	243	14.81	T
1000	255	14.12	V
1150	267	13.48	T
1250	278	12.95	V
1350	293	12.29	T
1450	313	11.50	T
1550	385	9.35	T
1600	381	9.45	V
1700	332	10.84	T
1800	367	9.81	T
1900	414	8.70	V
2000	432	8.33	T

Table 5.6: Empirical results of simulating SRV1 with FXB signalling system regarding theoretical line capacity with respect to block length

As a general rule, the longer the block is, the worse the performance in terms of LC are. However, there are outliers, such as for FBL close to 1600 m. This is due to the intricate combination of all factors that affect the trains in motion, which are not known a prior. In order to better explain this result, a prediction model is realized based on some of the data points in Table 5.6 and validated on the others. The fourth column of Table 5.6 specifies

the usage of the data: T identifies the training data used to realize the predictive model, while V stands for validation data used to evaluate the model fitting accuracy. Performing an exponential regression on the T-labeled data points leads to Equations 5.18 and 5.19 (which is obtained by taking the reciprocal of Equation 5.18). By representing Equation 5.18 graphically, Figure 5.16 is obtained. The blue dots represent the data points used for testing (generate the regression model) while the green dots represent the data points used for validation (evaluate the goodness of the model). The red line represents the exponential regression function obtained considering the testing data points.

$$d_{T2\ FXB}{}^{*}(FBL) = 152.88\ e^{(5\cdot 10^{-4} FBL)} \tag{5.18}$$

$$LC_{FXB}(FBL) = 6.5 \cdot 10^{-2}\ e^{(-5\cdot 10^{-4} FBL)} \tag{5.19}$$

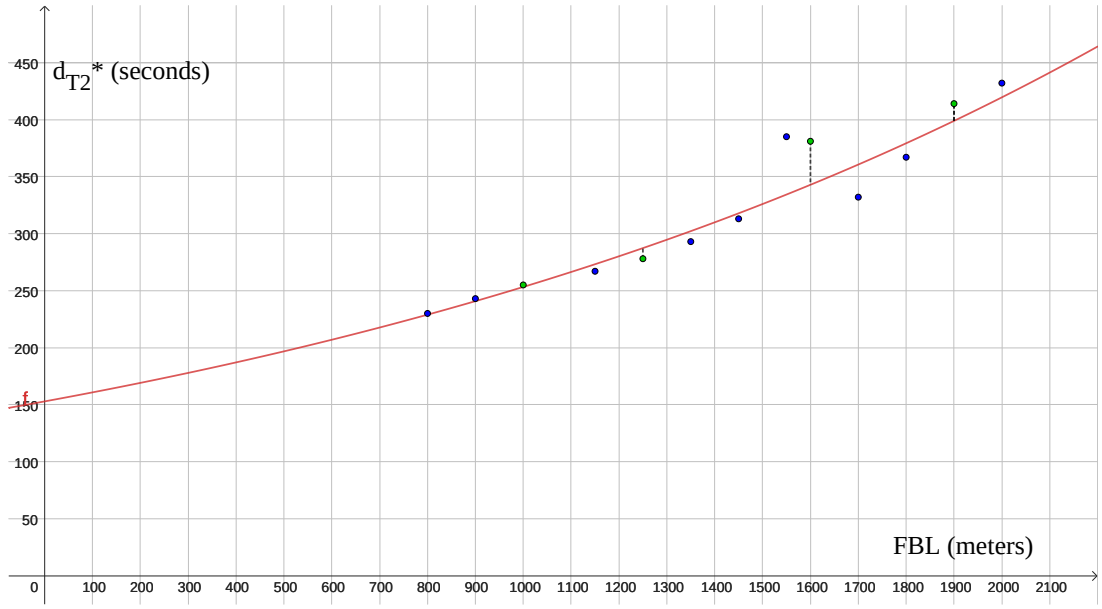

Figure 5.16: $d_{T2\ FXB}{}^{*}$ with respect to FBL and empirical data points.

Once the evaluation of line capacity of a FXB signalling system has been completed, attention is paid to MVB signalling. In this case there is no dependence on the block length; instead, the optimum delay and the theoretical line capacity are defined only once for the service. Empirically, it results:

$$d_{T2\ MVB}{}^{*} = 113\ s \implies LC_{MVB} = 31.86\ \text{trains/h} \tag{5.20}$$

That value is not obtainable with the FXB signalling system, as even if FBL = 0 could be set, it would still result $d_{T2\ FXB}{}^{*}(FBL = 0) = 152.88\ s > 113\ s = d_{T2\ MVB}{}^{*} \implies LC_{FXB} < LC_{MVB}$, meaning that in SRV1 the moving block signalling system returns to be better-performing than the fixed block one for any feasible block length.

In conclusion, the FXB signalling system is very sensitive to the increase in the number of stations. The reason lies in the fact that each station adds a level of complexity to the interaction between station positioning and block boundaries. Indeed, depending on the location of a station inside a block, two situations may occur. If the station is far from the block beginning when the first train stops it is fully contained in the block, and the second train only sees the station block as occupied. On the other hand, if the station is close to the block beginning when the first train stops its rear end is still in the previous block, and the second train sees both of them as occupied. Thus, it will have to be distanced significantly to prevent a yellow signal, as shown in Figure 5.17.

Figure 5.17: Influence on coloured signalling of the station positioning inside the block

The most general conclusion that can be reached through this analysis is that there are cases in which the moving block signalling system is favourable with respect to the fixed block one in terms of line capacity. Depending on the configuration of the line and the specifications considered in the implementation of the signalling system, the moving block

technology may be the best choice. After having discussed the line capacity considering various services of increasing complexity, in the next Section attention will be paid to the morion regularity KPI.

5.6. Motion regularity evaluation

Motion regularity (MR) is the second KPI used to compare the FXB and MVB signalling systems. Recalling Section 5.2.3 Equation 5.3, it is defined as the ratio between the areas under the static and dynamic reference speed curves (s-MRSP and d-MRSP). As the d-MRSP is obtained by diminishing the s-MRSP in the case of a yellow signal for FXB or a violation of the safety distance for MVB, their ratio will be smaller or equal to 1. It is interesting to evaluate motion regularity for all services. SRV0-A and SRV0-B will act as introductory cases, while the other services will be used to show how different forms of signalling affect the motion regularity of the second train when it tends to get closer to the first one on a realistic line.

As previously stated, motion regularity is a parameter proper to the single train, so it could be investigated on both the first and second vehicle. However, the MR of the first train will surely be 100%, as its motion is not affected by the presence of any other train, making signalling irrelevant in the definition of the MRSP. Thus, in all cases analysed below, the MR will be always computed with reference to the second train.

5.6.1. Motion regularity for SRV0-A

SRV0-A was used in Section 5.5.1 to evaluate the optimal delay of the second train, i.e., the one that prevents the reception of yellow signal lights for FXB signalling and the violation of the safety distance for MVB signalling. In that case, motion regularity would definitely be 1, as there would be no difference between static and dynamic MRSP. Thus, SRV0-A is useful to show the effect of the delay of the second train on the MR, especially when it becomes lower than ${d_{T2}}^*$ evaluated in Section 5.5.1.

First, the FXB signalling system will be considered. The value of the optimal delay of the second train is dependent on the block length FBL, as discussed in Section 5.5.1. To perform the simulations, it has been set FBL = 1350 m, making the time needed for the first train to reach the second and third block respectively $t_{B2} = 74\ s$ and $t_{B3} = 128\ s = {d_{T2}}^*$.

If $0 \leq d_{T2} < t_{B2}$, the second train is required to wait until t_{B2} before it can start moving, since otherwise the first block is still occupied by the first train. Please refer to Figure 5.18

(a) and (b). The only difference between these Figures is the presence of a grey rectangle at the beginning of the graph of Figure 5.18 with a base equal to the time needed for the first train to reach the second block, i.e., $t_{B2} = 74\ s$. Thus, the light-blue area A1 will be the same in both cases and in general, it does not vary with the second train delay in the considered interval. The grey area A2 will be a rectangle with a height equal to the reference speed allowed in the service, and a base equal to the total simulation time minus the initial second train delay. Thus, an analytical expression for A2 can be written:

$$A_2(d_{T2}) = (T - d_{t2}) \cdot v_{max} = (600\ s - d_{T2}) \cdot 90\ \frac{km}{h} \tag{5.21}$$

The value of A1 is found with empirical data (please refer to Table 5.7):

$$A_1 = A_2(d_{T2}) \cdot MR(d_{T2}) \tag{5.22}$$

This expression could be evaluated for any value of d_{T2} in the appropriate range, and it should always be the same. Taking the limits of the interval:

$$A_1 = A_2(0) \cdot MR(0) = A_2(t_{B2} = 74) \cdot MR(t_{B2} = 74) = 44861\ s\frac{km}{h} \tag{5.23}$$

Thus, after few algebraic steps:

$$0 \leq d_{T2} < t_{B2} \implies MR(d_{T2}) = \frac{A_1}{A_2(d_{T2})} = MR(0)\ \frac{T}{(T - d_{T2})} \tag{5.24}$$

If $t_{B2} \leq d_{T2} < t_{B3}$, the second train can start its motion promptly, but it will immediately receive a yellow signal, released only at t_{B3} as until then the second block is still occupied by the first train. Please refer to Figure 5.18 (c). In this interval, the second train will encounter the yellow signal along its motion, making the light-blue area not cover the grey one completely. If the second train delay is made to vary in this interval, the light-blue area A1 does not remain constant, but rather it increases with it. It is not easy to give an analytical expression of A1, thus, polynomial regression will be performed on the data points obtained by the simulations (reported in Table 5.7). It results:

$$t_{B2} \leq d_{T2} < t_{B3} \implies MR(d_{T2}) = -1.65\ {d_{T2}}^2 + 4.31 \cdot 10^{-2}\ d_{T2} + 0.72 \tag{5.25}$$

Finally, if $t_{B3} \leq d_{T2}$, the second train is delayed enough that it does not receive yellow signals through its motion, so MR = 100%. Please refer to Figure 5.18 (d). In this case, the second train does not encounter any yellow signal along its motion. Hence the light-

blue area perfectly overlaps the grey one, and both A1 and A2 are rectangles with the same value, obtained through Equation 5.22.

$$t_{B3} \leq d_{T2} \implies MR = 100\% \tag{5.26}$$

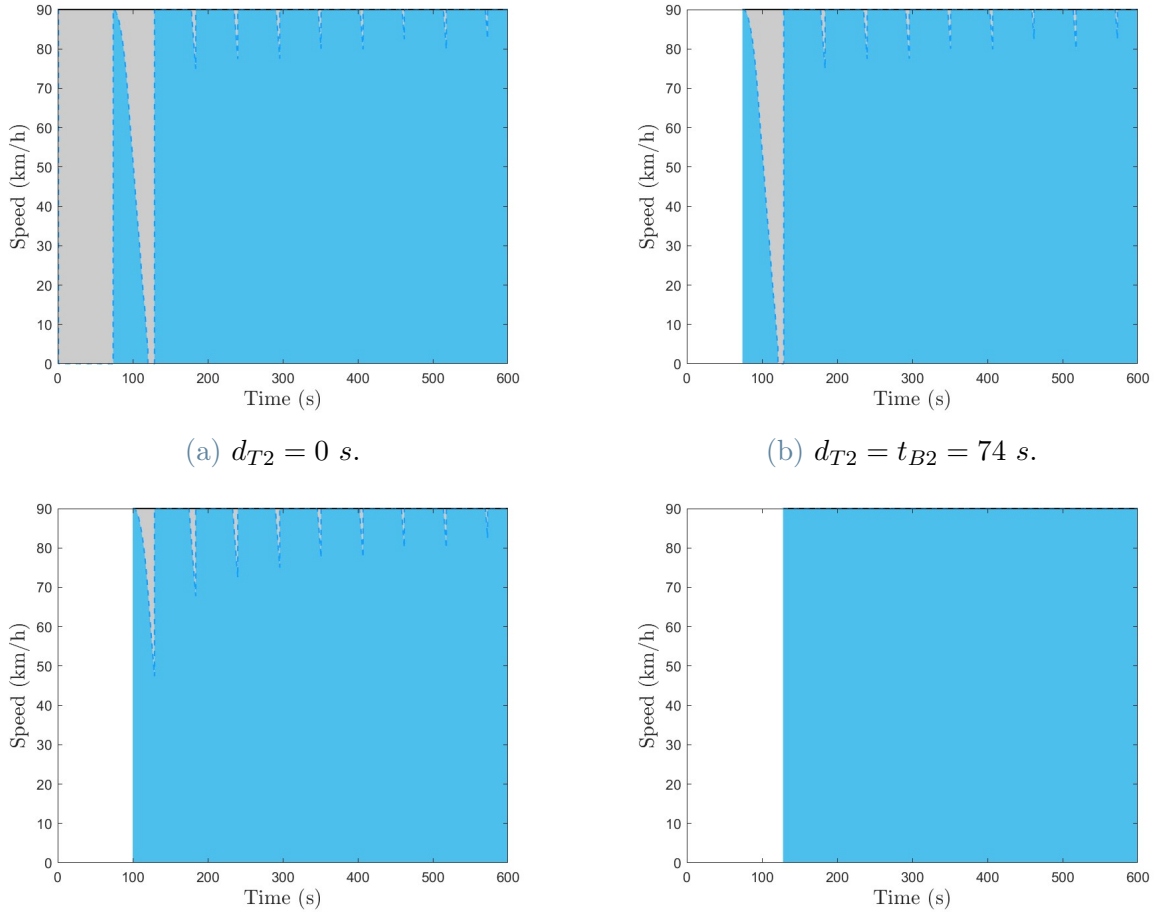

(a) $d_{T2} = 0\ s.$

(b) $d_{T2} = t_{B2} = 74\ s.$

(c) $d_{T2} = 100\ s.$

(d) $d_{T2} = t_{B3} = 128\ s.$

Figure 5.18: s-MRSP, d-MRSP and areas under them for various values of the initial delay of the second train. The light blue area is the one under the d-MRSP, referred to as A1, the grey area is the one under the s-MRSP, referred to as A2.

Table 5.7 collects the data obtained through the simulations of the two areas and the motion regularity for various values of the second train delay.

Now, the MVB signalling system will be considered. In this case, there are no thresholds t_{B2} and t_{B3} for the analysis of MR, but there still is a value for the delay of the second train that guarantees the non-violation of the safety distance through the whole service: recalling Section 5.5.1, Equation 5.13, ${d_{T2}}_{MVB}{}^{*} = 28\ s$. Thus, delaying the second train

d_{T2} [s]	A_1 $[s\frac{km}{h}]$	A_1 $[s\frac{km}{h}]$	MR
0	44 861	53 999	83.08
14	44 861	52 739	85.06
28	44 861	51 479	87.14
$t_{B2} = 74$	44 861	47 339	94.76
90	44 591	45 899	97.15
100	44 206	45 002	98.23
110	43 838	44 099	99.41
$t_{B3} = 128$	42 479	42 479	100
140	41 399	41 399	100

Table 5.7: SRV0-A, FXB with FBL = 1350 m: area below dynamic and static MRSP and motion regularity indicator for different values of second train delay.

of a quantity greater or equal to that value results in perfect motion regularity; on the other hand, a lower time delay makes motion regularity dependent on the second train delay, with a good linear approximation.

Table 5.8 collects the data obtained through the simulations of the two areas and the motion regularity for various values of the second train delay, which are considered to build a linear regression function of the MR in Equation 5.27.

d_{T2} [s]	A_1 $[s\frac{km}{h}]$	A_1 $[s\frac{km}{h}]$	MR
0	51 292	53 999	94.99
7	51 329	53 369	96.18
14	51 229	52 739	97.14
21	51 266	52 109	98.38
$d_{T2\ MVB}{}^{*}$ =28	51 479	51 479	100
40	50 399	50 399	100

Table 5.8: SRV0-A, MVB: area below dynamic and static MRSP and motion regularity indicator for different values of second train delay.

$$0 \leq d_{T2} < d_{T2\ MVB}{}^{*} \implies MR_{MVB} = 1.68 \cdot 10^{-3}\ d_{T2} + 0.949. \tag{5.27}$$

$$d_{T2\ MVB}{}^{*} \leq d_{T2} \implies MR = 100\% \tag{5.28}$$

Figure 5.19 shows the results for both FXB and MVB signalling systems, obtained by plotting the data in Tables 5.7 and 5.8.

Figure 5.19 (a) represents the areas under the dynamic (A_1) and static (A_2) MRSP respectively in blue and in black as a function of the initial delay of the second train (d_{T2}).

The solid lines refer to the FXB signalling system and the dotted lines to the MVB one. The Figure shows that while A2 is identical for both signalling systems, A1 varies significantly. In particular, A1 is always greater for the MVB signalling system, meaning that MVB guarantees a higher utilization of the static reference speed.

Figure 5.19 (b) represents the motion regularity indicator (MR) as a function of the initial delay of the second train (d_{T2}). Again, the solid line refers to the FXB signalling system and the dotted line to the MVB one. Coherently to what was observed in Figure 5.19 (a), the MR for the MVB signalling system is always greater than the one for the FXB one. Also, the Figure shows how faster the MVB signalling system is able to reach perfect regularity with respect to the FXB one: at FXB, the second train needs to be delayed almost five times more than at MVB so that its motion is not affected by the presence of the first train and its regularity is perfect.

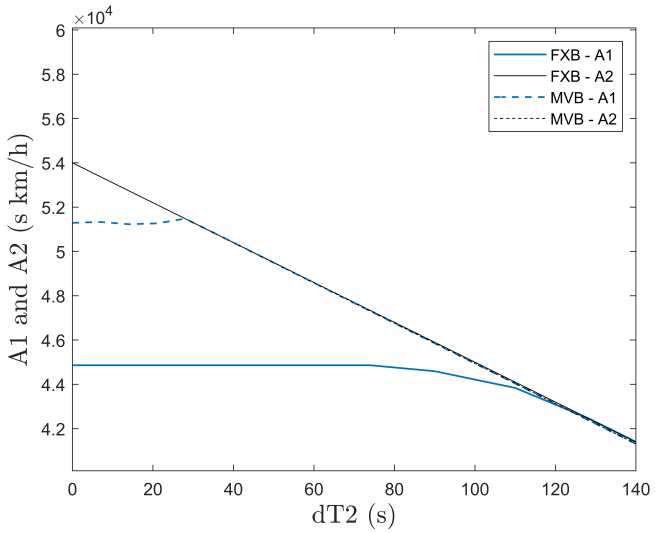

(a) A1 (in blue) and A2 (in black).

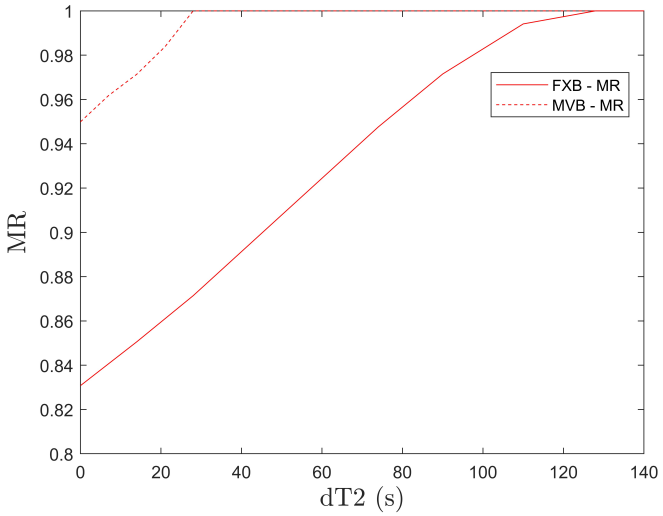

(b) MR.

Figure 5.19: SRV0-A FXB with FBL = 1350 m (solid lines) and MVB (dotted lines): A1, A2 and MR with respect to d_{T2}.

Once the analysis on SRV0-A has been presented, showing the advantages of the MVB signalling system with respect to MR, the next Section will pay attention to SRV0-B.

5.6.2. Motion regularity for SRV0-B

SRV0-B introduces a single station on the line. Also in this case, an optimal delay of the second train ${d_{T2}}^*$ can be evaluated. Thus,

- $d_{T2} < {d_{T2}}^* \implies MR < 1$
- $d_{T2} \geq {d_{T2}}^* \implies MR = 1$

First, the FXB signalling system will be considered. Recalling Section 5.5.3, Equation 5.19, if the block length is fixed to 1350 m, the time needed for the first train to reach the second and third block will be respectively $t_{B2} = 74\ s$ and $t_{B3} = {d_{T2\ FXB}}^* = 227\ s$. In this case, it is not trivial to provide an analytical expression for A_1, A_2 and MR. Thus, the empirical data obtained through the simulations and collected in Table 5.9 will be considered instead.

d_{T2} [s]	A_1 $[s\frac{km}{h}]$	A_2 $[s\frac{km}{h}]$	MR [%]
0	29 118	45 868	63.48
20	29 226	44 176	66.16
40	29 217	42 366	68.96
60	29 236	40 587	72.03
$t_{B2} = 74$	29 122	39 211	74.27
100	29 152	36 882	78.99
120	29 111	35 061	83.03
140	29 249	33 399	87.58
160	29 105	31 571	92.19
180	28 565	29 776	95.94
200	27 612	27 893	98.99
$t_{B3} = 227$	25 534	25 534	100
240	24 364	24 364	100

Table 5.9: SRV0-B, FXB with FBL = 1350 m: area below dynamic and static MRSP and motion regularity indicator for different values of second train delay.

Now, the MVB signalling system will be considered. Recalling Section 5.5.2 Equation 5.17, the optimal time delay for the second train is ${d_{T2\ MVB}}^* = 128\ s$. Thus, for lower values, the motion regularity of the second train will be lower than 100%. Also in this case, the most practical approach is to consider empirical data obtained through the simulations, collected in Table 5.10.

d_{T2} [s]	A_1 $[s\frac{km}{h}]$	A_2 $[s\frac{km}{h}]$	MR [%]
0	39 164	44 547	87.91
20	39 192	42 791	91.59
40	38 376	41 190	93.17
60	38 264	40 029	95.59
80	37 839	38 906	97.26
100	36 966	37 469	98.66
$d_{T2\ MVB}{}^{*} = 128$	34 992	34 992	100
140	33 912	33 912	100

Table 5.10: SRV0-B, MVB: area below dynamic and static MRSP and motion regularity indicator for different values of second train delay.

Figure 5.20 shows the results for both FXB and MVB signalling systems, obtained by plotting the data in Tables 5.9 and 5.10. The colour and line style code is the same as in Figure 5.19. Figure 5.20 (a) shows that while A2 is quite similar for both signalling systems, while A1 varies significantly. In particular, A1 is always greater for the MVB signalling system (dotted blue line with respect to solid blue line), meaning that the MVB system guarantees a higher utilization of the static reference speed. Coherently to what was observed in Figure 5.20 (a), Figure 5.20 (b) shows that the MR for the MVB signalling system is always greater than the one for the FXB one. Also, it shows how faster the MVB signalling system is able to reach perfect regularity with respect to the FXB one: for FXB signalling, the second train needs to be delayed almost twice more than what is needed at MVB so that it is motion is not affected by the presence of the first train and its regularity is perfect.

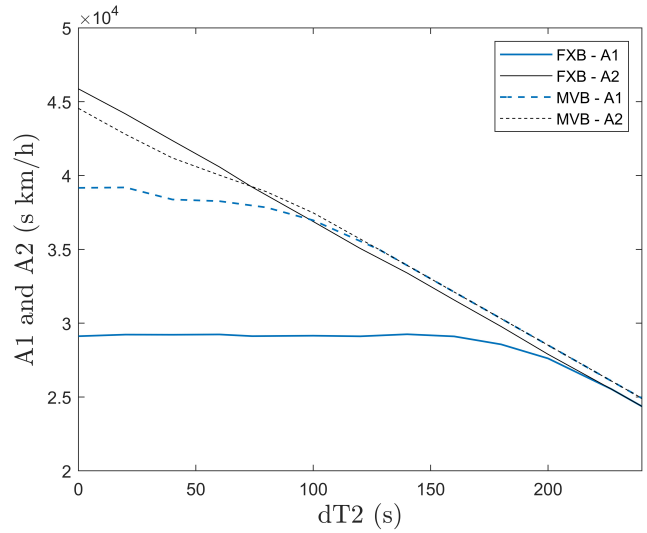

(a) A1 (in blue) and A2 (in black)

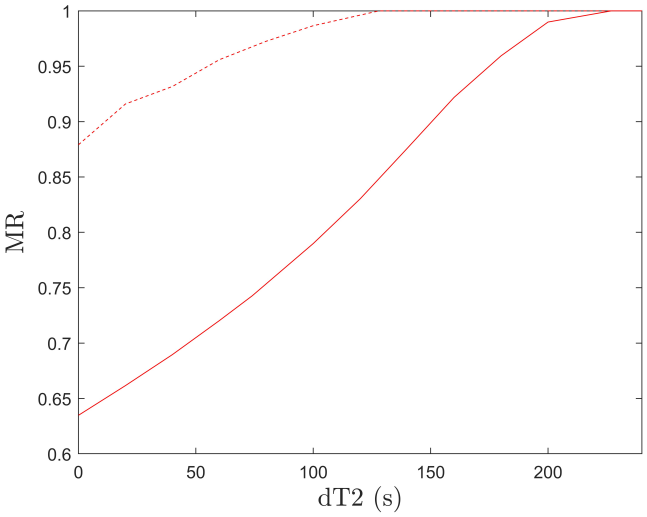

(b) MR

Figure 5.20: SRV0-B, FXB with FBL = 1350 m (solid lines) and MVB (dotted lines): A1, A2 and MR with respect to d_{T2}.

In conclusion, adopting a MVB signalling system is convenient with respect to a FXB one for motion regularity for both SRV0-A and SRV0-B. This advantage can be divided into two components: on the one hand, the performance for low values of second train delay; on the other hand, the minimum delay needed to guarantee perfect regularity. The MVB signalling system outperforms the FXB one with respect to both of these components. In particular, the presence of a station, which is peculiar of SRV0-B, makes the FXB performance drop with respect to the MVB one for low values of the second train delay. Therefore, the ratio between the motion regularities for null delay of the second train is

greater than 1 for both SRV0-A and SRV0-B, but it is the greatest for SRV0-B:

$$\left(\frac{MR(d_{T2}=0)_{MVB}}{MR(d_{T2}=0)_{FXB}}\right)_{SRV0-A} = 1.14 < 1.41 = \left(\frac{MR(d_{T2}=0)_{MVB}}{MR(d_{T2}=0)_{FXB}}\right)_{SRV0-B} \tag{5.29}$$

On the other hand, it makes the FXB performance more comparable to the MVB one in terms of minimum second train delay needed to guarantee perfect regularity (while still disadvantageous). Therefore, the ratio between the optimal initial delays of the second train is lower than one for both SRV0-A and SRV0-B, but it is the lowest for SRV0-A:

$$\left(\frac{{d_{T2\ MVB}}^*}{{d_{T2\ FXB}}^*}\right)_{SRV0-A} = 0.22 < 0.56 = \left(\frac{{d_{T2\ MVB}}^*}{{d_{T2\ FXB}}^*}\right)_{SRV0-B} \tag{5.30}$$

5.6.3. Motion regularity for SRV1

SRV1 is the first service built on a realistic line (recall Section 5.1.3 for its definition). Both trains have to serve 12 stations, and their models (in terms of their dynamics as well as their drivers' behaviour) are the same. Thus, if the trains were distanced enough at the start of the service, they would maintain the same time distance for the whole service, and the second train would not be influenced by the signalling system. Indeed, in Section 5.5.3, Table 5.6 reports the optimal delay of the second train for the FXB signalling system, i.e., the minimum delay needed to prevent the reception of the yellow signal: fixing the block length to FBL = 1350 m, it results ${d_{T2\ FXB}}^* = 239\ s$. Similarly, Equation 5.21 reports the optimal delay of the second train for the MVB signalling system, i.e., the minimum delay needed to guarantee the non-violation of the safety distance: ${d_{T2\ MVB}}^* = 113\ s$.

Given this short recap on the characteristics of SRV1, the motion regularity of the second train can be compromised in two ways: on the one hand, by choosing a lower delay than the optimal one; on the other hand, by choosing a higher delay than the optimal and disturbing the motion in other ways.

The first case would lead to a similar analysis to the one performed on SRV0-A and SRV0-B. Thus, an external disturbance will be introduced, making the second train get closer and closer to the first one even though it was delayed enough not to do so in nominal conditions. In particular, the first train will have to wait an unexpected time at a station in addition to the normal stop time, meaning that the second train will get closer to the first one during that time, potentially reaching a yellow signalled block or violating the safety distance, depending on the signalling system. Recall the stop time defined in

Section 5.1.3, Equation 5.1. In addition to that:

$$stopDelay_{t1}(5) = 300s \tag{5.31}$$

Meaning that there is an unexpected delay of the first train at the fifth station of 300 s.

First, the FXB signalling system will be considered. Figure 5.21 shows the block occupancy and continuous positioning inside the blocks of the trains, both regarding their front and rear end.

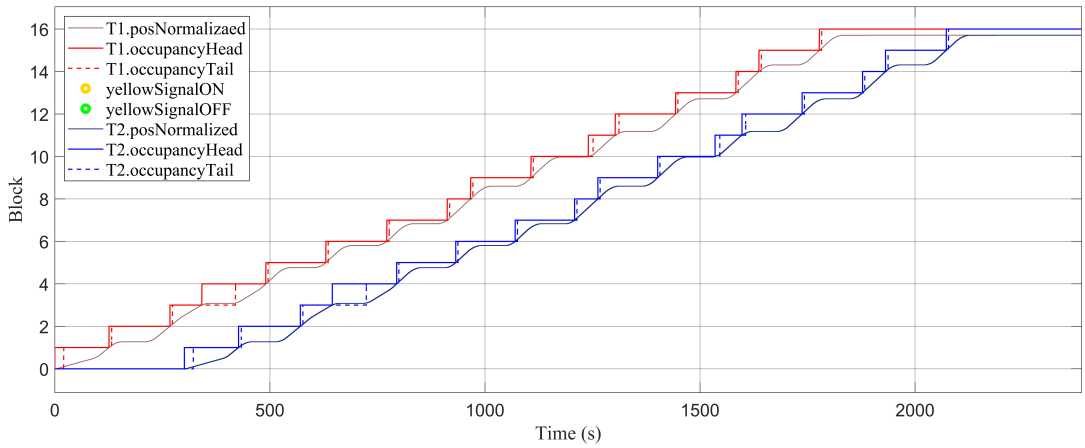

(a) Nominal scenario.

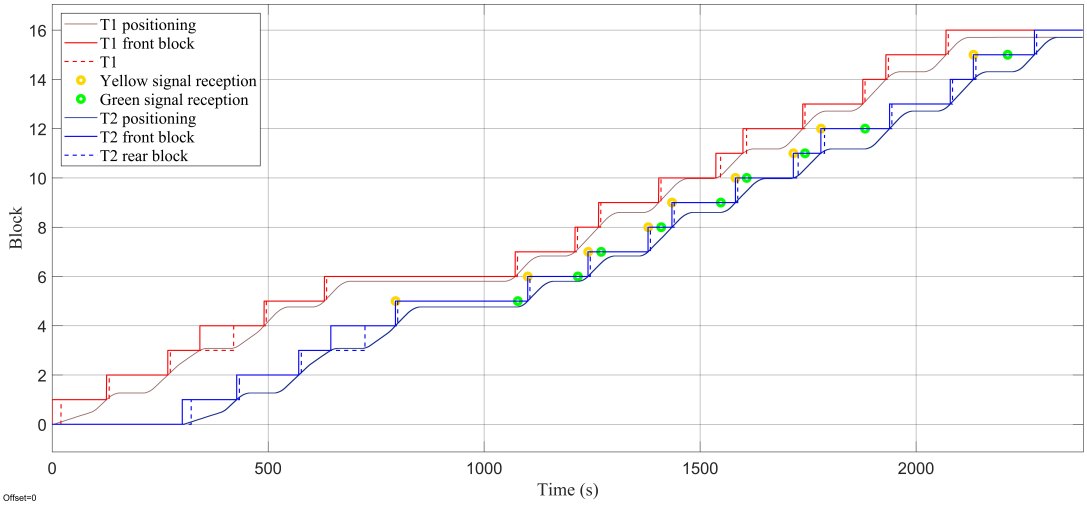

(b) Disturbed scenario, i.e., with an unexpected stop of the first train at the fifth station of 300 s.

Figure 5.21: SRV1, FXB with FBL = 1350 m: block occupancy of the trains (red lines for first train, blue lines for second train), both in their front ends (solid lines) and rear ends (dotted lines).

Figure 5.21 (a) represents the nominal service, meaning that there is no unexpected delay of the first train. If the initial time distancing is reasonably high, the second train never encounters a yellow signal. Figure 5.21 (b) represents the disturbed case, meaning that the first train has to wait for the unexpected delay at the fifth station. It is here reminded that the first station is located at position 0, meaning that the fifth station is located at the fourth plateau of the position curve. Even for reasonably high values of the initial time distancing, the second train reaches the first one and gets shown a yellow signal. Notice the yellow and green dots on the graph representing the moments in which the yellow signal is received and resolved.

Notice that the unexpected delay of the first train affects the signalling of the second train also after the first train has resumed its motion. This is because the second train starts moving as soon as the first train frees the block it had long occupied, without waiting for it to reach the further block. As an analogue example, consider a scenario in which the second train starts moving when the first train has left the first block, but it has not reached the third one yet, i.e., the interval (t_{B2}, t_{B3}). In that scenario, the second train can depart immediately, but it will encounter a yellow signal through its motion. Similarly, going back to the previous scenario, if the second train resumes the motion before the first train has reached the third block from it, it will encounter yellow signalling throughout all of its motion, also after the unexpected delay has resolved.

Figure 5.22 represents the MRSP curves and the areas under them: A1 (light blue area) under d-MRSP (dotted blue line), A2 (grey area) under s-MRSP (solid black line). By evaluating these areas and making the ratio between them, it is possible to obtain the motion regularity indicator for SRV1 at FXB, as shown in Equation 5.32.

$$MR_{FXB} = \frac{A_1}{A_2} = \frac{84975}{101240} = 83.94\% \tag{5.32}$$

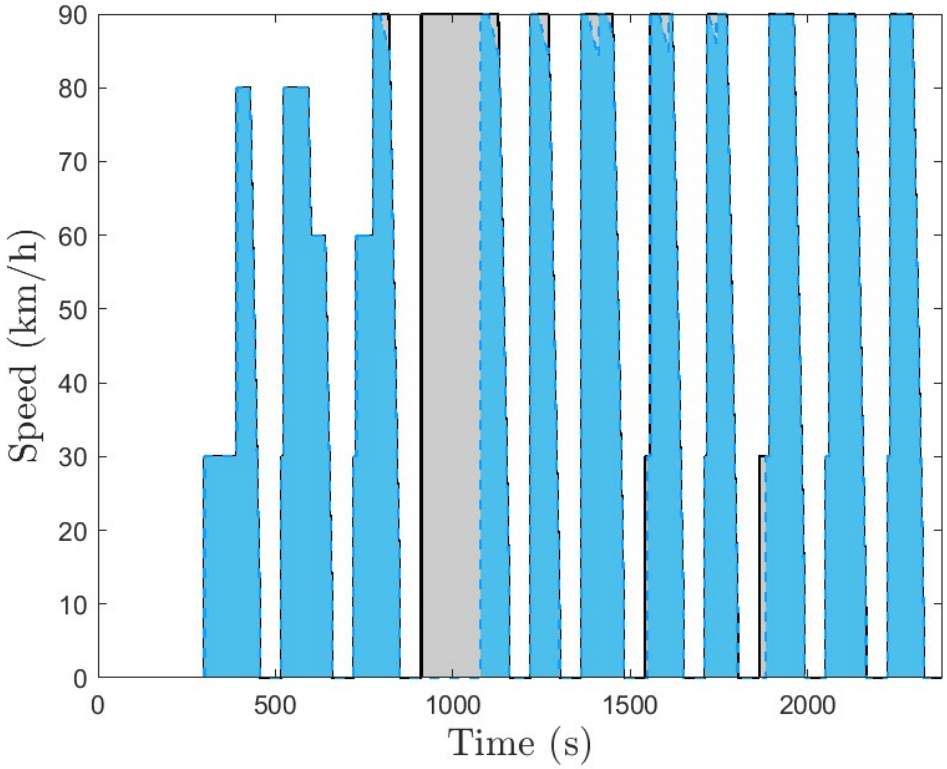

Figure 5.22: SRV1, FXB with FBL = 1350 m: Areas under s-MRSP (A2, grey) and d-MRSP (A1, light blue).

The results on motion regularity are that the biggest deviation of the d-MRSP from the s-MRSP happens when the second train catches up to the first one during its unexpected delay, but there are also other minor deviations afterwards.

Once the FXB case has been analysed, the MVB signalling system will be considered. Performing a simulation with the same unexpected delay leads to the results of Figure 5.23, which represents the position of the front and rear ends of both trains with respect to time.

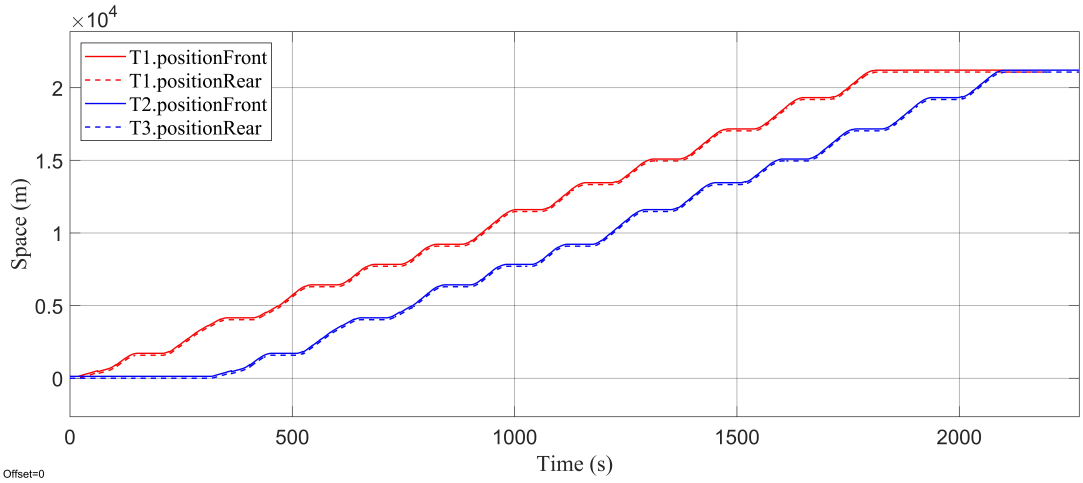

(a) Nominal scenario

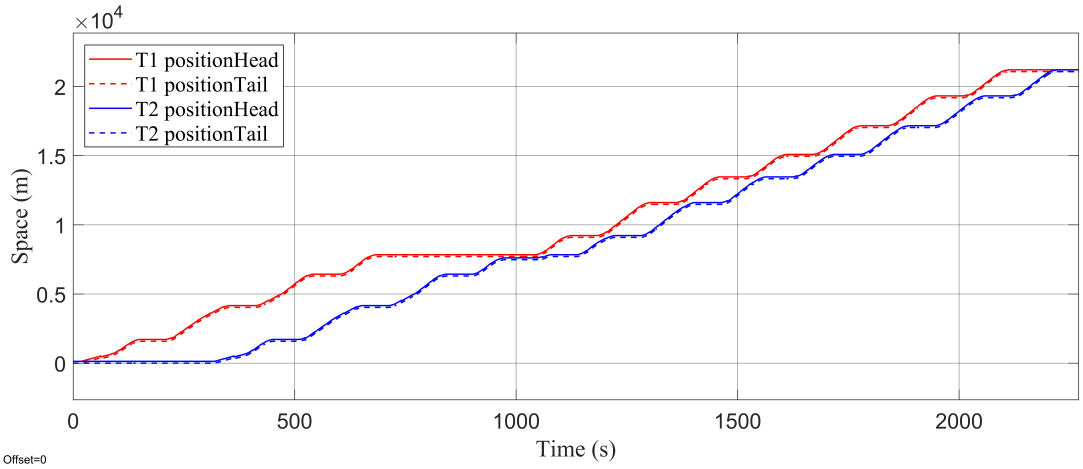

(b) Disturbed scenario, i.e., with an unexpected stop of the first train at the fifth station of 300 s

Figure 5.23: SRV1, MVB: Continuous position of the trains (red lines for first train, blue lines for second train), both in their front ends (solid lines) and rear ends (dotted lines).

Figure 5.23 (a) represents the nominal service. If the initial time distancing is realistically high, the second train will never violate the safety distance. Instead, Figure 5.23 (b) represents the disturbed case, i.e., the one with unexpected delay of the first train at the fifth station. Even for reasonably high values of the initial time distancing, the second train reaches the first one and violates the safety distance. Also in this case, the effect of the disturbance is not local, meaning that even after the safety distance has been restored the first time, there are other instances of safety distance violation. This effect can be evidenced by Figure 5.24, where the black line represents the safety distance evaluated at any time instant, while the red one represents the actual distance between the trains.

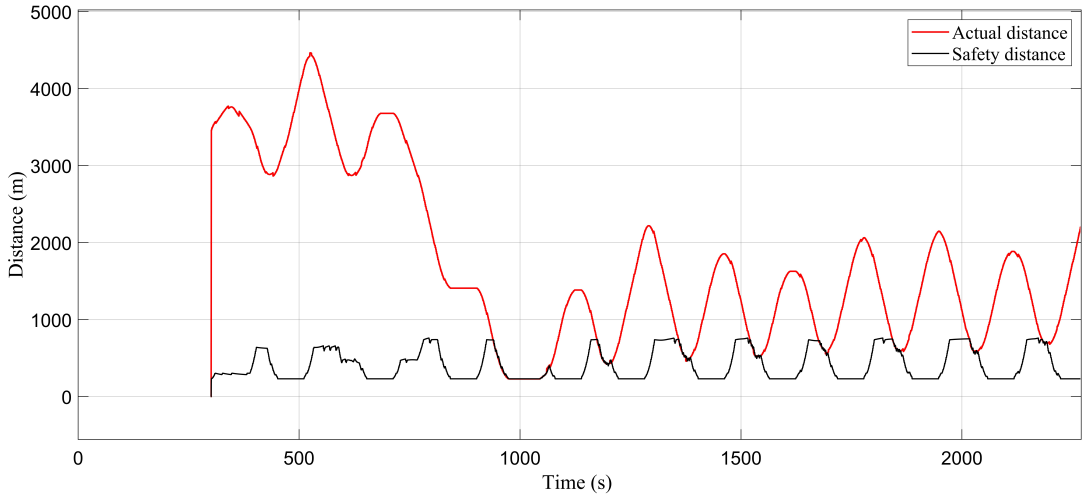

Figure 5.24: SRV1, MVB: Safety and actual distance between the trains in the disturbed scenario. The graph starts with the second train motion, i.e., at $d_{T2} = 360\ s$ for the presented simulation.

The results of motion regularity are similar to the ones obtained for FXB signalling. Figure 5.25 represents the MRSP curves and the areas under them (the color and style code is the same as Figure 5.22).

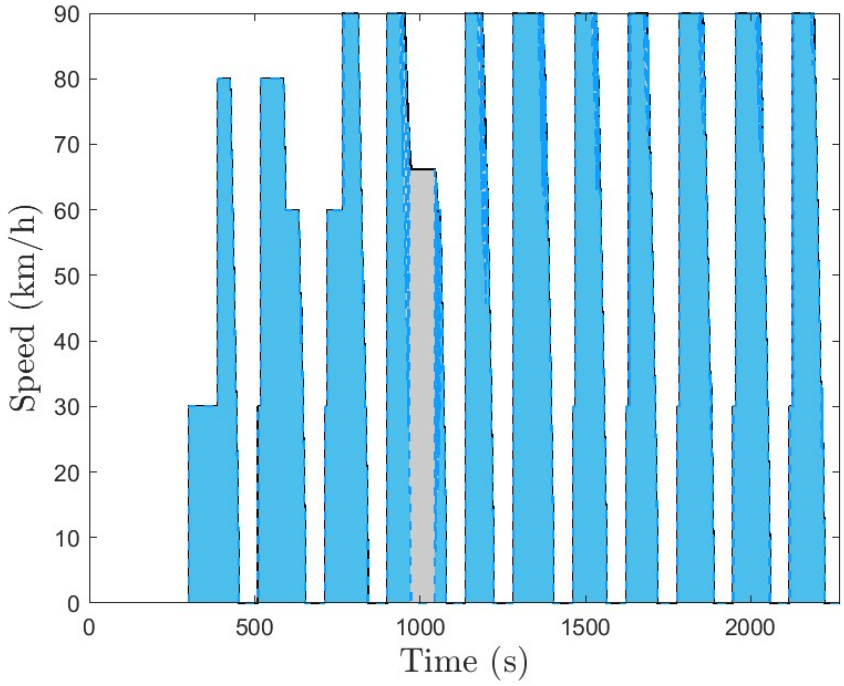

Figure 5.25: SRV1, MVB: Areas under s-MRSP (A2, grey) and d-MRSP (A1, light blue).

The main difference from the results obtained for FXB signalling is that while there are

still deviations of the d-MRSP from the s-MRSP after the unexpected delay has resolved, the d-MRSP is reduced more frequently but for less time. The reason lies in the fact that a yellow signal can only turn back green after the first train has overcome a specific point in the line, i.e., the end of the block it is currently occupying; on the other hand, when the safety distance is violated, it can be restored at any moment. As soon as that happens, the second train accelerates again, possibly violating the safety distance once more in a brief period of time. Then, it will decelerate again, starting the cycle over. This phenomenon can be seen in Figure 5.26, which is a zoom of Figure 5.25 showing examples of these slim notches in the static curve.

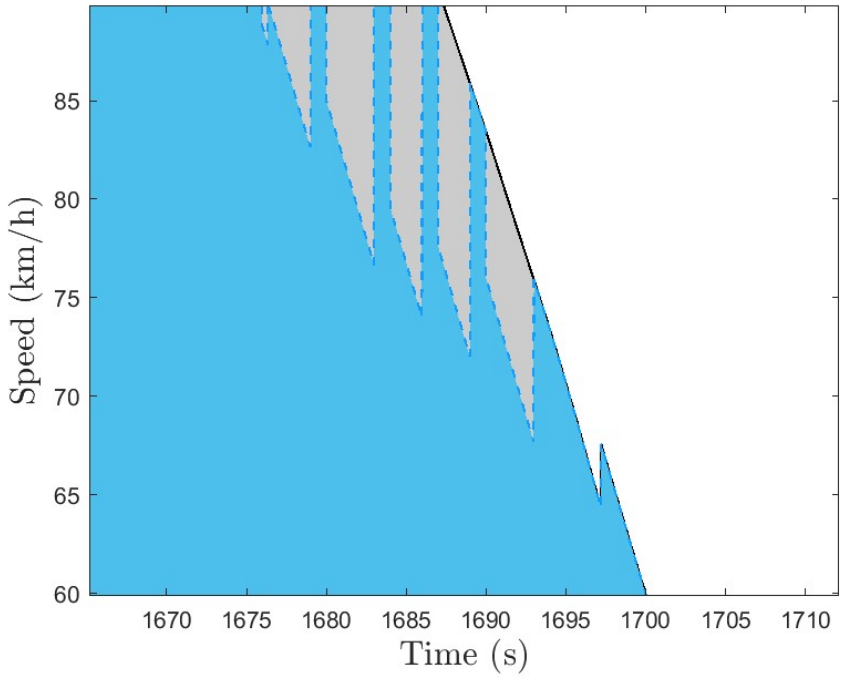

Figure 5.26: SRV1, MVB - Zoom on the slim deviation of the d-MRSP from the s-MRSP.

By evaluating the light blue and grey areas and making the ratio between them, the motion regularity indicator for SRV1 at MVB is obtained, as shown in Equation 5.33.

$$MR = \frac{A_1}{A_2} = \frac{95066}{102280} = 92.95\% \tag{5.33}$$

These results show that even for a realistic line the motion regularity is better preserved by adopting a moving block signalling system ($MR_{MVB} = 92.95\%$ with respect to a fixed block one ($MR_{MVB} = 83.94\%$, with a difference between the two performance indices of almost 10%. The next Section will be dedicated to the analysis of the motion regularity for SRV2.

5.6.4. Motion regularity for SRV2

In SRV2 the two trains travel on the same line introduced for SRV1, but the second train skips most of the intermediate stations, namely the ones from the fifth to the eleventh. Therefore, the distance between the trains will decrease also in nominal conditions, so there is no need to introduce a disturbance like in the case of SRV1 to evaluate the motion regularity.

First, the FXB signalling system will be considered (the block length has been set to FBL = 1350 m). Figure 5.27 shows the block occupancy and continuous positioning of the trains both regarding their front and rear ends.

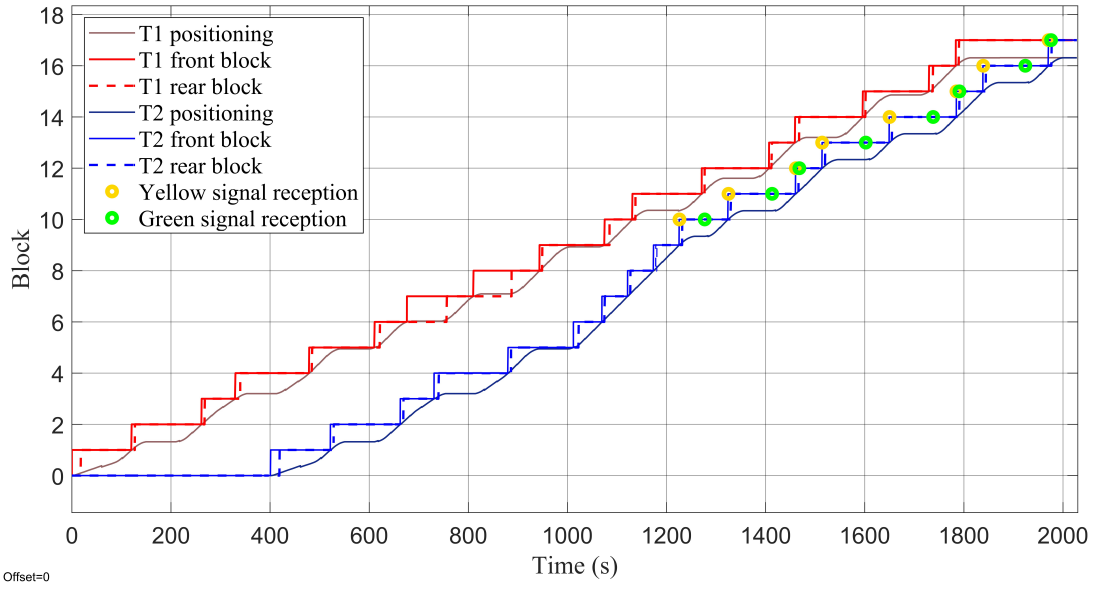

Figure 5.27: SRV2, FXB with FBL = 1350 m: Block occupancy of the trains (red lines for first train, blue lines for second train), both in their front ends (solid lines) and rear ends (dotted lines)

As expected, the second train gets close to the first one, eventually receiving a yellow signal and having to slow down or stop altogether. The result in terms of motion regularity is that the d-MRSP deviates from the s-MRSP multiple times and with great magnitude. Indeed, from the moment the second train reaches the first one (which, referring to Figure 5.27, happens roughly at time $t_0 = 1250\ s$), each station covered by the first train results in an unexpected stop of the second train. Figure 5.28 shows the d-MSRP, s-MRSP and the areas under their curves.

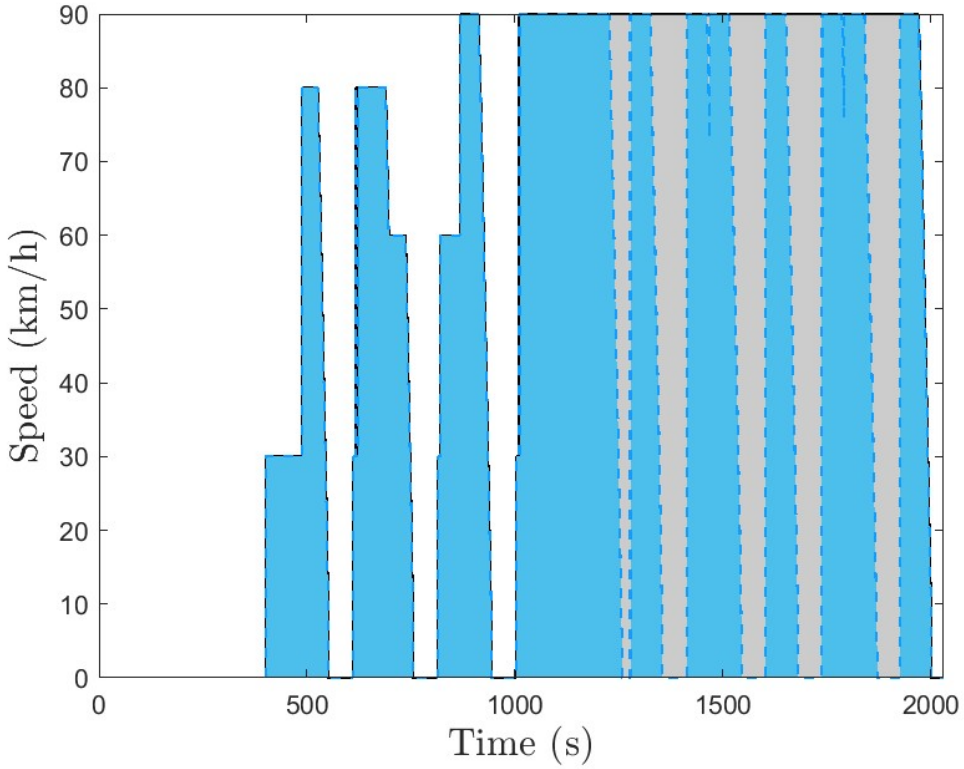

Figure 5.28: SRV2, FXB with FBL = 1350 m: Areas under s-MRSP and d-MRSP

As expected, after $t_0 = 1250\ s$ there are five drops of the d-MRSP, one for each station the first station has to stop at for its service. Note that there are also cases of the second train receiving a yellow signal for a short time so that it does not have to stop in that instance. Coherently, there are deviations of the d-MRSP from the s-MRSP that do not reach the null speed, meaning that they are only unexpected decelerations and not stops. By evaluating the light blue area A1 and the grey area A2 of figure 5.28 and performing the ratio between them, the motion regularity indicator for SRV1 at FXB is obtained, as illustrated in Equation 5.34.

$$MR = \frac{A_1}{A_2} = \frac{84208}{112750} = 74.68\% \tag{5.34}$$

As expected, this result is lower than the one obtained for SRV0-B, because of the increased number of stations, and thus, of deviations between d-MRSP and s-MRSP of the second train.

Now, the MVB signalling system will be considered. Figure 5.29 shows the position of the two trains both regarding their front and rear ends. As expected, the second train

gets close to the first one, eventually violating the safety distance and being required to slow down or stop altogether.

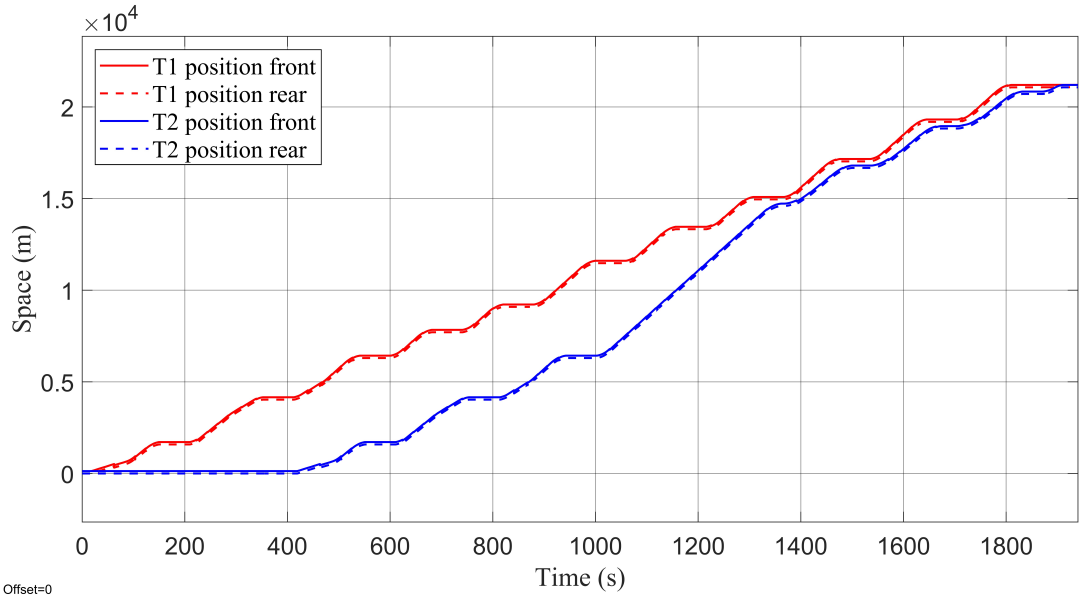

Figure 5.29: SRV2, MVB: position of the trains (red lines for first train, blue lines for second train), both in their front ends (solid lines) and rear ends (dotted lines)

The result in terms of motion regularity is that the d-MRSP deviates from the s-MRSP significantly in correspondence with the stations covered by the first train, but also frequently between the stations. Figure 5.30 shows the d-MSRP, s-MRSP and the areas under their curves. By zooming in, the shape of the frequent and narrow notches drawn by the d-MRSP would be similar to Figure 5.26.

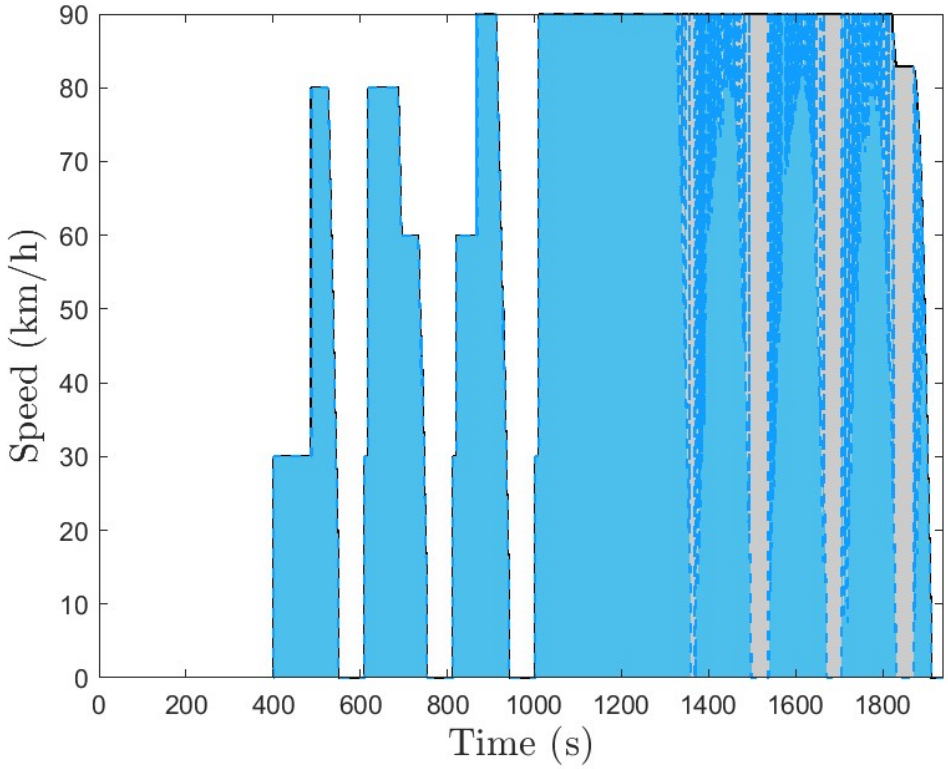

Figure 5.30: SRV2, MVB - Areas under s-MRSP and d-MRSP

By evaluating the light blue area A1 and the grey area A2 and performing the ratio between them, the motion regularity indicator for SRV1 and MVB signalling is obtained, as illustrated in Equation 5.35.

$$MR = \frac{A_1}{A_2} = \frac{85181}{104320} = 81.65\% \tag{5.35}$$

These results show that also for SRV2, the MVB signalling system outperforms the FXB one in terms of motion regularity. The reason for the better results of MVB signalling in terms of motion regularity lies in the fact that in the MVB case, the second train takes less time to complete the service. This has been observed in all presented simulations, and it stems from the fact that by adopting a MVB signalling system, the trains have to keep a smaller distance between them in general. Indeed, the second train takes roughly 2000 s for the FXB scenario and 1900 s for the MVB one to complete the service. This difference is not so significant in itself, but it becomes so when MR is evaluated: the grey area decreases by about 7% from one signalling system to the other, while the light blue area remains almost constant, in fact increasing slightly in the MVB signalling system. Thus, the ratio between the areas increases by about the same percentage.

In conclusion, the moving block signalling system seems advantageous with respect to the fixed block one in terms of motion regularity, regardless of the scenario in which it is implemented. Thus, it is extremely valuable to compare the two for future applications. Once the analysis of the KPI regarding motion regularity has been completed, in Section 5.7, attention will be paid to the evaluation of energy consumption.

5.7. Energy consumption evaluation

Energy consumption (EC) is the final KPI considered in the comparative analysis of the performances of the two signalling systems. This Section will cover the method used to evaluate the energy consumption of both trains, and will provide the results considering all services.

As stated in Section 5.2.4, the motor-generated force is already the force that is applied on the overall train to perform the motion as prescribed. Therefore, the computation of the required power reduces to the product of the motor-generated force and the train travelling speed. In particular, a positive motor force (traction) results in positive power consumption, while a negative motor force (braking) results in negative power consumption, which can be interpreted as power regeneration. Indeed, the model can simulate regenerative braking with a coefficient of performance (COP) η, which for the sake of simplicity is assumed to be constant for the entire simulation length. Referring to Figure 5.12, which represents the block diagram designed to perform EC evaluation, by setting the *regenerativeBrake* parameter to 1 and modifying the value of the COP a greater or smaller percentage of power can be regenerated, while by setting the *regenerativeBrake* parameter to 0 the power recovery can be neglected (this would be equivalent to setting $\eta = 0$), so that no energy can be recovered from braking operations.

The results will be presented by comparing the energy consumption computer in a FXB and MVB environment only in the case of the second train only. In fact, as in case of motion regularity, the first train is not influenced by the signalling system. Finally, the method considered for obtaining the results will be thoroughly described in Section 5.7.1, considering SRV0-B only, while for all other services, the results will be directly presented and commented in Section 5.7.2.

5.7.1. Energy consumption for SRV0-B

SRV0-B is the simplest service considered for energy consumption evaluation, in which two equal trains, driven by equal drivers, travel on a fictional line with one single station and

no velocity change points (VCPs). The reason behind this choice is that in SRV0-B the presence of the station guarantees that the second train has to brake even if its initial time delay was longer than the optimal value (recall Section 5.5.2, Figure 5.15). Thus, there is a difference in the evaluation of the EC in the cases with or without the consideration of regenerative braking. Finally, choosing SRV0-B instead of higher-complexity services for EC evaluation shows two advantages: it enhances a meaningful interpretation of the simulation results, as the presence of multiple stations and VCPs increases the complexity in a significant manner. Moreover, it allows the gradient of the line to be set freely, as the line is fictional and does not inherently carry the information on its gradient.

Therefore, the gradient of the line is a parameter of the simulations, meaning that the results will be presented considering different gradient profiles, such as null or uniform over the whole line. Clearly, the gradient configuration will be crucial in the evaluation of the energy consumption, since a downhill will be more convenient in terms of power usage, especially if regenerative braking is taken into consideration; vice-versa for an uphill. If the gradient follows a symmetrical, or at least balanced profile, meaning that the line is evenly split between uphill and downhill segments, the energy consumption will be equal to the null-gradient case.

For all simulations presented, the fixed block length has been set to FBL = 1350 m, and the station has been placed at S = 2500 m. By recalling Section 5.5.2, this implies that the optimal initial delay for the second train, i.e., the minimum delay that guarantees the non-reception of yellow signal lights for FXB and the non-violation of the safety distance for MVB, is:

- ${d_{T2\ FXB}}^* = 227\ s$ for FXB signalling systems;
- ${d_{T2\ MVB}}^* = 128\ s$ for MVB signalling systems.

Thus, to appreciate any difference between the two signalling systems, the prescribed initial delay for the second train must be smaller than the optimal value. Otherwise, the motion of the second train would be unaffected by the signalling system.

First, the case of motion with no regenerative braking will be examined: the force considered for the EC evaluation will be effectively saturated with a lower limit of 0 N, the power usage will be positive or null and the EC profile will be monotonically increasing with time, as shown in Figure 5.31. In the first graph of Figure 5.31, the solid black line represents the force considered in the EC evaluation, while the dotted line represents the overall motor-generated force (it assumes also negative values).

Note that this Figure has been obtained by simulating SRV0-B with a FXB signalling

system. However, if the analogous Figure for the MVB signalling system was represented, it would present very similar trends, so that the remarks made on the force, power and energy consumption profiles would still be valid. The most significant difference between the two signalling systems is that to obtain comparable results in terms of energy consumption, the initial delay of the second train would have to be much smaller for the MVB signalling system, in accordance with the optimality conditions reported earlier in this Section. In particular, the simulation reported in Figure 5.31 has been performed by prescribing an initial delay of the second train $d_{T2\ FXB} = 180\ s \tilde{=} 79\%\ d_{T2\ FXB}{}^{*}$, and a null gradient of the line.

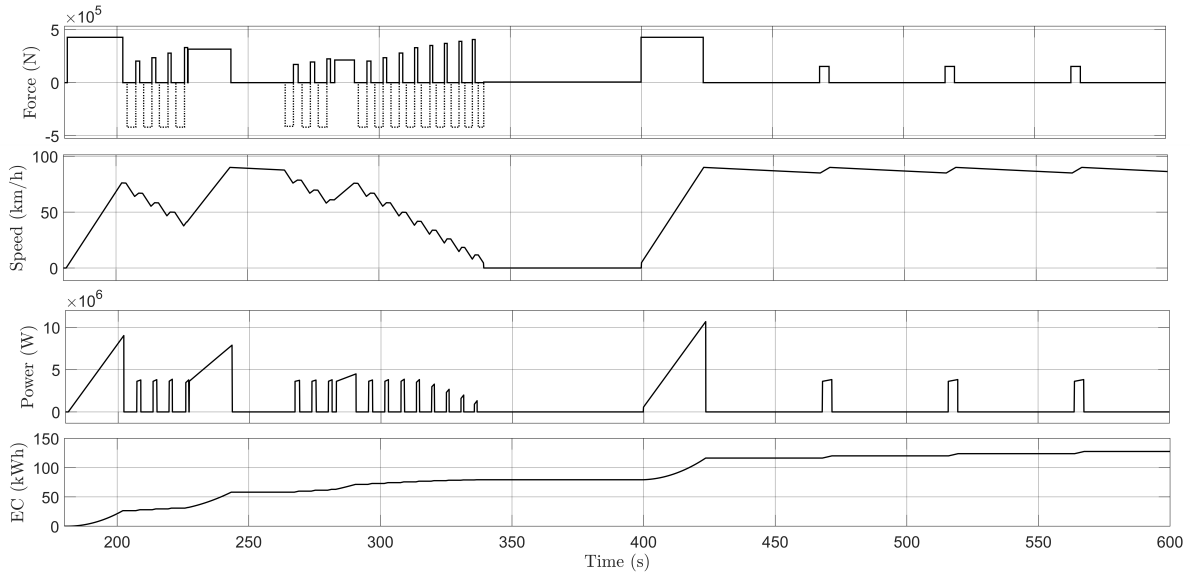

Figure 5.31: Force, speed, power and energy consumption graphs for SRV0-B FXB with null gradient along the whole line. The represented mode of operation presents no regenerative braking.

Now, the case of motion with regenerative braking will be examined. The power considered for the EC evaluation and the power consumption will be both positive and negative, and the EC profile will have both increasing and decreasing traits, as shown in Figure 5.32. In the first graph of Figure 5.32, the solid black line represents the force considered in the EC evaluation, while the dotted line represents the overall motor-generated force. Notice that as expected, this time the solid line assumes negative values when braking is issued, but it only reaches a portion of the overall motor-generated force accordingly to the value of the COP η, which has been set to 0.75 for the presented simulation.

Similar remarks can be made with respect to the difference between the results obtained with the two signalling systems as in the case without regenerative braking. Again, the simulation reported in Figure 5.32 has been performed by prescribing an initial delay of

the second train $d_{T2\ FXB} = 180\ s \tilde{=} 79\%\ d_{T2\ FXB}{}^{*}$, and a null gradient of the line.

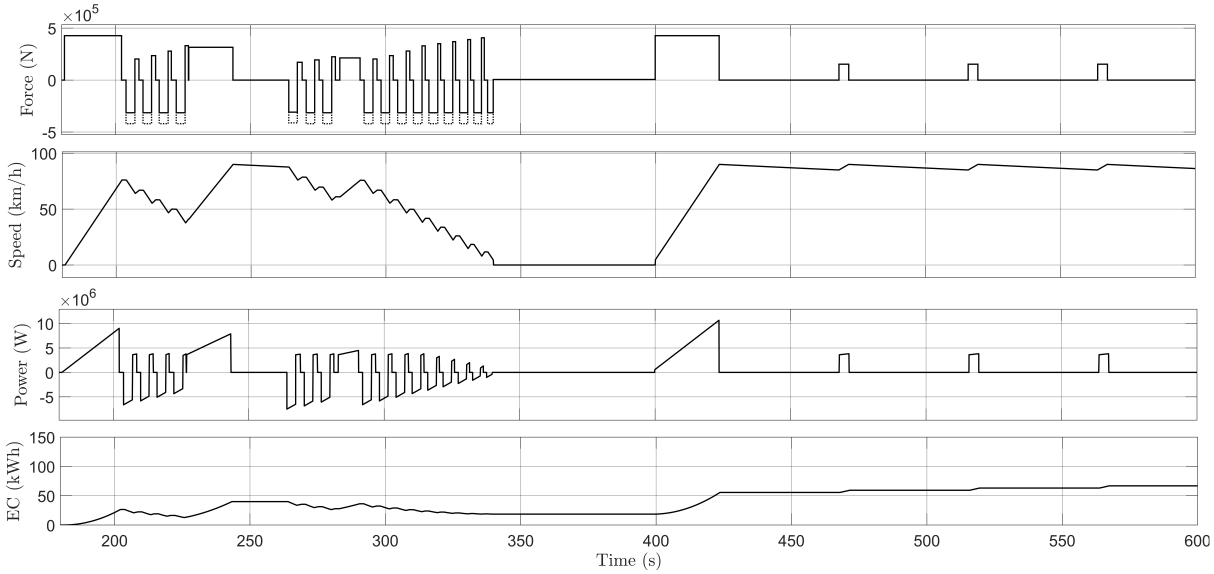

Figure 5.32: Force, speed, power and energy consumption graphs for SRV0-B FXB with null gradient along the whole line. The represented mode of operation presents regenerative braking.

Figures 5.31 and 5.32 have been obtained by performing a simulation with the aforementioned specifications, and as for the line gradient, it has been set to 0 for the whole line. Table 5.11 collects the results obtained by performing similar simulations in which different configurations of the line gradient have been considered, namely flat, uniform uphill and uniform downhill over the whole line. Moreover, the simulations have been performed with different values of the initial delay of the second train. For the FXB signalling system, the simulation have been performed considering the optimal delay and two cases of sub-optimal delay, namely at $100s$ and $180s = 79\% d_{T2\ FXB}{}^{*}$. For the MVB signalling system, the simulations have been performed considering the optimal delay and one case of suboptimal delay, namely at $100s = 79\% d_{T2\ MVB}{}^{*}$. This choice has been made to investigate whether equivalent performances of the two signalling systems can be achieved in case of equal delays of the second train. To do so, both the absolute sense (hence, $d_{T2} = 100\ s$ and in relation to the optimal time delay (hence, $d_{T2} = 79\%\ d_{T2}{}^{*}$ have been selected as a simulated scenario for both systems. Of course, the numbers reported in the Table represent the amount of energy consumed to perform the service, thus lower values are to be preferred to greater ones.

	Energy consumption without regenerative braking				
	FXB			MVB	
d_{T2} Line gradient	100 s	79% $d_{T2\ FXB}{}^{*} = 180$ s	$d_{T2\ FXB}{}^{*} = 227$ s	79% $d_{T2\ MVB}{}^{*} = 100$ s	$d_{T2\ MVB}{}^{*} = 128$ s
Flat	141.1 kWh	127.5 kWh	99.3 kWh	113.4 kWh	103.5 kWh
Uphill	188.8 kWh	182.1 kWh	146.4 kWh	195.1 kWh	183.3 kWh
Downhill	126.4 kWh	128.6 kWh	126.4 kWh	159.2 kWh	150.9 kWh
	Energy consumption with regenerative braking				
	FXB			MVB	
d_{T2} Line gradient	100 s	79% $d_{T2\ FXB}{}^{*} = 180$ s	$d_{T2\ FXB}{}^{*} = 227$ s	79% $d_{T2\ MVB}{}^{*} = 100$ s	$d_{T2\ MVB}{}^{*} = 128$ s
Flat	72.2 kWh	66.8 kWh	65.0 kWh	73.6 kWh	72.2 kWh
Uphill	127.7 kWh	126.7 kWh	116.8 kWh	157.2 kWh	152.3 kWh
Downhill	28.4 kWh	29.3 kWh	31.1 kWh	20.1 kWh	22.6 kWh

Table 5.11: Energy consumption results expressed in kWh for the second train in SRV0-B, with respect to operation mode (without or with regenerative braking), signalling system, initial delay and gradient of the line.

To critically analyse the results, the different line gradient configurations and operation modes (without or with regenerative braking) will be considered separately. In particular, note that the results obtained by selecting the optimal initial delay for the second train are very similar for the two signalling systems. This result was expected since the signalling does not affect the motion of the second train. The small difference in the values reported in the Table comes from numerical aspects related to the simulation. Thus, only the results obtained by selecting a sub-optimal initial delay of the second train will be considered, and the comparison will be performed on the results obtained with equivalent initial delays, both in an absolute and relative sense, i.e., columns 1 and 2 will be compared to column 5. The data reported in columns 1 and 2 will be hereafter reported as X/Y kWh, where X and Y are the contents of the cells at interest; for example, considering the first row, the result obtained for a FXB signalling is 141.1/127.5 kWh. Note that the enumeration of the rows and columns only takes into account the ones that contain numeric data, which are highlighted in light blue in Table 5.11.

First, the flat line scenario is considered, making reference to the first and fourth rows of Table 5.11. Without regenerative braking, the MVB signalling system produces better results with respect to the MVB one, as by comparing columns 1/2 and 4, energy consumption decreases from 141.1/127.5 kWh to 113.4 kWh (about 15%). By introducing regenerative braking, the two signalling systems become almost equivalent. This means that the implementation of regenerative braking is more beneficial to trains controlled with FXB signalling systems rather than with MVB ones, as they will perform longer and deeper decelerations. this was already evident in Section 5.6.3, where an explanation of the difference in the shape of the notches of the d-MRSP between the two signalling systems was provided considering a different service (SRV1), but the exact same reasoning holds for SRV0-B, which is the case considered in this Section.

Then, the uphill line scenario is considered, making reference to the second and fifth rows of Table 5.11. Both without and with regenerative braking, the FXB signalling system produces better results than the MVB one, as by comparing columns 1/2 and 4, energy consumption increases from 188.8/182.1 kWh to 195.1 kWh (about 5%), for row 2 (withohut regenerative braking) and from 127.7/126.7 kWh to 157.2 kWh (almost 20%), for row 5 (with regenerative braking). As in the previous case, the implementation of regenerative braking is more beneficial to trains controlled with FXB signalling systems rather than with MVB ones. An interesting conclusion is that in case of an uphill line, the adoption of MVB is found to be a less favourable choice compared to FXB from an energy consumption point of view.

Finally, the downhill line scenario is considered, making reference to the third and sixth

rows of Table 5.11. Without regenerative braking, the FXB signalling system produces better results with respect to the MVB one, as by comparing columns 1/2 and 4, energy consumption increases from 126.4/128.6 kWh to 159.2 kWh (about 7%). By introducing regenerative braking, the MVB signalling system becomes better performing than the FXB one. The downhill case represents the most meaningful case with respect to regenerative braking, since the only possibility for the train to slow down consists in the application of the braking force. Thus, the amount of energy restored through regenerative braking is very high, making the overall energy consumption very low. In particular, the MVB signalling systems produces better results than the FXB one, as by comparing columns 1/2 and 4, energy consumption decreases from 28.4/29.3 kWh to 20.1 kWh (about 30%). The implementation of regenerative braking is significantly more beneficial to trains controlled with MVB signalling systems rather than with FXB ones, in case of downhill line. The reason behind this discrepancy with the other cases lies in the fact that in downhill segments, the signalling is more impactful on the trains, as they will tend to move with higher average speed. Thus, a more reactive signalling system, like MVB with respect to FXB, is more prone to handle this kind of scenario. A train controlled with a MVB system will perform more frequent (although shorter and milder) decelerations, but for a downhill, this has a beneficial effect on energy consumption.

Once the simple case of SRV0-B has been examined, the next Section will be devoted to the synthetic exposition of the results obtained in the more complex cases of SRV1 and SRV2.

5.7.2. Energy consumption for SRV1 and SRV2

For SRV1 and SRV2 the line gradient is not a parameter of the simulation anymore, and the delay of the second train can be selected according to a reasonable choice of service scheduling. Thus, only one simulation will be presented for both services. In particular, SRV1 will be simulated with the addition of the unexpected delay of 300 s of the first train at the fifth station (please recall Section 5.6.3), while SRV2 will be simulated without any external disturbance, as the different station coverage of the two trains is sufficient to highlight the effect of the signalling system on the energy consumption of the second train.

Figures 5.33 and 5.34 show the graphs of the force, speed, power and energy consumption for SRV1 (with an unexpected delay of train 1) and SRV2 respectively. For each service, the results obtained without or with regenerative braking have been condensed into a single figure, in which red and blue lines respectively represent the scenarios without and

with regenerative braking. Note that for the force and power graphs, the blue lines are only traced in the negative half-plane, but the complete graph would overlap with the red lines in the positive half-plane. As explained for SRV0-B, the graphs are only represented for the FXB signalling system. One can reasonably expect the MVB-related graphs to have similar shapes.

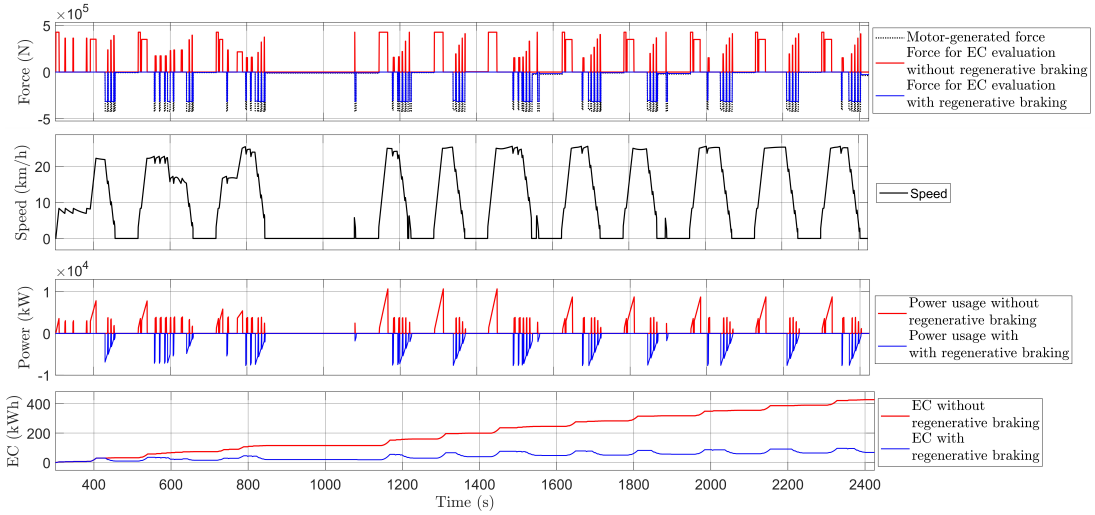

Figure 5.33: Force, speed, power and energy consumption graphs for SRV1 FXB with the inclusion of an unexpected delay of the first train of 300 s at the fifth station. Both modes of operation (without and with regenerative braking) are represented.

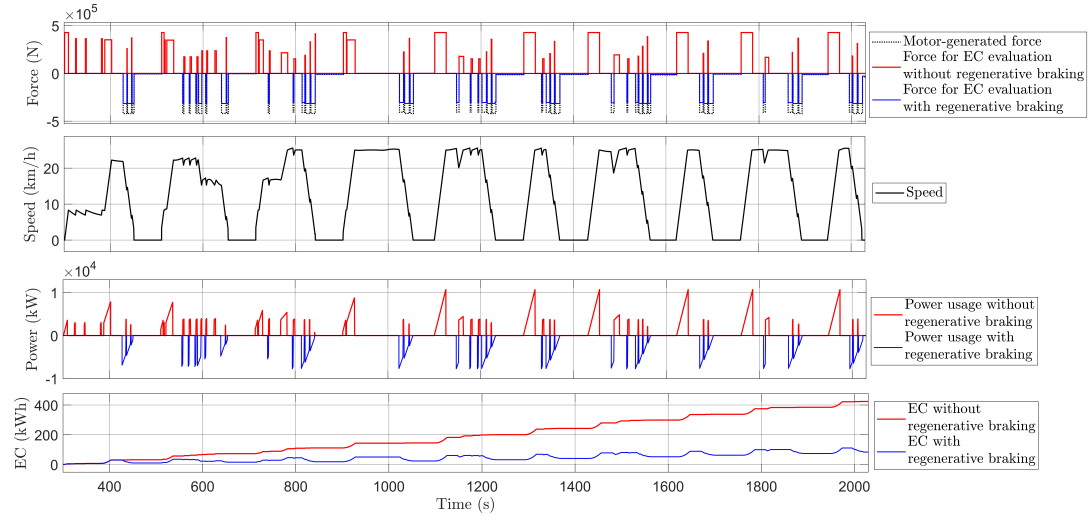

Figure 5.34: Force, speed, power and energy consumption graphs for SRV2 FXB with the inclusion of an unexpected delay of the first train of 300 s at the fifth station. Both modes of operation (without and with regenerative braking) are represented.

Table 5.12 collects the results obtained from the simulation. Note that, for the FXB signalling system, the fixed block length has been set to FBL = 1350 m, and the initial delay of the second train has been set to 300 s for all simulations.

	EC without regenerative braking	
	FXB	MVB
SRV1	428.0 (kWh)	471.9 (kWh)
SRV2	423.7 (kWh)	410.0 (kWh)
	EC with regenerative braking	
	FXB	MVB
SRV1	68.9 (kWh)	73.8 (kWh)
SRV2	82.9 (kWh)	53.5 (kWh)

Table 5.12: Energy consumption results expressed in kWh for the second train in SRV1 and SRV2 with respect to operation mode (without or with regenerative braking) and signalling system.

The results show that for SRV1, the FXB signalling system performs better than the MVB one for both operation modes (without or with regenerative braking). In particular, comparing the first and second columns of Table 5.12, the energy consumption of the second train increases from 428.0 kWh to 471.9 kWh (about 7%) without regenerative braking (first row) and from 68.9 kWh to 73.8 kWh (about 10%) with regenerative braking (third row). For SRV2, the MVB signalling system performs better than the FXB one for both operation modes. In particular, the energy consumption of the second train increases from 423.7 kWh to 410 kWh (about 3%) without regenerative braking (second row) and from 82.9 kWh to 53.5 kWh (about 45%) with regenerative braking (third row). This is the most outstanding result, and it stems from the fact that in a service like SRV2, the second train keeps on getting close to the first one because of the difference in station coverage. In this situation, if the signalling system adopted is MVB, the second train will perform a much greater number of unexpected brakes with respect to FXB signalling case(please, recall Figures 5.28 and 5.30). Thus, regenerative braking provides an extremely positive effect on this kind of service considering the MVB signalling system.

5.8. Final remarks

In conclusion, the evaluation of the KPIs produced interesting results, which are the effect of an intricate system of causes. The outcome of the comparison between FXB and MVB signalling systems is not trivial, since it is dependent on several factors other than the signalling system, such as line inclination, line scheduling (initial delay of the second train), traffic perturbation and their combination in the considered operational scenario.

To provide an overview of the results presented in this chapter:

- with respect to line capacity, the MVB signalling system is capable of reaching better results than the FXB one, but it is still possible to design a FXB signalling system that outperforms the MVB one by dimensioning the fixed blocks optimally;
- with respect to motion regularity, the MVB signalling system performs better than the FXB one in all analysed cases;
- with respect to energy consumption, the FXB signalling system performs better than the MVB one in most analysed cases with two main exceptions: on the one hand, if the line is generally downhill and regenerative braking is implemented; on the other hand, if the second train tends to get closer and closer to the first one to the point that its motion is severely constrained by the signalling (also in this case, the advantage is much more significant if regenerative braking is implemented).

This paragraph concludes the dissertation on the results of the simulations performed on the two signalling systems. The next Chapter will be devoted to the description of the application of the simulation tool presented in Sections 3 and 4 to a real-time environment, together with some preliminary results carried out with the designed system.

6 | Real-time application

This Chapter will present the results obtained by performing simulations in real-time. This has been achieved with the use of the performance real-time target machine by Speedgoat [30], which is a test equipment ideal for Hardware-in-the-Loop (HiL) simulation with MATLAB and Simulink workflow integration through the Simulink Real-Time toolbox. The aim of this Section is not to present extensive results, but rather it has to be intended as a first step towards the realization of a Hardware-in-the-Loop laboratory for signalling system comparison and certification. In particular, it will be shown that the simulation environment described in Chapters 3 and 4 is compatible with the Speedgoat device and suitable for real-time applications.

6.1. Speedgoat target machine

Hardware-in-the-Loop (Hil) testing is an ever-growing practice that has replaced traditional testing methods in a lot of applications in the field of railway signalling, at least in some portions of the system verification process [31]. The greatest advantage it offers is the possibility to verify the controller design without the complete system hardware. Instead, it relies on a real-time simulator that acts as a digital twin of the whole system or parts of the system. This allows for growing the range of scenarios that can be tested, reducing the cost and practical difficulties of test performance and easily controlling test inputs.

The performance real-time target machine by Speedgoat is a high-performance target computer, i.e., the machine on which the Simulink software is run instead of the source computer, that allows for Hil testing and verification. Its main strengths are the presence of embedded controllers and the possibility to realize a digital or hybrid physical and digital twin of the system to be controlled. Applying the target machine to the simulation tool, different choices could be made regarding the components to deploy from the virtual Simulink environment to the real-time Speedgoat target machine, such as the radio block center (RBC), the reference speed profiles generator, the vehicle/driver model or any combination of those, up to the whole system.

Another extremely useful feature of the Speedgoat target machine is that it offers a vast range of options for input/output (I/O) connectivity through the I/O modules. There is a multitude of modules that can be implemented, depending on the particular application. In the case of signalling system testing, these could be used to simulate the injection of disturbances or exogenous inputs. Just to provide few examples, the data received by the balises (Section 3.2.1), the loss of integrity of a train (Section 4.2) or the unexpected delay of a train at a station (Section 5.5.3) could be included in the analysis making use of these modules.

Figure 6.1 shows the Speedgoat target machine. It is connected to the source computer through the blue Ethernet cable, while the boards placed on top of it are the I/O modules.

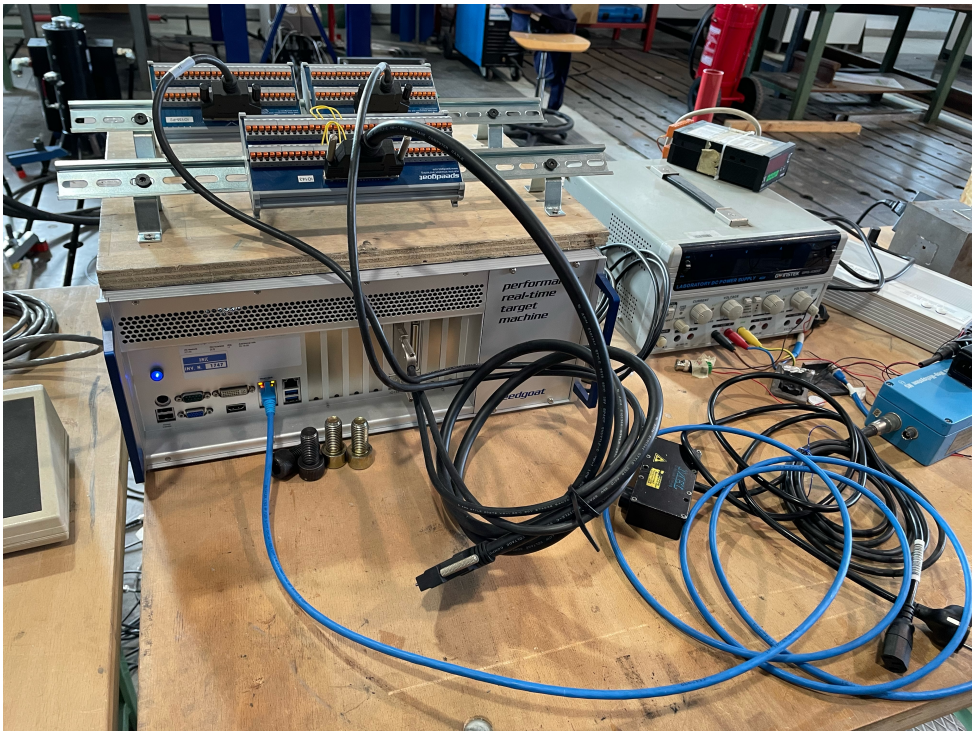

Figure 6.1: Speedgoat target machine, Ethernet cable for source computer and I/O modules.

This Section provided a brief overview of the HiL testing, the Speedgoat target machine and its potential application together with the Matlab and Simulink simulation environment described in this Thesis. Next, the results of a simulation performed by utilising the Speedgoat as the target machine will be presented.

6.2. Real-time simulation results

Two simulations of SRV1 in a real-time environment have been considered, adopting both FXB and MVB signalling. SRV1 has been chosen since it was extensively analysed in terms of KPIs in Chapter 5, as reported in Table 5.2. Thus, it will be possible to make a comparison between full-virtual and real-time simulations. More in detail, SRV1 has been considered in two slightly different versions: the nominal case, which is the one described in Section 5.1.3 and has been considered for line capacity evaluation; the disturbed case, which contains an unexpected delay of the first train at the fifth station, and has been considered for motion regularity and energy consumption evaluation. In this case, the simulation has been performed considering SRV1 in the disturbed case.

Figure 6.2 shows the simulation performed under the FXB signalling system: Figure 6.2 (a) represents the block occupancy of the trains; Figure 6.2 (b) represents their static and dynamic reference speed profiles (s-MRSP and d-MRSP) as well as the actual speed of the trains; finally, Figure 6.2 (c) represents the energy consumption of the second train, both with and without regenerative braking.

Likewise, Figure 6.3 shows the simulation performed under the MVB signalling system: Figure 6.3 (a) represents the position of the trains; Figure 6.3 (b) represents the s-MRSP, d-MRSP and actual speed of the second train; finally, Figure 6.3 (c) represents the power and energy consumption of the second train, both with and without regenerative braking.

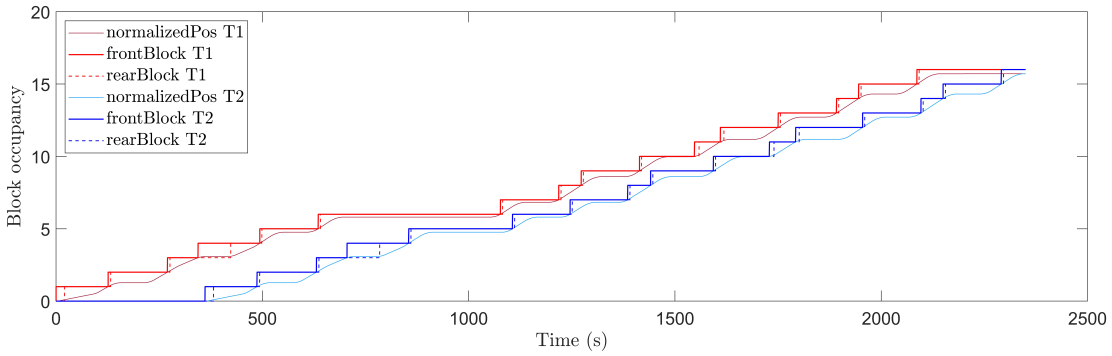

(a) Block occupancy and normalized continuous position of both trains.

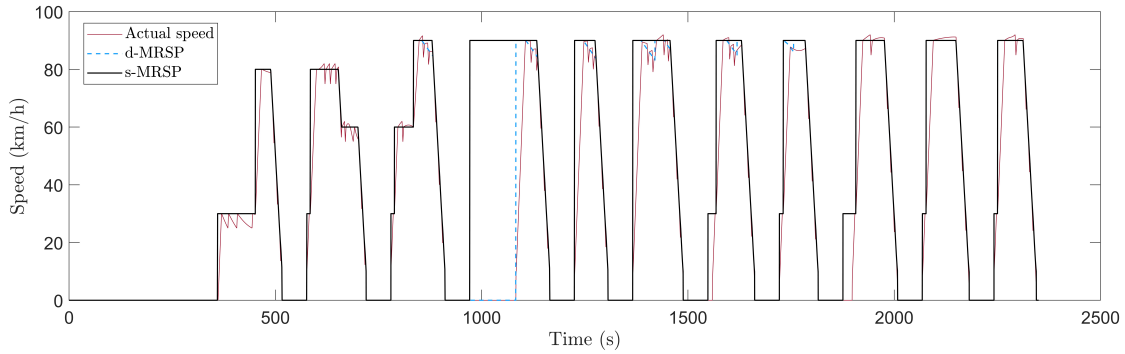

(b) s-MRSP, d-MRSP and actual speed of the second train.

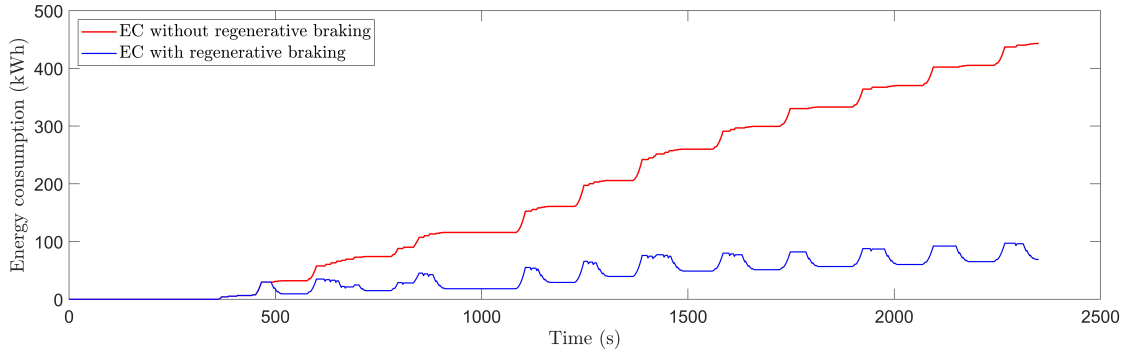

(c) Energy consumption of the second train with both modes of operation (without and with regenerative braking)

Figure 6.2: Real-time simulation of SRV1 with an unexpected delay of the first train at the fifth station of 300 s, FXB signalling system with FBL = 1350 m, initial delay of the second train dT2 = 360 s.

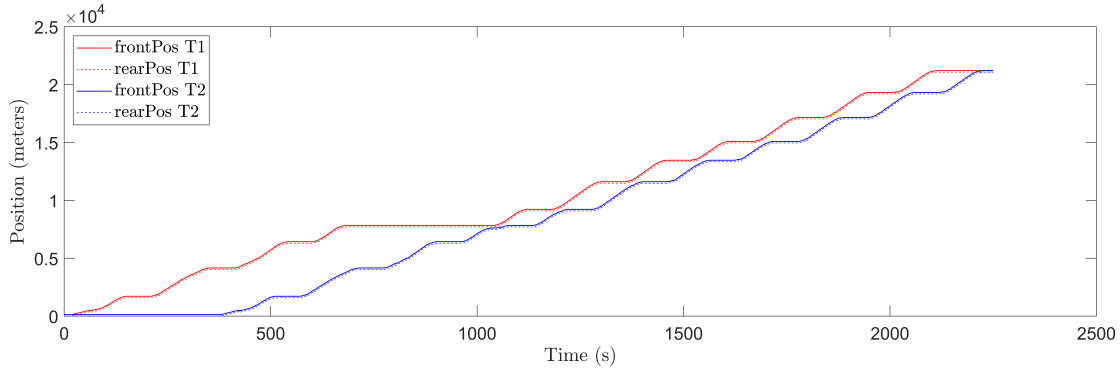

(a) Position of both trains.

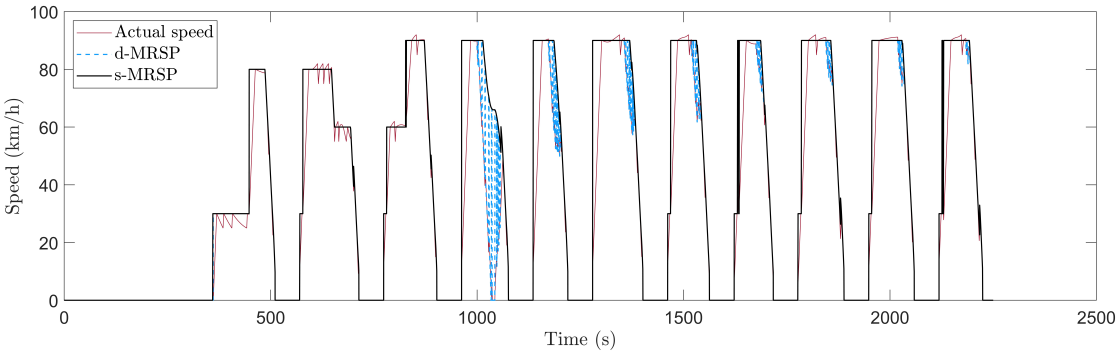

(b) s-MRSP, d-MRSP and actual speed of the second train.

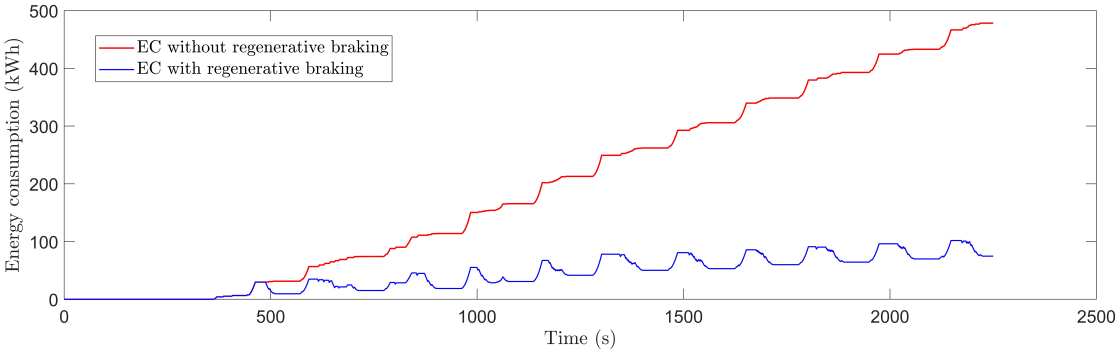

(c) Energy consumption of the second train with both modes of operation (without and with regenerative braking)

Figure 6.3: Real-time simulation of SRV1 with an unexpected delay of the first train at the fifth station of 300 s, MVB signalling system, initial delay of the second train dT2 = 360 s.

The results presented in Figure 6.2 and 6.3 are analogous to the one obtained in a fully virtual environment. This was expected to some extent, but still worth veryfing to allow the realization of the Hil test bench. To this end, the results will be analysed from a quantitative point of view, comparing them with the results presented in Chapter 5 for the simulation of SV1 with an unexpected delay of the first train.

Table 6.1 collects the data obtained from these simulations, organized with respect to the KPIs. For each variable, two values have been reported in two separate rows: the first one refers to the simulation run in a real-time environment, while the second one, refers to the simulation run in a virtual environment. Note that for line capacity, the result of SRV carried out in virtual environment was never shown in Section 5.5.3, since no unexpected delay was previously introduced in the computation of this KPI. Instead, they have been evaluated through a new simulation and with the same empirical method described in Section 5.5.3: performing multiple simulations with increasing values of the second train initial delay, until the reception of a yellow signal light at FXB or the violation of the safety distance at MVB is prevented. On the other hand, the computation and presentation of the other values obtained in a virtual environment can be found in Section 5.6.3 for motion regularity and Section 5.7.2 for energy consumption.

A difference in the values of the KPIs between the two simulation environments can be found when comparing the simulations carried out in full virtual and real-time configurations. Since the Simulink model and all the specifications considered in the real-time environment are the same as the ones considered in the virtual environment, the difference in the results can be attributed to numerical errors of the simulator, which are emphasized in a real-time environment. However, the general comparison between the FXB and MVB signalling systems provides the same results with both virtual and real-time environments. For instance, the difference in the motion regularity indicator between the signalling system is still about 10% in favour of the MVB system, even though the actual MR values differ of about 2% from virtual and real-time environments.

Aside from the numerical differences in the results, the main objective of this Section is to show that the simulation tool is suitable to be integrated into a real-time environment. Given this final alim, some modelling choices previously presented can be furtherly justified. For instance, consider the zero-order hold blocks (Section 3.2.2) purposely designed and adopted to discretize the communication between the components, instead of the Simulink built-in ones, which in fact are not compatible with a real-time environment. With these devices, the simulation tool is fully compatible with the Speedgoat target machine.

	Line capacity	
	FXB	MVB
Real-time environment	6.12 trains/h	8.49 trains/h
Virtual Environment	6.14 trains/h	8.49 trains/h

	Motion regularity of the second train	
	FXB	MVB
Real-time environment	85.98%	94.76%
Virtual Environment	83.94%	92.95%

	Energy consumption of the second train		
	FXB	MVB	
Real-time environment	443.0 kWh	478.2 kWh	without RB
	69.1 kWh	74.7 kWh	with RB
Virtual Environment	428.0 kWh	471.9 kWh	without RB
	68.9 kWh	73.8 kWh	with RB

Table 6.1: Results of the simulation of SRV1 (with unexpected delay of the first train at the fifth station) with both signalling systems in a real-time environment, compared to the equivalent results obtained in a fully virtual environment. RB stands for regenerative braking.

The next step in the integration of the Speedgoat target machine is the partition of the Simulink program into two parts which run on separate machines. For example, the RBC could be dislocated on the Speedgoat and connected to the rest of the model through the I/O modules described in Section 6.1.1. Thus, the handle of connectivity, potential asynchrony and loss of information become relevant topics of study.

This Section was dedicated to the description of one possible approach to the integration of the Simulink software in a real-time environment, as well as the presentation of the results of one simulation performed following that approach. It should be interpreted as a point of connection between this research and further research that will be performed within the same scope. The next Section will be devoted to summarizing the results obtained in this work and proposing the possible next step to advance this work.

Conclusions

This thesis work dealt with railway signalling system, investigating on the advantages and disadvantages of moving block signalling in comparison with fixed block signalling. The former, not yet in operation, is currently the subject of intensive research: this work intends to be a contribution in this field, focusing on the comparison of the performance of the two signalling systems in different operational scenarios, to identify in which ones it is really worth implementing a moving block system.

The main goals of the work were:

- the development of a simulation tool implementing the rules of fixed and moving block signalling, considering the longitudinal dynamics of the train, the train driver behaviour in response to signalling alerts, the capability to manage different scenarios of service of the leading and the trailing trains;
- the investigation on the comparative performance of moving block and fixed block signalling;
- the possibility to inject disturbances at different levels, in order to evaluate the capability of the simulation tool to respond to them;
- the implementation of the simulation tool in a real time computing system, in the prospect of the setup of a virtual laboratory, where some of the sub-elements anc be substituted by a real device.

In the work of this thesis, to achieve these goals a simulation tool for the management of railway traffic was implemented in a Simulink model containing the most relevant elements concerning railway signalling, namely the trains with their dynamics, the drivers' behaviour and response to signalling alerts, the positioning devices and the radio block center (RBC).

The radio block center (RBC) provides the trains with their movement authority (MA) in terms of coloured signal lights for FXB signalling and safety distancing for MVB signalling. Regardless of the signalling system adopted, the trains are also provided with the reference speed profile to follow in order to prevent collisions with other vehicles.

Starting from this speed profile, referred to as dynamic most restrictive speed profile, additional references are designed to perform the speed control: the lower curve (LC) and warning curve (WC) determine the range around the d-MRSP inside of which the speed varies in nominal conditions; the service brake intervention (SBI) and emergency brake intervention (EBI) are defined above the WC as additional safety measures in case the speed exceeds the nominal interval (LC-WC). The train is modelled in terms of vehicle dynamics, considering the force generated by the motor, the motion resistance and the effect of line gradient. Moreover, the driver behavioural model is defined to implement the speed control algorithm considering the aforementioned speed reference profiles. Finally, the train speed and position are evaluated and, only in the case of FXB signalling, the block occupancy is computed by discretizing the line into fixed blocks. The state of the train (block occupancy for FXB signalling and position and speed for MVB signalling) is then reported to the RBC.

This simulation tool has been adopted to perform a diverse set of simulations, and some underlying assumptions have been considered in each of them for the sake of simplicity. First, only two trains are considered, referred to as first (leading) and second (following) train. Furthermore, the line consists of a single track for each direction of motion, thus, no overtake is allowed between the trains. Finally, only longitudinal gradient is considered (uphills and downhills), rather than transversal gradient (curves).

Two lines were considered to perform the simulations. The first one is an ideal line which can account for a desired number of stations, with arbitrary location. Moreover, also the reference speed and the gradient profiles can be modified as simulation parameters. The second line is a real one containing 12 stations and prescribed reference speed and gradient profiles. On this line, the trains can perform different services depending on the subset of stops at the stations.

Coming to the comparison between the FXB and MVB signalling systems with respect to a set of key performance indicators (KPIs). The selected KPIs are representative of the diverse points of view under which the signalling systems may be compared. The adopted KPIs were:

- line capacity (LC), which measures the number of trains that can perform a service over the time of an hour;
- motion regularity (MR), which describes how the signalling system constrains the motion of the trains;
- energy consumption (EC) measures the energetic efficiency of the trains, with or

without considering regenerative braking.

The results of the simulations show that the signalling systems outperform each other differently if a different service and KPI are considered. To be more specific, in terms of line capacity, the MVB signalling system generally performed better than the FXB one for the simplest cases, with same service of both trains. However, as the simulated service scenario became more complicated there have been instances of the FXB environment performing better than the MVB one for well-designed block systems with optimally or nearly optimally dimensioned fixed blocks.

As far as motion regualrity is concerned, the MVB signalling systems performed better than the FXB one in all considered cases, which means that MVB signalling is generally favourable on the motion of the trains.

Finally, in terms of energy consumption, the FXB signalling system outperformed the MVB one, especially without the implementation of regenerative braking. This may suggest that in order for the moving block to be more competitive also with regard to energy consumption, modern and efficient infrastructure must be combined with it.

The last objective of this thesis was the preliminary application of the simulation tool to a real-time environment, to check the capability to integrate the simulation in a future test bench with mixed simulated and physical subsystem. Which has been performed with the Speedgoat target machine. This device is used to run simulations in real-time, and the simulation tool has been designed to be compatible with it. The simulations of a service with two trains travelling on a line with 12 stations (and stopping at all of them) have been performed both with FXB and MVB signalling. The results correspond to the ones obtained in a fully virtual environment. This is the first step towards a broader objective of designing a virtual-physical test bench in which some of the simulated functions are carried out by the corresponding physical device. On this topic, the European projects and regulations will be taken into consideration to define the most important scenarios to simulate and test.

This thesis was developed within the framework of a project of the Italian Piano Nazionale di Ripresa e Resilienza (PNRR). Thus, the work presented in this document will be expanded in various directions. On the front of virtual simulation, more features are planned to be added to the simulation tool and already existing features can be furtherly refined. Among them, the resistance force acting on a train due to the effect of transverse line curvatures, the modelling of the traction including the creepage formulation of the contact forces, a more refined simulation of RBC and the insertion of the simulation of the protocols of transmission. On the front of the realization of the Hardware-in-the-

Loop laboratory for signalling system comparison and certification, further research will be crucial in the next phases of the project to determine the laboratory components, the communication protocols to be implemented and which virtual components to transpose into physical ones.

Bibliography

[1] Sajed K Abed. European rail traffic management system - an overview. pages 173–180, 2010.

[2] C.J. Goodman, L.K. Siu, and T.K. Ho. A review of simulation models for railway systems. pages 80–85, 1998. doi: 10.1049/cp:19980101.

[3] R.J. Hill and L.J. Bond. Modelling moving-block railway signalling systems using discrete-event simulation. pages 105–111, 1995. doi: 10.1109/RRCON.1995.395162.

[4] Murray A. Geisler and Harry Max Markowitz. *A Brief Review of SIMSCRIPT as a Simulating Technique*. RAND Corporation, Santa Monica, CA, 1963. doi: 10.7249/RM3778.

[5] C.S. Chang, C.S. Chua, H.B. Quek, X.Y. Xu, and S.L. Ho. Development of train movement simulator for analysis and optimisation of railway signalling systems. pages 243–248, 1998. doi: 10.1049/cp:19980123.

[6] D. Basile, M. H. ter Beek, A. Ferrari, and A. Legay. Modelling and analysing ertms l3 moving block railway signalling with simulink and uppaal smc. 11687 LNCS:1–21, 2019. URL `www.scopus.com`. Cited By :25.

[7] Bruce Powel Douglass. *Real-Time UML*. Springer Berlin Heidelberg, Berlin, Heidelberg, 2002.

[8] Gerd Behrmann, Alexandre David, and Kim G. Larsen. *A Tutorial on Uppaal*. Springer Berlin Heidelberg, Berlin, Heidelberg, 2004. ISBN 978-3-540-30080-9. doi: 10.1007/978-3-540-30080-9_7. URL `https://doi.org/10.1007/978-3-540-30080-9_7`.

[9] T.K. Ho, B.H. Mao, Z.Z. Yuan, H.D. Liu, and Y.F. Fung. Computer simulation and modeling in railway applications. *Computer Physics Communications*, 143(1):1–10, 2002. ISSN 0010-4655. doi: https://doi.org/10.1016/S0010-4655(01)00410-6. URL `https://www.sciencedirect.com/science/article/pii/S0010465501004106`.

[10] P. Martin. Train performance and simulation. 2:1287–1294 vol.2, 1999. doi: 10.1109/WSC.1999.816855.

[11] David Barney, David Haley, and George Nik. Calculating train braking distance. 02 2002.

[12] Volodymyr Havryliuk. An overview of the etcs braking curves. *ELECTROMAGNETIC COMPATIBILITY AND SAFETY ON RAILWAY TRANSPORT*, 06 2017. doi: 10.15802/ecsrt2017/136811.

[13] Bertil Friman. An algorithm for braking curve calculations in ertms train protection systems. *WIT Transactions on the Built Environment*, 88:421–429, 2006.

[14] Valeria Vignali, Federico Cuppi, Claudio Lantieri, Nicola Dimola, Tomaso Galasso, and Luca Rapagnà. A methodology for the design of sections block length on etcs l2 railway networks. *Journal of Rail Transport Planning and Management*, 13:100160, 2020. ISSN 2210-9706. doi: https://doi.org/10.1016/j.jrtpm.2019.100160. URL `https://www.sciencedirect.com/science/article/pii/S2210970619300605`.

[15] E. Quaglietta. A simulation-based approach for the optimal design of signalling block layout in railway networks. *Simulation Modelling Practice and Theory*, 46:4–24, 2014. URL `www.scopus.com`. Cited By :32.

[16] A. Mazini, M. Samra, L. Chen, M. Blumenfeld, and G. Nicholson. Specification and design of a modular and extensible architecture for testing moving block systems. 213:147–158, 2022. URL `www.scopus.com`.

[17] Gonzalo Solas, Leonardo J. Valdivia, Javier Añorga, Adam Podhorski, Jaizki Mendizabal, Stanislas Pinte, and Luis Marcos. Virtual laboratory for on-board etcs equipment. pages 2013–2018, 2015. doi: 10.1109/ITSC.2015.326.

[18] Gonzalo Solas, Jaizki Mendizabal, Leonardo Valdivia, Javier Añorga, Iñigo Adin, Adam Podhorski, Stanislas Pinte, Luis Gerardo Marcos, Jesús Mª González, and Francisco Cosín. Development of an advanced laboratory for etcs applications. *Transportation Research Procedia*, 14:1894–1903, 2016. ISSN 2352-1465. doi: https://doi.org/10.1016/j.trpro.2016.05.156. URL `https://www.sciencedirect.com/science/article/pii/S2352146516301570`. Transport Research Arena TRA2016.

[19] Mohamed Ghazel. A control scheme for automatic level crossings under the ertms/etcs level 2/3 operation. *IEEE Transactions on Intelligent Transportation Systems*, 18(10):2667–2680, 2017. doi: 10.1109/TITS.2017.2657695.

[20] Qi Wang, Ming Chai, Haifeng Wang, Hao Zhang, Jinchuan Chai, and Bingyue Lin.

Cloud-based simulated automated testing platform for virtual coupling system. pages 2738–2743, 2022. doi: 10.1109/ITSC55140.2022.9922450.

[21] Geordie Roscoe and C. Tyler Dick. Comparing the efficiency and effectiveness of different train-following control algorithms for fleets of heavy-haul freight trains under moving blocks. *Transportation Research Record*, 2677(1):446–459, 2023. doi: 10.1177/03611981221099917.

[22] Mohammad taghi HAMIDI BEHESHTI and Mohammad hasan and MIRAN BEYGI. A comparison study of fixed and moving-block signalling in rapid transit railways. *The Modares Journal of Electrical Engineering*, 3(1), 2003. URL `http://mjee.modares.ac.ir/article-17-2294-en.html`.

[23] Yoshinao Isobe, Faron Moller, Hoang Nga Nguyen, and Markus Roggenbach. Safety and line capacity in railways – an approach in timed csp. pages 54–68, 2012.

[24] Rob M.P. Goverde, Francesco Corman, and Andrea D'Ariano. Railway line capacity consumption of different railway signalling systems under scheduled and disturbed conditions. *Journal of Rail Transport Planning and Management*, 3(3):78–94, 2013. ISSN 2210-9706. doi: https://doi.org/10.1016/j.jrtpm.2013.12.001. URL `https://www.sciencedirect.com/science/article/pii/S2210970613000504`. Robust Rescheduling and Capacity Use.

[25] V. Ranjbar, N. O. E. Olsson, and H. Sipilä. Impact of signalling system on capacity – comparing legacy atc, etcs level 2 and etcs hybrid level 3 systems. *Journal of Rail Transport Planning and Management*, 23, 2022. URL `www.scopus.com`. Cited By :1.

[26] M. Abril, F. Barber, L. Ingolotti, M. A. Salido, P. Tormos, and A. Lova. An assessment of railway capacity. *Transportation Research Part E: Logistics and Transportation Review*, 44(5):774–806, 2008. URL `www.scopus.com`. Cited By :277.

[27] Jyh-Cherng Jong. Models for estimating energy consumption of electric trains. *Journal of the Eastern Asia Society for Transportation Studies*, 5, 01 2005. doi: 10.11175/easts.6.278.

[28] Christian Dullinger, Walter Struckl, and Martin Kozek. Simulation-based multi-objective system optimization of train traction systems. *Simulation Modelling Practice and Theory*, 72:104–117, 2017. ISSN 1569-190X. doi: https://doi.org/10.1016/j.simpat.2016.12.008. URL `https://www.sciencedirect.com/science/article/pii/S1569190X16301435`.

[29] Jinghui Wang and Hesham A. Rakha. Electric train energy consumption modeling.

Applied Energy, 193:346–355, 2017. ISSN 0306-2619. doi: https://doi.org/10.1016/j.apenergy.2017.02.058. URL https://www.sciencedirect.com/science/article/pii/S0306261917301861.

[30] https://www.speedgoat.com/products-services/real-time-target-machines/performance-real-time-target-machine.

[31] Jonathan Millitzer, Dirk Mayer, Christian Henke, Torben Jersch, Christoph Tamm, Jan Michael, and Christopher Ranisch. Recent developments in hardware-in-the-loop testing. pages 65–73, 2019.

List of Figures

List of Tables

Acknowledgements

This study was carried out within the MOST - Sustainable Mobility National Research Center and received funding from the European Union - NextGenerationEU (PIANO NAZIONALE DI RIPRESA E RESILIENZA (PNRR) - MISSIONE 4 COMPONENTE 2, INVESTIMENTO 1.4 - D.D. 1033 17/06/2022, CN00000023). This manuscript reflects only the authors' views and opinions, neither the European Union nor the European Commission can be considered responsible for them.

Studio condotto nell'ambito del MOST - Centro Nazionale per la Mobilità sostenibile, finanziato dall'Unione Europea - NextGenerationEU (PIANO NAZIONALE DI RIPRESA E RESILIENZA (PNRR) - MISSIONE 4 COMPONENTE 2, INVESTIMENTO 1.4 - D.D. 1033 17/06/2022, CN00000023). I punti di vista e le oprinioni espressi sono tuttavia solo quelli degli autori e non riflettono necessariamente quelli dell'Unione Europea o della Commisione Europea. Né l'Unione Europea né la Commissione Europea possono essere ritenute responsabili per essi.

Ringrazio l'intero team di lavoro coinvolto in questo progetto. Ho appreso da ognuno di voi. Inoltre, non posso scordarmi dei miei amici per avermi alleggerito nei momenti di fatica e spronato in quelli di ozio. Infine, un pensiero va ai miei genitori che mi hanno supportato con amore in tutti questi anni. Vi voglio bene.